

Rowan University

Rowan Digital Works

Theses and Dissertations

9-8-2021

INVESTIGATION OF THE ROLE OF HYDROPHOBIC AMINO ACIDS ON THE STRUCTURE-ACTIVITY RELATIONSHIP IN PONERICIN L1 FROM NEOPONERA GOELDII

Nicholas Patrick Schifano
Rowan University

Follow this and additional works at: <https://rdw.rowan.edu/etd>

 Part of the [Medicinal and Pharmaceutical Chemistry Commons](#)

Recommended Citation

Schifano, Nicholas Patrick, "INVESTIGATION OF THE ROLE OF HYDROPHOBIC AMINO ACIDS ON THE STRUCTURE-ACTIVITY RELATIONSHIP IN PONERICIN L1 FROM NEOPONERA GOELDII" (2021). *Theses and Dissertations*. 2943.

<https://rdw.rowan.edu/etd/2943>

This Thesis is brought to you for free and open access by Rowan Digital Works. It has been accepted for inclusion in Theses and Dissertations by an authorized administrator of Rowan Digital Works. For more information, please contact graduateresearch@rowan.edu.

**INVESTIGATION OF THE ROLE OF HYDRPHOBIC AMINO ACIDS ON THE
STRUCTURE-ACTIVITY RELATIONSHIP IN PONERICIN L1 FROM
NEOPONERA GOELDII
&
EFFECT OF CHARGE AND HYDROPHOBICITY IN ANTIMICROBIAL
POLYMETHACRYLATE POLYMERS**

By

Nicholas Schifano

A Thesis

Submitted to the
Department of Chemistry and Biochemistry
College of Science and Mathematics
In partial fulfillment of the requirement
For the degree of
Master of Science in Pharmaceutical Sciences
at
Rowan University
July 29, 2021

Thesis Chair: Gregory A. Caputo, Ph.D.

Committee Members:
Gregory A. Caputo, Ph.D.
Timothy Vaden, Ph.D.
Venkatesh Nemmara, Ph.D.

© 2021 Nicholas Schifano

Dedication

This thesis is dedicated to my brother Bryan, who has acted not just as a brother but also as a mentor and most importantly a role model. I am honored to say that you are one of the biggest influences in my life that helped make me the scientist I am today. Ever since I was little, being seven years apart made me believe I would always walk in your shadow, to only be recognized as a “little brother”. However, as I have walked this path, you have helped me see that I was not walking in your shadow but creating my own set of footsteps alongside of yours. Your unrelenting support, generosity, and ability to always instill confidence in me is the reason why I made it as far as I have. My journey into science started out as way to get you to notice me; a topic we can relate on. Your ability to make science seem so enjoyable and effortless made it even more appealing. I have gained such much of an appreciation of your talents and intellect through this process; because science, although enjoyable, is not easy nor effortless. Being able to go down this path and escape the type of town we are from, I have you to be grateful for. I never would have made it for if it were for my big brother, thank you for everything.

Acknowledgments

I would like to start by expressing my deep gratitude and appreciation to my thesis advisor Dr. Gregory A. Caputo. He has gone above and beyond the duties of a mentor. He took me as a student when I was at the end of my undergrad career when I still had little direction or purpose. Other than the copious lab techniques he has taught me, he taught me that science is a mindset. My skills and aspirations have grown exponentially within the small amount of time I have been in his lab. I have been recently accepted into the biochemistry program at University of Maryland, I hope to make him a proud mentor through the next steps in my career as a scientist.

I would also like to recognize both previous lab colleagues Alexandria Senetra and Mathew Necelis for not only the hard work they put in before me but helping me through this process. Both colleagues went out of their way to help prepare me for the challenges I would face. When I first entered the program, I did not think that I would even consider continuing my education. However, watching both thrive and be accepted into different Ph.D. programs it gave me motivation to continue and set new goals. Thank you for always helping and being great role models. Lastly, I would like to thank family and friends who understood the importance of this thesis and what this degree means to me. Also, for helping me stay calm and collected and ensuring me that I could make it every bit of the way. I would also like to thank all my coworkers and boss at IVDS. It is not easy working while obtaining any degree let alone a master's degree, however, IVDS helped me grow as a scientist, allowed for flexible scheduling when needed, and most importantly allowed me to form strong bonds and friendships. Thank you got all the support and experience.

Abstract

Nicholas Schifano

INVESTIGATION OF THE ROLE OF HYDRPHOBIC AMINO ACIDS ON THE
STRUCTURE-ACTIVITY RELATIONSHIP IN PONERICIN L1 FROM *NEOPONERA*
GOELDII

&

EFFECT OF CHARGE AND HYDROPHOBICITY IN ANTIMICROBIAL
POLYMETHACRYLATE POLYMERS
2020-2021

Gregory A. Caputo, Ph.D.

Master of Science in Pharmaceutical Science

Due to the increase prevalence of antimicrobial resistance (AMR) antibiotic alternatives have been of great interest. Antimicrobial peptides (AMPs) and polymers like polymethacrylates that mimic AMPs are two non-traditional antimicrobial agents that have been investigated thoroughly over the years as a potential solution to the AMR problem. This study will further the understanding of the L1 peptide by investigating the role hydrophobic amino acids have on the antimicrobial activity. Biophysical and microbiological techniques were utilized to show that the L1 hydrophobic derivative showed enhanced binding to anionic lipid bilayers while maintaining low hemolytic activity. This study also elucidates the effect of charge and hydrophobicity on polymethacrylate polymers by imploring the same techniques and methods used to investigate the Ponericin L1 peptide. These results indicate that both charge and hydrophobicity have an impact on activity and selectivity. As hydrophobicity increased, so did the hemolytic activity, suggesting a balance between hydrophobicity and charge is needed to optimize antimicrobial activity as well as selectivity. Overall, the results show that these AMPs and polymethacrylates have great potential as a platform against AMR.

Table of Contents

Abstract	v
List of Figures	ix
List of Tables	x
Chapter 1: Antimicrobials and a Need for Alternatives.....	1
History of Antimicrobials	1
Traditional Antibiotics	2
Multidrug Resistance	4
History of Antimicrobial Peptides	6
Structures and Characteristics of Antimicrobial Peptides	8
Mechanism of Action of Antimicrobial Peptides	9
Physiochemical Properties of Antimicrobial Peptides.....	12
Venom-Derived Antimicrobial Peptides.....	14
Background on Antimicrobial Polymers	17
Chapter 2: Investigation of the Role of Hydrphobic Amino Acids on The Structure- Activity Relationship in Ponericin L1 from <i>Neoponera Goeldii</i>	19
Background on Ponericins	19
Materials and Methods.....	22
Peptide Preparation	22
Lipid Preparation	22
Fluorescence Spectroscopy	23
Binding Experiments	24
Red-Edge Excitation Spectroscopy.....	24
TCE Quenching	24
Acrylamide Quenching	25
Circular Dichroism Spectroscopy	25

Table of Contents (Continued)

Minimum Inhibitory Concentration (MIC)/Minimum Bactericidal Concentration (MBC).....	25
Bacterial Inner Membrane Permeabilization Assay	26
Bacterial Outer Membrane Permeabilization Assay.....	27
Hemolysis	28
Results.....	29
Peptides	29
Antimicrobial Activity	29
Solution Aggregation Properties.....	30
Peptide-Lipid Interactions.....	33
Peptide Secondary Structure	40
Membrane Permeabilization	42
Discussion.....	48
Effects of Hydrophobic Substituents	48
Chapter 3: Effect of Charge and Hydrophobicity in Antimicrobial Polymethacrylates	53
Antimicrobial Polymers	53
Polymethacrylates	53
Indole Polymers	55
Materials and Methods.....	59
Preparation of Polymethacrylates	59
Lipid Preparation	59
Binding Experiments	59
Acrylamide Quenching	60
10-DN Quenching.....	60

Table of Contents (Continued)

Inner and Outer Membrane Permeabilization.....	60
Hemolysis	61
Results.....	61
Lipid Interactions	62
Membrane Permeabilization	67
10-DN Quenching	73
Discussion.....	75
Chapter 4: Conclusions.....	77
L1 Ponericin Data	77
Polymethacrylate Data	78
References.....	79

List of Figures

Figure	Page
Figure 1. Peptide Sequences and Helical Wheel Diagrams	21
Figure 2. Peptide Solution Assays	32
Figure 3. Binding to Lipid Vesicles	35
Figure 4. Normalized Trp Emission Spectra.....	36
Figure 5. Acrylamide Quenching.....	39
Figure 6. Circular Dichroism (CD) Spectrum.....	41
Figure 7. Membrane Permeabilization of <i>E. coli</i>	43
Figure 8. <i>E. coli</i> Outer Membrane Permeabilization Assay	44
Figure 9. <i>E. coli</i> Inner Membrane Permeabilization Assay	45
Figure 10. Hemolysis of Human Red Blood Cells (RBCs)	47
Figure 11. iTasser Structures	51
Figure 12. MMA & PMMA.....	54
Figure 13. Polymethacrylate Structures	58
Figure 14. Binding to Lipid Vesicles	62
Figure 15. Normalized Barycenter Shifts	63
Figure 16. Acrylamide Quenching.....	66
Figure 17. Membrane Permeabilization of <i>E. coli</i>	68
Figure 18. <i>E. coli</i> Outer Membrane Permeabilization Assay	69
Figure 19. <i>E. coli</i> Inner Membrane Permeabilization Assay	70
Figure 20. Hemolysis.....	72
Figure 21. 10-DN Quenching	74

List of Tables

Table	Page
Table 1. Minimum Inhibitory Concentration (MIC) and Minimum Bactericidal Concentration (MBC)	30
Table 2. TCE Quenching	33
Table 3. Fluorescence Quenching	38
Table 4. Fluorescence Quenching	66

Chapter 1

Antimicrobials and a Need for Alternatives

History of Antimicrobials

Antibiotics are a major line of defense against infectious bacteria, a progression in the development of antibiotics has allowed for significant progress in medical practices [1]. Alexander Fleming was known for the discovery of penicillin, and the impact it had on the field of medicine. Although the revolutionary nature of penicillin, it was not until 1943 that penicillin was mass produced and used commercially [2]. This was because the stability of the compound and the science that was available made it tougher than expected to purify this compound. Penicillin encompassed Paul Ehrlich's idea of the "magic bullet", which is the idea that a drug selectively targets a disease-causing microbe and not the host themselves. However, the unexpected problem of the purification almost led to the extinction to this concept until 1930 when the development of sulfa drugs became prevalent. A compound that was derived from oil dyes by the name of sulfamidochrysoidine or commonly referred to as prontosil. This was discovered to have limited success with its bacteriologic activity in animals but not invitro. This was resolved in 1935, when it was elucidated that sulfanilamide was the primary active compound within prontosil. This discovery not only led to a Nobel prize in 1939 but revived the search for the perfect "magic bullet" [3]. From 1944 to 1972 deaths caused from bacterial infection had decreased and a new life expectancy had jumped by eight years. This era is now referred to the golden age of antibiotics [4].

Traditional Antibiotics

Drug-target interactions are the mechanisms of a drug that occur during the interaction with the intended target. Four most common antibiotic target mechanisms are the inhibitions of DNA, RNA, cell wall, and protein syntheses. Quinolones inhibit chromosomal topology that is essential for the synthesis of DNA, mRNA transcription, and cell division. Quinolone antimicrobial agents target one of two enzymes more efficiently depending on the type of bacteria. Topo IV is the target in Gram-positive bacteria; however DNA gyrases are the target in Gram-negative [5-8]. RNA synthesis is another quintessential part of every cell. Antibiotics that inhibit this synthesis have a selectivity to target RNAP or RNA polymerase. This method of action permits a wide range of activity, specificity of the drug, and high efficacy. Four different classes that participate in this mechanism are rifamycin, sorangicin, streptolydigin, and myxopronin. Each class has a different binding site but have the same outcome of disrupting RNA synthesis [5,9,10]. Antibiotics also can affect the cell wall of a bacterial cell. Cell wall Biosynthesis Inhibitors (CBIs) are one of the most effective classes of antibiotics that are available. There are three stages of cell biogenesis that the antibiotics target to cause cell lysis. In the first stage or the cytoplasmic stage, an antibiotic like Fosfomycin will inhibit a specific enzyme to starve the bacteria cell. Tunicamycin will target the lipid II component of a cell, causing cell death from the second stage, the membrane associated stage. Beta-lactam antibiotics like penicillin are a classical example of an antimicrobial agent that targets proteins like the lactam binding protein to inhibit the third stage, extracytoplasmic stage. There are a wide range of activities for CBI's which lead to lytic or non-lytic death [11]. Antibiotics also have the capability to inhibit protein synthesis

and is the broadest of classes of antibiotics. 30s and 50s are two subclasses and refer to the ribonucleoprotein that organize the initiation phase for protein synthesis. A 30S inhibitors like aminoglycosides will bind tightly to the 30S subunit that will cause a misreading in mRNA, or like tetracycline will bind to 30S and prevent addition of amino acids containing tRNA. Protein synthesis inhibitors of the 50S subclass have a wider range of activities. These inhibitors can bind to the 50S subunit and inhibits the formation of peptide bonds. They can also, prevent peptide elongation via binding to the peptide exit tunnel. Lastly, an integral part of protein synthesis is the formation of the ribosomal complex that initiates the process of protein synthesis. The 50S subclass can affect the formation of this complex preventing the process [10,12].

Antibiotics with their wide range of activities do not affect different types of bacteria the same, some are more effective at killing Gram-positive than Gram-negative. Gram-negative bacteria have a thinner peptidoglycan layer as well as it resides between an outer membrane composed of lipopolysaccharides, proteins, and a plasma inner membrane. Gram-positive bacteria only have a doubly thick peptidoglycan and inner membrane. Penicillin affects Gram-positive more effectively because of its ability to disrupt the formation of peptidoglycan. This is because of the composition of cell wall for Gram-positive versus the composition of Gram-negative. The full exposure of the peptidoglycan layer leaves it prone to inhibition by penicillin. After this inhibition, the bacteria cell is fragile and more likely to burst, and because human cells do not contain a peptidoglycan layer it acts as a “magic bullet” and targets the bacteria specifically [13,14]. *Staphylococcus Aureus* is a Gram-positive bacterium that is selectively targeted by penicillin-like or beta lactam antibiotics.

Multidrug Resistance

A need for antibiotic alternatives has been strongly recognized since the 1960's as the rise of antimicrobial resistance accelerated. Some *S. Aureus* strains as well as other bacterial strains have the capability of avoiding imminent death by mediation from a gene that encodes β -lactamase. Once staphylococci gain exposure to the antibiotic, a gene will produce the β -lactamase and this enzyme then hydrolyses the β -lactam ring of penicillin. *S. Aureus* can also develop resistance to methicillin as well. Methicillin was introduced as an antibiotic to combat the penicillin resistant strains of *staphylococcus*. This antimicrobial agent is a semisynthetic derivative of penicillin. It is in a class of antibiotic called penicillinase-resistant-penicillin. Penicillinase refers to the enzyme β -lactamase, and the modifications made to penicillin as an attempt at a solution to this problem. The strain of *staphylococcus* that are resistant to methicillin is referred to as MRSA or Methicillin Resistant *Staphylococcus Aureus* and the mechanism of defense against the antibiotic is different. This strain has a gene called *mecA* which produces penicillin-binding protein 2a (PBP2). This type of protein is responsible for the cross-linking of peptidoglycan chains. Beta-lactam antibiotics have a poor affinity for binding to PBP2a, this allows MRSA to survive even at high concentrations [14,15].

Multidrug Resistance (MDR) much like the notorious case of *S. aureus* is a threat especially in clinical settings. MDR occurs when the active concentration of a drug is insufficient in killing the bacteria. This can happen by an accumulation of resistant plasmids or transposons that encode the resistance of specific antimicrobial agents. Bacteria can also use energy-dependent efflux pumps to impair the accessibility to the target [17,18]. In a clinical setting, nosocomial infections are a concern when considering

multidrug resistance. Nosocomial infections and MDR for over a century have caused a burden on the healthcare system, particularly in the intensive care unit (ICU). ICUs have extensive antimicrobial usage which may promote an emergence of MDR. This coupled with a patient having a compromised immune system can cause life-threatening situations [19]. To put this in perspective, the World Health Organization (WHO) reported an estimated 480 thousand new cases of a Multidrug Resistant Tuberculosis (MDR-TB) that occurred in 2014. Of the 480 thousand cases, 190 thousand patients died proving MDR-TB to pose a threat to control worldwide [20].

Non-typhoidal Salmonella (NTS) are infections caused by all serotypes of *Salmonella enterica* with the exception of serovars Typhi and Paratyphi. Fluoroquinolones drugs are a common choice for treating gastrointestinal infections, for example NTS infections. However, several studies have shown that NTS have a decreased susceptibility to this treatment. According to data reported by WHO, fluoroquinolone resistance in NTS are high in some countries of Africa (30%-35%), of Eastern Mediterranean region (46%-49%) and in Peru (96%) yet relatively low in the European region [125]. These problems highlight the need for the development of new antibiotics, ideally with low potential for resistance.

Although MDR has a large impact and is life threatening or clinical environments, there are approaches to combat this problem. One of the common approaches is the use of a combination of antimicrobial agents. This can result in an antibiotic-antibiotic combination, or an antibiotic-non antibiotic adjuvant molecules to inhibit the B-lactamase enzyme. This approach can also use two components that will indirectly affect the bacterial resistance by interfering with the signaling pathway [21]. Macromolecular

approaches to eradicate the clinical problems of multidrug resistance are also common. Synthetic cationic polymers have shown to be useful, one of the most beneficial characteristics is the ability to reuse polymers without leading to antimicrobial resistance [22]. A renewed interest in western medicine is the approach of phage therapy. This approach uses virulent phages that act as parasites performing lytic cycles on the bacteria. The mode of action for phages are highly selective, however complex difficulties led to slow development [23,24]. Metal-based Antimicrobials (MBAs) have also shown to be an effective approach against AMR. Metal ions are known to be toxic to bacteria, and transition metals in the D-block have been gaining increasing amount of attention for this approach. Metals exhibit cytotoxic effects and have seemingly endless complex formations, and with their electron deficiency metals readily interact with electron-rich biomolecules [25,26].

History of Antimicrobial Peptides

In 1939 substances under the class of gramicidin were isolated from the *bacillus brevis*. This peptide falls under a broad class of antimicrobials called antimicrobial peptides (AMPs). This AMP has a wide range of antimicrobial activity against Gram-positive bacteria. Antimicrobial peptides are used in organisms as a defensive or offensive mechanism in nature. The difference between a small molecule antibiotic and an AMP is that an AMP does not rely on an enzymatic mechanism leading to cell death. A common well accepted mechanism of an AMP targets the envelope of the bacterium and not proteins or other compounds in the biosynthesis processes [27,28]. Targeting an integral part of cell structure is a core reason for diminished antimicrobial resistance. It was also elucidated in a recent investigation that the pharmacodynamics of peptides may

also have a part to play [29]. Antimicrobial peptides consist of a sequence of amino acids that can vary in length and a variation of different amino acid residues. There is a class of AMPs derived from the secretions of an Indian native frog called Tigerinins. This class of peptide is one of the smallest sequences, and the smallest represented of the antimicrobial peptides derived from amphibians. This class of peptide is a short sequence only containing 11-12 amino acids. Reported in a study done in 2001 it has shown to have antimicrobial activity against a broad spectrum of bacteria Gram-positive and Gram-negative [30]. Large amino acid sequences are also effective at causing cell death. The range in length for AMPs can be around 12-50 amino acid residues. A recent review was done in 2019 comparing different antimicrobial peptides derived from multiple sources. This review described LL-37, an antimicrobial peptide that has 37 amino acids with two leucine residues at the N-terminus with traditional antimicrobial activity against Gram-positive and Gram-negative bacteria [31].

Isolating antimicrobial peptides from mammals and other organisms is not an unusual practice in present day. AMPs have been isolated from vertebrates, invertebrates, plants, and even fungi. In animals AMPs are commonly found in the tissues and organs that are easily exposed to airborne pathogens, these AMPs act as a first line of defense. The progression into studies done on host defense peptides (HDPs) started in 1956 when the first animal host defense peptide was isolated from rabbit leukocytes. This discovery led to a rapid expansion into the field of antimicrobial peptides. Host defense peptides do as the name suggests and work directly as an antimicrobial agent, or in immune signaling, and in some cases work in both fashions. Defensins are an HDP were identified in the early 1980's. They were described as cationic, and cysteine rich components residing in

mammal neutrophil phagocytes. More than 5,000 naturally occurring AMPs were discovered or synthesized as of 2013 [32,33] and as of 2016 there were over 23,000 AMPs that were discovered [34]. As technology improves, more and more computer assisted simulations can predict valid peptide structures for antimicrobial activity [35].

Structures and Characteristics of Antimicrobial Peptides

As briefly mentioned, antimicrobial peptides have a range in length typically between 11-50 amino acids. These sequences are amphipathic and vary in hydrophobic and cationic amino acids. Due to these characteristics and a positive net charge AMPs have shown strong activities against bacteria. However, these activities are not limited to just bacteria and can affect a broad spectrum of organisms. AMPs have shown antiviral activity [36], antifungal activity [37], perturb protozoan homeostasis in parasites [38], and can even cause apoptosis in cancer cells [39]. These activities are largely impacted by the sequence and structure of the antimicrobial peptide.

AMPs can be characterized by their secondary structure. These secondary structures can be characterized into 4 classifications including: α -helix, β -sheet, loop structure, and extended structures. Using peptide backbone torsion angles as an alternative to structural classification will show many different AMP folds [40]. AMPs that are classified as an α -helical structure are usually amphipathic and cationic. Helical peptides are the most widely distributed with a level of hydrophobicity and the broadest spectrum of activity [40]. β -sheet AMPs are characterized by a disulfide bond between at least two β -strands. These structures are more complicated, and the degrees of β -sheet can be extremely different between peptide sequences [31,41,42]. Antimicrobial peptide secondary structures are still considered poorly understood. Most will belong to the four

mentioned classifications however, in some cases AMPs can belong to neither of those classifications [40].

Experimental and theoretical data have shown that most AMPs are either partially or fully disordered in solution [43-45]. Some AMPs are unstructured in solution. However, AMPs have the ability to adopt an active secondary structure due to the hydrophobic and hydrophilic regions being in energetically favorable positions upon interaction with lipid membranes [46-49]. The formation of an α -helical secondary structure allows peptide bonds to form hydrogen bonds that will reduce the energetic cost of transfer. β -sheet induced secondary structures often display discrete cationic and hydrophobic patches [50]. AMP amphiphilicity is promoted through a steep decrease in polarity across the membrane and align peptide with the interface gradient. This results in an interface-partitioned AMP that is orientated with hydrophobic residues directed toward non-polar region of the bilayer and cationic residues remain close to the charged and zwitterionic head groups [51]. Due to the poor understanding of the active secondary structure, the underlying issue that if it is necessary to form this structure for disruption of bacterial membranes can be viewed as controversial.

Mechanism of Action of Antimicrobial Peptides

Since the discovery of AMPs the mode of action (MOA) has been extensively studied to be used as a therapeutic agent at full potential. It was previously thought that the only MOA of AMPs was membrane targeting. However, as understanding MOA progresses there is increasing evidence that there are several mechanisms [52]. The two major classes are direct killing or immune modulation. It was briefly mentioned that AMPs target the envelope however, they can also act like traditional antibiotics and target

DNA, RNA synthesis as well as target other specific molecules in the cell [53,54]. The Multi-hit mechanism upon interactions with a bacterial cell increases the efficiency of antimicrobial peptides [55].

AMPs adopt an active secondary structure upon interaction with the bacterial cell membrane. Amphiphilic peptides show their nature upon interaction by folding into amphipathic α -helices with hydrophobic and hydrophilic faces when adsorbed into lipid membrane. The initial interactions occur because of electrostatic interactions. The positively charged AMP interacts with the negatively charged cell membrane and undergo both adsorption and a conformational change [56]. AMPs generally show selectivity with non-hemolytic activity well above their Minimum Inhibitory Concentration. Magainin 2 a peptide that is derived from the skin of an African claw frog *Xenopus laevis* inhibits growth of bacteria at 2-50uM. However, the concentration that causes hemolysis in human erythrocytes is as high as 1000uM [57,58]. The main factor in an AMPs ability to selectively target a bacterial cell opposed to a host cell can be attributed to the cationic property and the composition of membrane for bacteria. Bacteria cell membranes are rich in phosphatidylglycerol and cardiolipins. The cell walls also contain anionic lipopolysaccharides making them susceptible to being targeted by AMPs. Mammalian cells lack this anionic surface charge however, this isn't the only reason for the prevention of AMP interaction. Mammalian cells contain a molecule called cholesterol that has membrane stabilizing characteristics and helps protect attack against AMPs [59,60].

It is difficult to elucidate a full understanding of the mechanism of action for AMPs, due to the scale of observation and myriad of pathways that AMPs can take to

disrupt a bacterial cell membrane. The four significant models that have been described are barrel-stave model, toroidal pore model, carpet model and the detergent like model. In the barrel-stave model peptides are initially oriented parallel to the membrane and eventually insert themselves perpendicularly which promotes lateral peptide-peptide interactions. These interactions act in a similar fashion to that of protein ion channels and for this model an amphipathic peptide structure is crucial. This allows for the hydrophobic region of the peptide to interact with the membrane and the hydrophilic regions to form the lumens of the channel. Similarly, the toroidal pore model will insert itself perpendicularly. The difference between the models is that the arrangement of hydrophobic and hydrophilic lipid portions is maintained and in a toroidal pore model they are disrupted. In this model there are alternate surfaces for the head or tail groups to interact with and adds ion selectivity and a discrete size. Pore formation is not the only model that can designate a pathway to membrane disruption. In the carpet model the peptides are adsorbed in a parallel manner to form a “carpet” to cover the surface, which then leads to unfavorable reactions. The carpet model can produce interactions to disrupt the membrane with a detergent like effect disintegrating the membrane by forming micelles. The final collapse that comes from carpet model can be explained by the detergent-like model or a pore forming model. However, it does not require specific peptide-peptide interactions, it also does not require the peptide to bury itself into the hydrophobic core to form a channel, nor does it need the formation of specific peptide structures [61-65].

Physiochemical Properties of Antimicrobial Peptides

It is relatively easy to perform modifications to AMP sequences to help modify activity and target spectrum, as well as aid in stabilization and bioavailability [65,66]. The modifications that can be done physiologically to affect antimicrobial activity and target specificity are size, net charge, hydrophobicity, amphipathicity, and solubility [67]. Length is an important property and can be crucial to biological activity. Due to an entropic balance, short peptide sequences are less likely to form regular secondary structures. Longer sequences can overcome this with energetically favorable facial properties [68]. Length can also contribute to different 3D structures; however, it also has the possibility of increasing cytotoxicity. An investigation published in 2006 was done to elucidate possible effects when increasing chain length. Simple sequence repeats, $(RW)_n$ (where n equals 1,2,3,4, or 5) were used to investigate a possible role of sequence length by comparing the antimicrobial activity as well as hemolytic activity. The conclusion was that for this sequence that the optimal length was at n equals 3. As the length increased so did antimicrobial and hemolytic behaviors. Although results were similar for $n = 3,4$, or 5 the sequence where n equals 3 is the best choice for efficiency in synthesis [69]. When designing synthetic AMPs, it is important to consider length in a manner of a cost and time effective product as well.

The net charge is determined by the summation of ionizable groups in the peptide. Majority of cationic AMPs (CAMPs) have two unique features one of the being a positive net charge of at least +2 and the other is an amphipathic character. It is theorized that the net positive charge is the main cause for the initial interaction due the bacterial membrane being negatively charged. It has been elucidated from a study that the net

charge of an AMP impacts the antimicrobial activity as well as hemolytic activity. A study was done using an established AMP named L-V13K which is a 26 amino acid that adopts an α -helical structure in a hydrophobic environment and has a hydrophilic positively charged lysine residue at the center. The V13K analogs had a net charge that ranged from -5 to +10. In the study it was observed that lowering the net charge to $<+4$ rendered the peptide completely inactive, while systematically increasing the charge from +4 to +8 increased the overall antimicrobial activity while sustaining low hemolytic activity. However, an increase to +9 and +10 increased antimicrobial activity as well as unwanted hemolytic activity [70].

Hydrophobic residues that reside within a given AMP have also shown to have influence over antimicrobial activity and hemolytic activity. Natural AMPs exist with a broad range of hydrophobicity and charge, commonly natural AMP sequences contain 40-60% hydrophobic residues with a +4 to +6 charge [71]. The cationic nature contributes to the initial interaction with a negatively charged bacterial cell membrane, where the hydrophobic components facilitate partitioning into the membrane. Studies have shown that the hydrophobicity of an AMP has a more complex nature to the interactions of the cell membrane. For example, data provided by a study done on an AMP called C18G, when the phenyl alanine residues are replaced by less hydrophobic leucine residues it drove antimicrobial activity and cytotoxicity. One possible solution presented from the paper was that the physical orientation of the side chains could also play an important role in activity as well. The side chains of the hydrophobic residues could part take in a phenomenon similar to that of cationic side chains that exhibit “snorkeling” or extending out of the non-polar core of the bilayer. Although this was an

interesting result of the study, It was also displayed that when the AMP dropped below a threshold of hydrophobicity will contribute to the reduction of membrane binding, membrane activity, and antimicrobial activity [72].

Amphipathicity is a result of having both hydrophilic and hydrophobic properties. This property is important because it ensures that there will be an initial interaction and activity with selectivity. A study done on cecropins, a family of AMPs that have an amphipathic N-terminal domain and a hydrophobic C- terminal domain. It was evident that a substitution of proline residues in the N-terminus significantly reduced antimicrobial activity, highlighting the importance of an amphipathic α -helix [73,74].

The solubility of an AMP is vital for an initial interaction between the AMP and the bacterial cell membrane. A lack of solubility can cause inappropriate aggregation leading to a reduction of the membrane permeabilization effects [75]. Despite this potential flaw there are some methods to improve solubility of peptides in aqueous solutions. It is not uncommon to synthesize “hybrid” or “chimeric”, which combines AMPs or fragments of AMPs to improve properties. Polyethylene glycol moieties although not extensively explored, are commonly attached to AMPs to increase solubility. Not only does it increase solubility but improves pharmacokinetics, and half-lives [76,77].

Venom-Derived Antimicrobial Peptides

Natural AMPs are diverse which causes difficulties in classification. AMPs can be classified on activity, structural characteristics, amino acid- rich species, and on source of the peptide [45]. Venom derived peptides have been a focus of studies and

modifications and can be a valid example of an AMP being classified by source. Venoms are complexed mixtures comprised of various enzymes and protein of different sizes that serve as a defense against microbes. Peptides are a major component in venoms and are capable but not required to be biologically active [78]. The peptides that do exhibit biological activity can do so in a myriad of ways. This activity includes membrane permeabilization, neurotoxins, and even GPCR agonist and antagonists [79]. With a Small size, acute specificity, significant structural stability these biologically active peptides are also relatively easy to synthesize making them ideal components for novel antimicrobial agents [80].

Venoms can be classified into their mode of action and their effect. These include: Neurotoxins, cardiotoxins, hemotoxin, and cytotoxin. Neurotoxins can inhibit nicotinic acetylcholine receptors (nAChRs) and interfere with nerve transmission [115] These toxins can also inhibit ion movement through cellular membrane blocking the movement of neurons. Cardiotoxins bind to the cells of the heart and block muscle contraction which generally affect the heart muscle. Hemotoxins cause the destruction of red blood cells which primarily affect the circulatory system, blood function, and muscle tissue. Lastly, one of the most researched components of venoms are cytotoxins. Cytotoxins can affect the cell membrane, interfere with the transportation of substances, or even interfere with the transduction of signals across the membrane [116]

An increasing amount of studies have been done on membrane active peptides over the last 20 years. AMPs fall into one of the two classes of membrane peptides, and the other are cell penetrating peptides (CPP's) [117]. A well known example of a membrane active AMP is a peptide derived from honey bee venom called melittin.

Melittin is a lytic peptide that binds to the membrane surface followed by insertion at threshold levels of bound peptide. This AMP can bind to membranes in milliseconds and adopts an amphipathic α -helical structure oriented either parallel or perpendicular to the plane of the membrane [118]. As the membrane active peptide melittin gained interest it has been shown to have anticancer activity [119], antifungal activities [120], antiviral [121], and not only antibacterial but in some cases specifically target drug resistive forms [122]. CPP's are short sequence peptides with a positive charge and facilitate penetration into the cell across the membrane [123]. CPPs like transportan, a chimeric peptide derived from wasp venom, can act as a cargo carrier as a potential drug delivery system [124].

Venoms like snake or spider venom are notorious for being toxic and deadly. However, the safety and pharmacodynamics are not the only issues with venom peptides. Peptides derived from venoms need to be sufficiently stable to avoid degradation, and these peptides go through Post Translational Modifications (PTMs) to achieve this stability. PTMs that are common are amidation (C-terminal), γ -carboxylation (Glu), hydroxylation (Pro), sulfation (Tyr), bromination (Trp), glycosylation (Thr), pyroglutamation, N-C-cyclization, and isomerization from into D-amino acids [80]. These modifications enhance peptide properties however for possible therapeutic applications may not be enough or optimal. Optimizing venom peptides as therapeutics comes with a list of issues including formulation, cost of production, stability, selectivity, and MOA.

One of the key weaknesses of venom peptides as potential therapeutic agents is their low bioavailability which can be attributed to their hydrophilic nature and even their

small size (10-50 amino acids) [81]. This weakness results in an unfavorable mode of administering the peptide, which is a site of injection. A previously discussed technique such as the development of chimeric peptides is often utilized as a possible method to overcome this issue but is not the only method. Another common method is to use N-alkylation of amino acids, typically N-Methylation is used to improve pharmacokinetics. Studies were done by N-methylating the cyclic peptide somatostatin. These studies elucidated that N-methylating at certain points of the peptide it increases the bioavailability by 10% [82]. Despite these issues that need to be addressed in further investigations, Venom-derived peptides hold valuable potential for being a model or a therapeutic agent.

Background on Antimicrobial Polymers

AMPs may be ancient weapons, evolving for millions of years and attacking bacterial membranes for quite some time, but they are not the only effective defense. Methacrylate random copolymers that can be classified as an AMP-mimetic polymers can inhibit the growth of Methicillin-resistant *S. aureus* (MRSA) and Vancomycin-resistant *S. aureus* (VRSA). Synthetic polymers can be used as an advantageous antibiotic that mimics an AMPs cationic amphiphilic structure while having diverse compositions, shapes, and architecture [83]. Due to this feature, polymers can be relatively easily synthesized to mimic AMPs and gain more insight into peptide SAR. Polymers have a myriad of advantages over peptides that include inexpensive to manufacture, easier to produce and alter chemically, and are more amendable in the integration of drug delivery systems [84]. These strengths and advantages may allow for the use of polymers to overcome the chemical limitations like bioavailability and oral

availability that prevent the use of AMPs in clinical settings. Many classes of AMP mimicking polymers exist already such as polynorbornenes, polycarbonates, polyalanines, and polymethacrylates. Also, these synthetic polymers can be chemically altered via facile route and obtain a broader range of chemical structures [85]. The ability to alter and manipulate to optimize activities is a favorable characteristic of both polymers and AMPs. Structure Activity Relationship (SAR) studies are relatively easy to perform to optimize these potential therapeutic agents.

Chapter 2

Investigation of the Role of Hydrphobic Amino Acids on The Structure-Activity Relationship in Ponericin L1 from *Neoponera Goeldii*

Background to Ponericins

Neoponera, a ponerine ant genus is comprised of 57 species of ant composed of very diverse morphology and behavior. This diverse genus ranges from southern Texas and northern Mexico to southern Brazil and northern Argentina. Within the ponerine ant genus, the *Neoponera* can be considered a cryptic species complex, this is defined as two or more species being classified as a single nominal species due to being superficially morphologically indistinguishable. This includes sympatric species and species with a wide distribution [86,87]. A predatory ant in the subfamily Ponerinae, called *Neoponera Goeldii* (previously misclassified as *Pachycondyla Goeldii*) has been previously studied for the antimicrobial activities the peptides that reside in the venom exude [88].

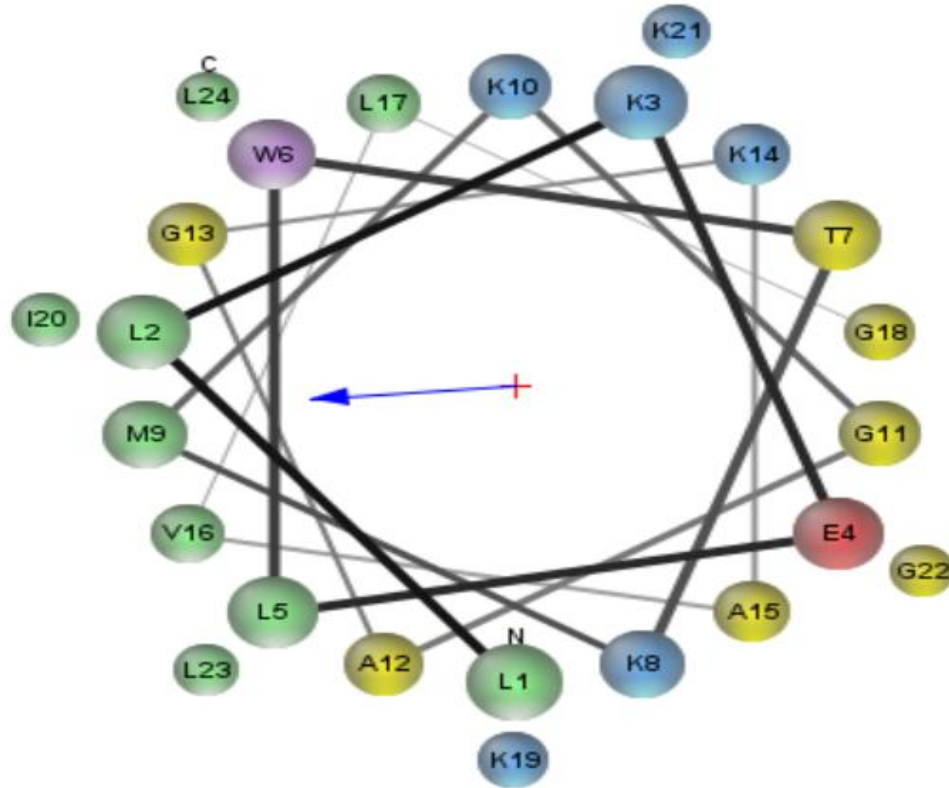
The AMPs that are isolated from the venom of this ant are called Ponericins. There are fifteen novel peptides that have been extracted that display antibacterial and insecticidal activities. Of the fifteen peptides all contain cationic, amphiphilic sequences. Only twelve of the peptides contain a Trp residue in the N-terminal region. There are three classifications that a ponericin peptide can belong too: G, W, or L. Each class shares high sequence relationships with different known existing AMPs; Ponericins belonging to the G classification show similarities with cecropin-like peptides, W with gaegurins and melittin, and finally L sharing similarities with the natural polycationic peptides dermaseptins [88].

The G family has seven of the fifteen novel peptides and has more than half of its sequence in common with cecropins. Cecropins have activity against Gram-negative and Gram-positive bacteria cells. These AMPs can also inhibit the uptake of proline, as well as cause leaky membranes. Ponericins in the W family make up another large portion of the fifteen novel peptides. This family has spectrum of activity against yeast, bacteria but also show hemolytic activity. In most sequences for both G and W families there is a proline residue near the middle of the sequence (11/13). In cell membranes ponericins naturally adopt α - helix structure [89].

The L family is the smallest and the most poorly understood of the ponericins. This family consist of two peptide sequences (L1 and L2) each with similarities to peptides derived from amphibians called dermaseptins. These peptides have had little recognition, only two papers report the activities and characteristics one of which being the original report by Orivel *et al.*. This reported only on the L2 peptide, which elucidated that ponericin L2 had a broad-spectrum of activity with no hemolytic activity. Ponericin L1 was reported in a recent study and had shown that this peptide adopts an α -helical confirmation, has enhanced binding to lipid vesicles with anionic lipids and little to no hemolytic activity. This study also had shown SARs that displayed the significance that net charge and group identity had on antimicrobial activity [90]. Ponericin L1 and L2 have identical sequences except for a single amino acid at position 9, where L1 contains a Met and L2 has an Ile. Although the recent study elucidated information on ponericin L1, there still is a general lack of understanding when it comes to the L-family of ponericins.

Figure 1

Peptide Sequences and Helical Wheel Diagrams



Peptide sequences, nomenclature, and properties				
Name	Sequence	Net Charge	M.W calculated	M.W Found
L1	LLKELWTKMKGAGKAVLGKIKGLL	5+	2596	2595.4
L1V	VVKEVWTKMKGAGKAVVGKVKGVV	5+	2498	2497.4
L1I	IIKEIWTMKGAGKAIIGKIKGII	5+	2610	2608.6
L1L	LLKELWTKMKGAGKALLGKLGKLL	5+	2610	2609.2
L1A	AAKEAWTKMKGAGKAAAGKAKGAA	5+	2274	2273.5
L1F	FFKEFWTKMKGAGKAFKFKGFF	5+	2883	2881.2

Note. Helical wheel diagram of L1, L1V, L1I, L1L, L1A, and L1F. Cationic residues are shown in blue, anionic in red, hydrophobic in green, polar uncharged in yellow, and aromatic are in purple. Peptide sequences and relevant properties are shown below the helical wheel. Helical wheel representations were made using MPEX [91].

Materials and Methods

Peptide Preparation

Peptide variants L1A and L1F were synthesized using standard FMOC-chemistry in-house. The parent peptide L1 along with L1-V, L1-I, and L1-L were purchased from Synthetic Proteomics (Carlsbad, California). Using a Zorbax C3 column, all peptides were purified via RP-HPLC eluted by a linear gradient of water to acetonitrile (both supplemented with 0.1% TFA). Peptide identity was confirmed using MALDI-TOF mass spectrometry. HPLC fractions containing the peptide were collected, pooled, lyophilized, and stored at -20 C. Peptides were dissolved in H₂O:ethanol 3:1 prior to use. Each peptide stock was made to a final concentration of 150 -200 μM then stored at 4 C.

Lipid Preparation

Lipids 1,2-dioleoyl-sn-glycero-3-phosphocholine (DOPC; PC), 1,2-dioleoyl-sn-glycero-3-phospho-(10-*rac*-glycerol) (DOPG; PG), and 1-palmitoyl-2-oleoyl-sn-glycero-3-phosphoethanolamine (POPE; PE) were purchased from Avanti Polar Lipids (Alabaster, Alabama), and stored as stocks in chloroform at -20 C. Lipids were prepared as 100% DOPC, 3:1 DOPC:Cholesterol (PC:Chol), 3:1 DOPC:DOPG (PC:PG), or 3:1 POPE:DOPG (PE:PG). Isopropyl β-D-1-thiogalactopyranoside (IPTG) (Chem-Impex Int'l INC.), ortho-nitrophenyl-β-galactoside (ONPG) (Research Products International Co.), nitrocefin (Biovision, Milpitas, California). All other chemicals and reagents were from Thermo Fisher Scientific (Waltham, Massachusetts), VWR (Radnor, Pennsylvania), or Sigma-Aldrich (St. Louis, Missouri).

To form small unilamellar vesicles (SUVs) sonication or ethanol dilution methods were implemented [92]. In all cases, lipid vesicle preparation was the same. Depending on the lipid composition, appropriate volumes of lipids in chloroform were mixed in a glass tube and then allowed to dry under N₂ gas for 15 minutes. The lipid films were then placed in a vacuum desiccator and allowed to dry further under a vacuum for 1 hour. For vesicles formed through ethanol dilution methods, 10 µL of pure ethanol was added to the film, and then vortex until the dissipation of the film. While continuing to vortex, the appropriate amount of PBS was added. For vesicles formed using the method of sonication, PBS was added directly to the tube while being vortexed to create multilamellar vesicles (MLVs). The MLV suspension was covered with parafilm and then placed in a high-powered bath sonicator (Avanti Lipids) and subjected to sonication for 20 minutes to create SUVs.

Fluorescence Spectroscopy

All fluorescence spectroscopy experiments were performed using a JY-Horiba Fluoromax4 instrument. Excitation and emission slit widths were kept consistent at 2.5 nm. Semi-micro quartz cuvettes were utilized for each experiment. The following formula was used to calculate a spectral barycenter for each experiment:

$$B = \frac{\sum \lambda * i}{\sum i}$$

where B is the barycenter, λ is the wavelength, and i is the intensity at the specified wavelength. An entire emission spectrum from 300-400 was used to carry out the calculation of barycenter.

Binding Experiments

Lipid binding protocols from previous experiments were used as a basis for the following reported data. Peptide samples were prepared at final concentration of 2 μ M in PBS buffer (150 mM NaCl, 50 mM Na₂HPO₄, pH 7.0) and titrated with lipid vesicle stock (usually [1.0] mM total lipid). The standard for all binding assays is $\lambda_{\text{ex}} = 280$ nm and $\lambda_{\text{em}} = 300$ to 400 nm. A sample containing only PBS and no peptide was used as a background to correct spectra after each addition of vesicles.

Red-Edge Excitation Spectroscopy

Red edge excitation shift (REES) experiments utilized excitation at 6 different wavelengths ($\lambda_{\text{ex}} = 280, 290, 295, 300, 305, \text{ and } 307$ nm) and the same emission range of 310 to 410 nm. Samples were similarly prepared as above. A blank only containing PBS buffer was used as background to correct the spectra after each addition.

TCE Quenching

Trichloroethanol (TCE) quenching was monitored by titration of samples with 10 μ L aliquots of 10M TCE (Alfa Aesar, Haverhill, Massachusetts) into peptide samples prepared as described above. After each addition of TCE, Trp fluorescence intensity was measured using $\lambda_{\text{ex}} = 280$ nm and $\lambda_{\text{em}} = 340$. Corrections to the emission intensity were made for background subtraction and dilutions. The slope of the linear best fit equation to the data (eqn 2) was used as the Stern-Volmer quenching constant (K_{sv}).

2

$$\frac{F_0}{F} = 1 + K_{sv}[Q]$$

where F_0 is the fluorescence intensity in the absence of quencher, and F is the fluorescence intensity in the presence of a given concentration of quencher $[Q]$.

Acrylamide Quenching

Acrylamide quenching was monitored by titration of samples with 10 μ L aliquots of 4M acrylamide titrated into peptide samples prepared as described above. These samples contained either [0] or [0.25] mM total lipid. After each addition of acrylamide, Trp fluorescence intensity was measured using $\lambda_{ex} = 295$ nm and $\lambda_{em} = 340$. Corrections to the emission intensity were made for background subtraction, dilutions, and inner filter effects in the excitation path as described previously. The same method to calculate K_{sv} was used as above.

Circular Dichroism Spectroscopy

Circular Dichroism (CD) spectra were collected via Jasco J-810 spectropolarimeter. CD experiments with samples containing SUVs with 200 μ M total lipid and 3 μ M peptide in 0.1 x PBS buffer. Each measurement was an average of at least 64 scans and was corrected by subtracting background spectra that did not contain peptide.

Minimal Inhibitory Concentration(MIC)/Minimal Bactericidal Concentration(MBC)

Six different strains of bacteria were streaked on LB-Miller agar plates from a frozen glycerol stock derived from the original samples shipped from CGSC (Coli

Genetic Stock Center, Yale University) or ATCC (American Type Culture Collection) (*Escherichia coli* D31 CGSC 5165 , *Staphylococcus aureus* ATCC 35556. *Pseudomonas aeruginosa* PA-01 ATCC 47085, *Acinetobacter baumannii* ATCC 19606). For each of the strains a liquid overnight culture was prepared using a single colony into fresh LB broth and placed in a shaking incubator for ~ 18 hours at 37 C at 225 rpm. After the incubation period, a 1:200 dilution was made in fresh LB broth and then used for experimentation. Minimal Inhibitory Concentration (MIC) determinations were performed using mid-log phase bacteria diluted to 5×10^5 CFU/mL. Next, 90 μ L of this diluted culture was then pipetted into a sterile 96-well plate that contains serially diluted aliquots of the peptide variants to consist of a total volume of 100 μ L. This plate was then incubated for 18 hours at 37 C. Bacterial growth was determined by taking an OD₆₀₀ measurement using a Spectramax M5 multimode plate reader post incubation. Minimal Bactericidal Concentration (MBC) was performed by taking 1 μ L of the culture from the MIC plate and then pipetting it on to a fresh LB agar plate. After plating this culture, the plate was then incubated overnight at 37 C. MBC was determined by the growth or the lack of growth from each well on the agar plate.

Bacterial Inner Membrane Permeabilization Assay

A single colony of *E.coli* D31 was inoculated into LB broth and placed in a shaking incubator and set to 225 rpm at 37 C for ~ 18 hours. A 1:250 dilution was made using the overnight culture into fresh LB broth. To induce the expression the expression of β -galactocidase, A final concentration of 100mM of IPTG was introduced. This dilution plus the IPTG was placed back into the shaking incubator for about 2 hours until an OD₆₀₀ of 0.2-0.4 was achieved.

A 96 well plate was prepared with the following solutions in order: 10 μL of each peptide variant 2-fold serially diluted down the plate with the exception of the final row (used as a negative control 10 μL of 0.01% acetic acid), 56 μL Z-buffer (60mM Na_2HPO_4 , 40mM NaH_2PO_4 , 10mM KCl, 1mM MgSO_4 , 50mM β -mercaptoethanol pH 7), 19 μL of the *E.coli* culture, and 15 μL of 4 mg/ml ONPG that was prepared in Z-buffer added immediately before the assay began. Absorbance measurements were taken at 420 nm every 5 minutes for a total run time of 90 minutes. The detergent cetyltrimethylammonium bromide (CTAB) was used as a positive control. The data presented is an average of three replicates.

Bacterial Outer Membrane Permeabilization Assay

A single colony of *E.coli D31* was taken from an LB agar plate and inoculated into fresh LB broth with 100 $\mu\text{g}/\text{mL}$ ampicillin (LB-Amp), then place in a shaking incubator at 37 C (225 rpm) for ~ 18 hours. After the incubation period 100 μL was taken from the culture and diluted with 25 mL of fresh LB-Amp. The dilution was further incubated in the same conditions until an OD_{600} of 0.2 to 0.4 was obtained. Once the specified OD_{600} was reached the culture was then centrifuged at 2500 rpm for 15 minutes in a tabletop clinical centrifuge. The supernatant was discarded and then an equal amount of PBS (100 mM NaH_2PO_4 , 200 mM NaCl, pH7) was used to resuspend the pellet.

Experimental samples were prepared in a 96-well plate in the order as follows: 10 μL of the six peptide variants that were serially diluted starting a concentration of 15 μM with the exception of the last row (used as a negative control 10 μL of 0.01% acetic acid). 80 μL of the resuspended bacteria culture, and 10 μL of 50 $\mu\text{g}/\text{mL}$ nitrocefin in PBS. The absorbance was recorded at 486 nm in 5-minute intervals for a total run time of 90

minutes immediately following the addition of nitrocefin. The antimicrobial agent polymyxin B was used as a positive control. The values presented are the average of three replicates.

Hemolysis

Hemolysis on Sheep red blood cells (RBCs) was used to quantify the destabilization of membranes by leakage of hemoglobin. Sheep blood was obtained through Hemostat Laboratories and stored at 2 – 8 C. A 7 mL aliquot of whole sheep blood was mixed with 7 mL of sterile PBS at pH 7.4. The solution was sedimented via centrifugation for 7 minutes at 2500 rpm. Supernatant was removed and the pellet was resuspended to the original volume of 14 mL. This was repeated three times and the final pellet was resuspended to 14 with PBS. Next, 90 µl of the cell suspension was pipetted into all wells of a conical bottom 96-well plate. 10 µL of serially diluted peptide variant or the detergent TX-100 (positive control) were added to the wells prior to addition of the RBC's. The plate was covered and left in a shaking incubator at 37 C at 150 rpm for 1 hour. Post incubation the plate was then centrifuged for 10 minutes at 200 rpm at 4 C. 6 µL of the supernatant was added to 94 µl of fresh PBS in a flat bottom plate. The absorbance of the plate was taken at 415 nm using a Spectramax M5 multimode plate reader. By using the absorbance of each well compared to the wells without additive and those with Triton-X 100 a percentage of hemolysis was calculated. The data presented are the average of three replicates.

Results

Peptides

All peptides in this study were synthesized via solid-*phase* peptide synthesis approaches and purified by reversed-phase HPLC. The sequences used in this study and relevant physio-chemical properties are shown in Figure 1A. As the L1 peptide has previously been shown to adopt an α -helical conformation when bound to lipid bilayers, a helical wheel diagram of the parent L1 sequence is shown in Figure 1B.

Antimicrobial Activity

The ability of L1 and the hydrophobic variants to act as antimicrobials was investigated using the Minimal Inhibitory Concentration (MIC) and Minimal Bactericidal Concentration assays as previously described [96]. The MIC is determined as the lowest concentration of peptide required to inhibit bacterial growth in solution, while the MBC is the lowest concentration required to act in a bactericidal mechanism (as opposed to bacteriostatic) and is determined by plating MIC cultures on antimicrobial-free media. Peptides were screened against *E. coli*, *S. aureus*, *A. baumannii*, *P. aeruginosa*, *B. subtilis*, and *K. pneumoniae*. The results are shown in Table 1.

Table 1

Minimum Inhibitory Concentration (MIC) and Minimum Bactericidal Concentration (MBC)

	<i>S. aureus</i>		<i>E. coli</i>		<i>A. baumannii</i>		<i>P. aeruginosa</i>		<i>B. subtilis</i>		<i>K. pneumoniae</i>	
	MIC	MBC	MIC	MBC	MIC	MBC	MIC	MBC	MIC	MBC	MIC	MBC
L1	7.50	15	0.94	0.94	1.875	3.75	>15	>15	0.469	0.938	3.75	>15
L1V	>15	>15	>15	>15	>15	>15	>15	>15	>15	>15	>15	>15
L1I	15	15	0.469	3.75	1.875	1.875	>15	>15	0.469	0.469	7.5	7.5
L1L	1.875	3.75	0.469	0.938	0.938	0.938	15	>15	0.469	0.938	3.75	>15
L1A	>15	>15	>15	>15	>15	>15	>15	>15	>15	>15	>15	>15
L1F	0.938	1.875	0.938	>15	0.469	0.938	7.5	>15	1.875	1.875	1.875	7.5

Solution Aggregation Properties

Considering that the first step in the mechanism of action of many AMPs is the binding to the bacterial cell surface, any aggregation or oligomerization of peptides can impact the binding equilibrium. If amino acid substitutions promote the aggregated state, this will then reduce the amount of free peptide available to bind the bacteria and exert antimicrobial activity. This is especially relevant in reference to hydrophobic substitutions as hydrophobicity of a peptide is a significant driver of peptide aggregation in solution [93-95].

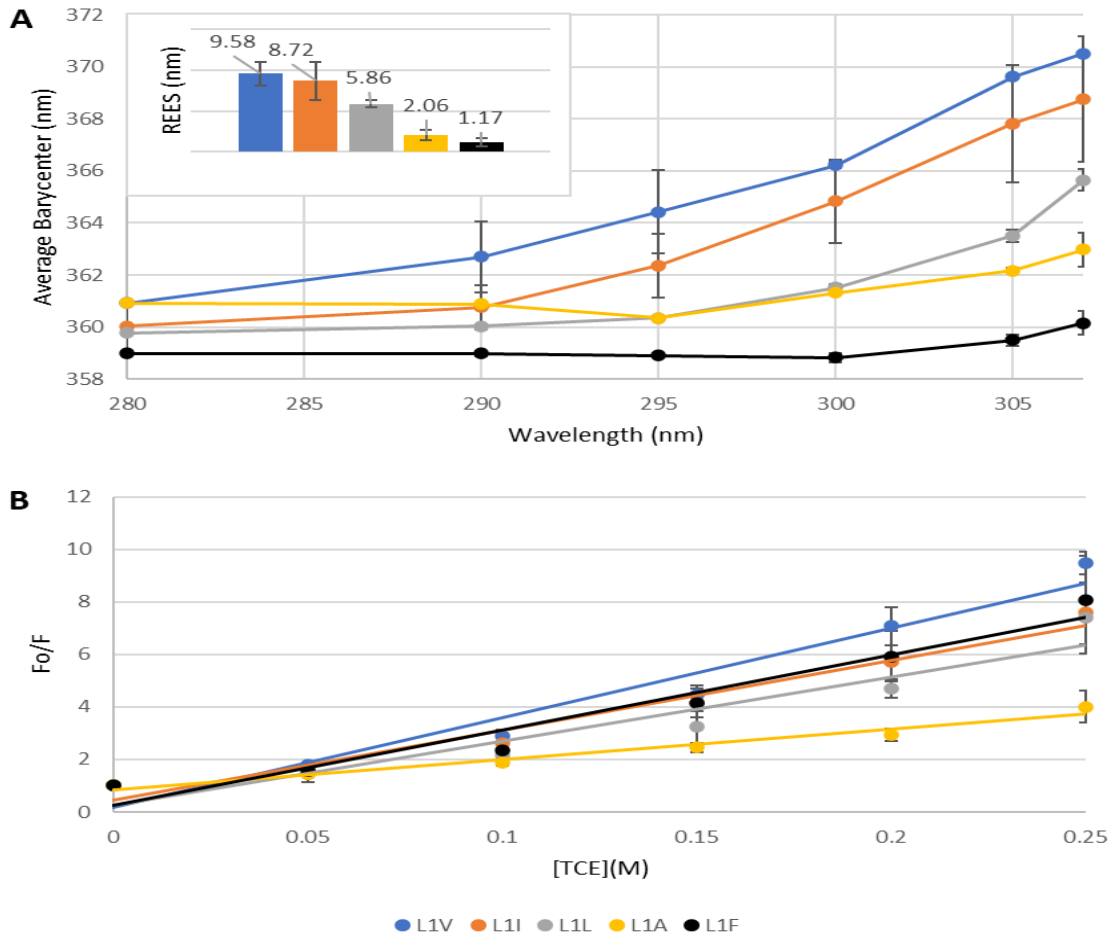
Aggregation of peptides was assessed utilizing the intrinsic fluorescence properties of the Trp residue in the L1 sequence. Since L1 contains a single Trp, this residue can serve as a reporter for a variety of peptide characteristics, most notably the environment that the Trp, and thus the peptide, is sampling. Differences in the side chain motion/dynamics of the Trp residue and the local environment around the Trp can be observed by

monitoring the red-edge excitation shifts (REES). This approach monitors shifts in the emission spectrum as a function of varying the excitation wavelength which is directly influenced by the mobility and solvent accessibility of the Trp side chain [96]. When a Trp is exposed to the aqueous milieu and is free to sample rotational conformations, no REES is exhibited, while if the Trp is constrained or shielded from bulk water REES is observed as the excitation wavelength is increased. The REES results are shown in Figure 2A. Notably, all peptides exhibited some degree of REES, with L1V exhibiting the strongest REES of ~10 nm. Conversely, the L1F peptide exhibited the least REES, only ~2 nm.

The environment of the L1 Trp residue was further probed using fluorescence quenching by trichloroethanol (TCE) which selectively exerts quenching on Trp residues which are shielded from the aqueous milieu, such as at the interior of a peptide aggregate. The results are shown in Figure 2B, with the K_{sv} values for the quenching shown in table 2. The majority of the peptides showed similar extent of quenching by TCE except the L1A variant. The Trp quenching in this peptide sample was markedly lower than the others. However, considering the reduced overall hydrophobicity of this peptide and thus higher aqueous solubility, decreased TCE quenching is not surprising. Importantly, the L1V showed the most quenching, consistent with the REES results.

Figure 2

Peptide Solution Assays



Note. (A) Red Edge Excitation shift (REES) and (B) Trichloroethanol (TCE) quenching. The inset column in panel A represents the total shift (nm) for each peptide. In both panels L1V is shown in Light blue, L1I orange, L1L grey, L1A yellow, and L1F black. Peptide concentration was 2 μ M in all samples. All data are averages of three replicates and SD is represented by error bars.

Table 2*TCE Quenching*

Sequence	Ksv[M-1]		
L1V	9.47	±	1.3
L1I	7.59	±	4.9
L1L	7.39	±	3.5
L1A	4.01	±	0.91
L1F	8.08	±	5

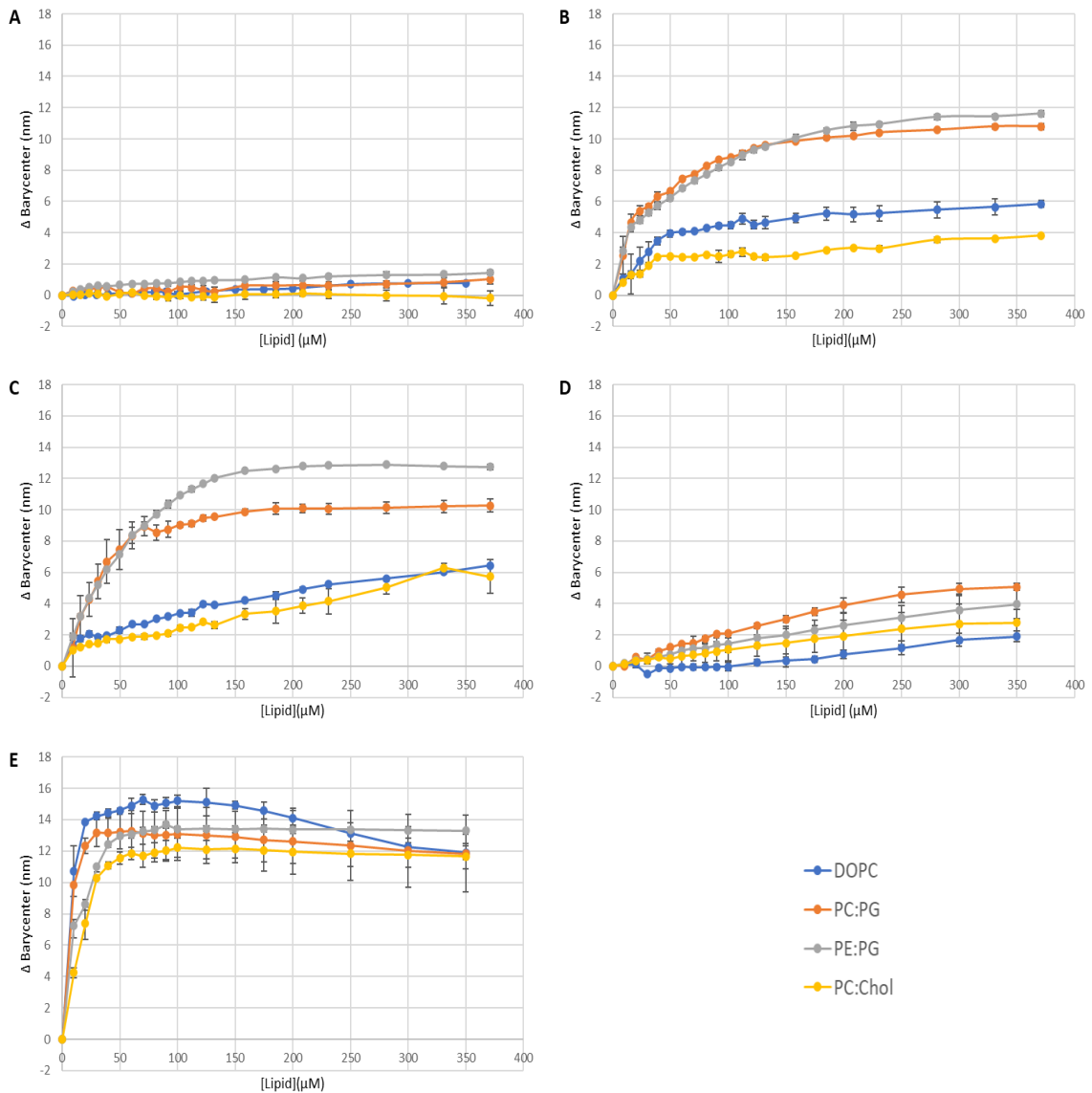
Peptide-Lipid Interactions

Considering that the first step in the mechanism of action of many AMPs is the binding to the bacterial cell surface, binding to model lipid vesicles was performed. These experiments exploited the inherent environmental sensitivity of Trp as a reporter for binding to bilayers. In aqueous solution, the Trp fluorescence exhibits a red shifted emission barycenter, while when bound to bilayers and thus in a more non-polar environment the Trp emission blue-shifts to lower wavelengths [97,98]. The impact of lipid composition on binding to model vesicles was investigated using a simple vesicle titration experiment in which Trp fluorescence was measured after addition of lipid vesicles. The change in the emission barycenter compared to that in absence of vesicles was plotted as a function of total lipid concentration (Figure 3). Lipid composition of vesicles was either 100% DOPC, 3:1 DOPC:DOPG, 3:1 POPE:DOPG, or 7:3 DOPC:Cholesterol. The results show varied behavior that is both peptide and lipid

composition dependent. The L1L and L1I variants show significantly larger shifts in Trp emission barycenter when binding PG-containing bilayers, indicating that electrostatic forces are a strong driver in the bilayer association of these peptides. In contrast, L1F, L1V, and L1A showed no significant preference for anionic vs. zwitterionic bilayers. However, only the L1F showed significant shifts in barycenter with the addition of lipid while L1A and L1V did not. The L1F results indicate that binding in this case is driven more strongly by hydrophobic interactions independent of the electrostatic contribution. The L1A and L1V results indicate little interaction with the bilayer, or perhaps only very shallow interactions with the surface of the bilayer which does not result in a significant environmental change around the Trp.

Figure 3

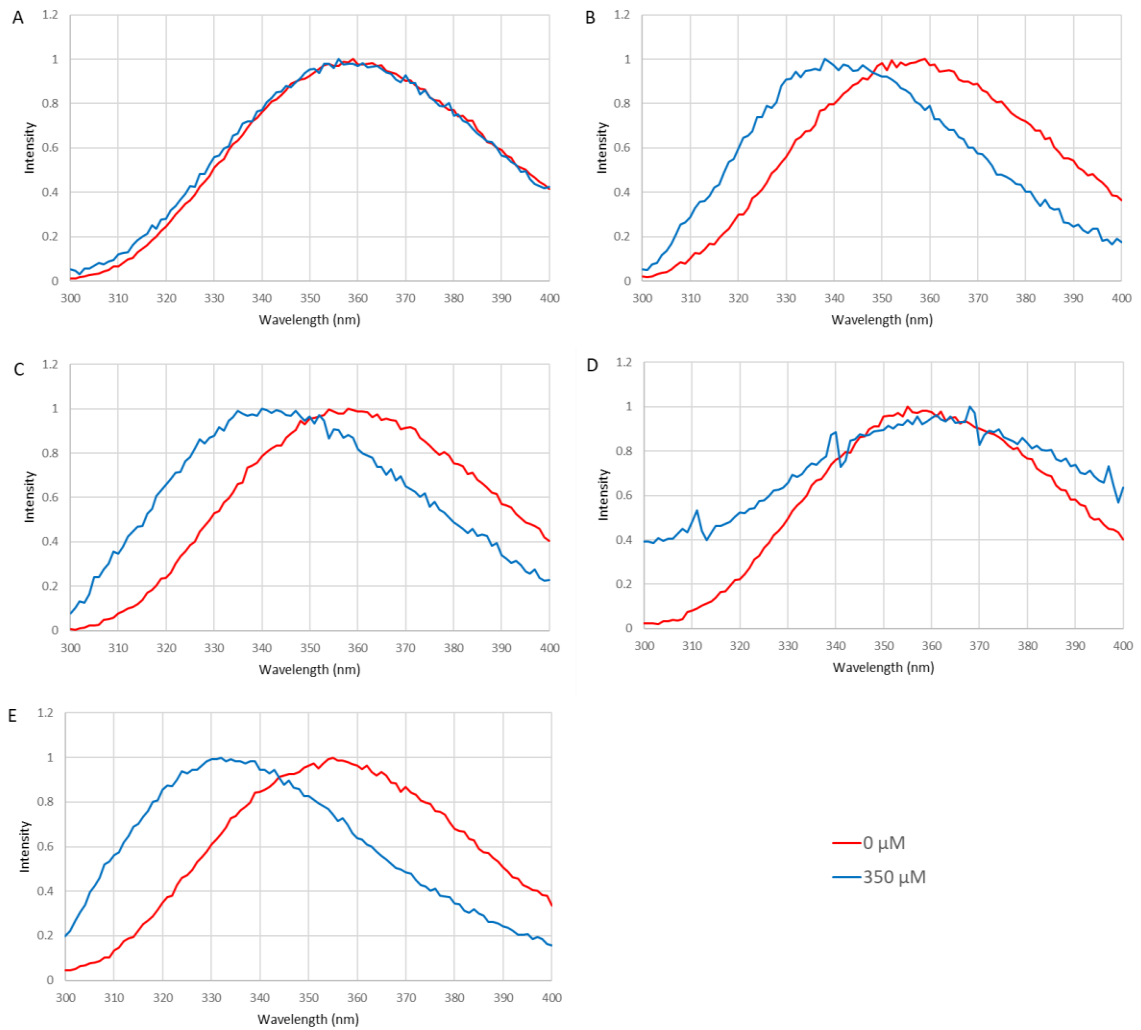
Binding to Lipid Vesicles



Note. Peptide binding was assayed using TRP fluorescence by titrating SUVs into a peptide containing sample with a final concentration of 2 μ M. After each addition the spectral barycenter was calculated and then a Δ barycenter was calculated by taking the difference between the initial barycenter and that of each addition. Peptide variants that were assayed were (A) L1V, (B) L1I, (C) L1L, (D) L1A, (E) L1F. In all panels Blue represents PC, Orange 3:1 PC:PG, Grey 3:1 PE:PG, and Yellow 3:1 PC:Chol. All data are averages of 3 replicates and SD is represented by error bars.

Figure 4

Normalized Trp Emission Spectra



Note. Normalized Trp emission spectra for L1V (A), L1I (B), L1L (C), L1A (D), and L1F (E) peptides before (red) and after (blue) interacting with lipid vesicles. Data are representative spectra after subtraction of a background spectrum. All shifts representative of samples containing 0 μM and 350 μM lipide (PC:PG).

In order to gain more insight into the bilayer interactions, fluorescence quenching approaches were utilized. The peptides were exposed to the aqueous quencher acrylamide in solution or when bound to vesicles. Acrylamide is known to strongly quench Trp fluorescence in aqueous environments but does not exert the quenching effect if the Trp is buried in the non-polar core of the bilayer [99]. Thus, peptide Trp exposure to the aqueous milieu can be gauged by the extent of quenching by acrylamide. Stern-volmer quenching plots were created to analyze the data and K_{sv} (slopes of a linear fit to the data) are shown in Table 2. The trends in this data are consistent with the barycenter shift data in Figure 3. In the case of L1L and L1I, there was a significant reduction in quenching between the solution (free) state of the peptide and when bound to anionic vesicles, but a much smaller reduction if any when interacting with zwitterionic vesicles. This is consistent with a more deeply buried Trp in anionic bilayers. The L1V and L1A exhibited differential behavior in this experiment with L1V showing a reduction in quenching with vesicles, indicating some interaction while the L1A did not exhibit significant reductions indicating that the Trp is significantly exposed under all conditions. Importantly, the L1F was the only peptide to exhibit extensive reductions in quenching when bound to PC:Chol vesicles, consistent with the strong binding to both anionic and zwitterionic vesicles.

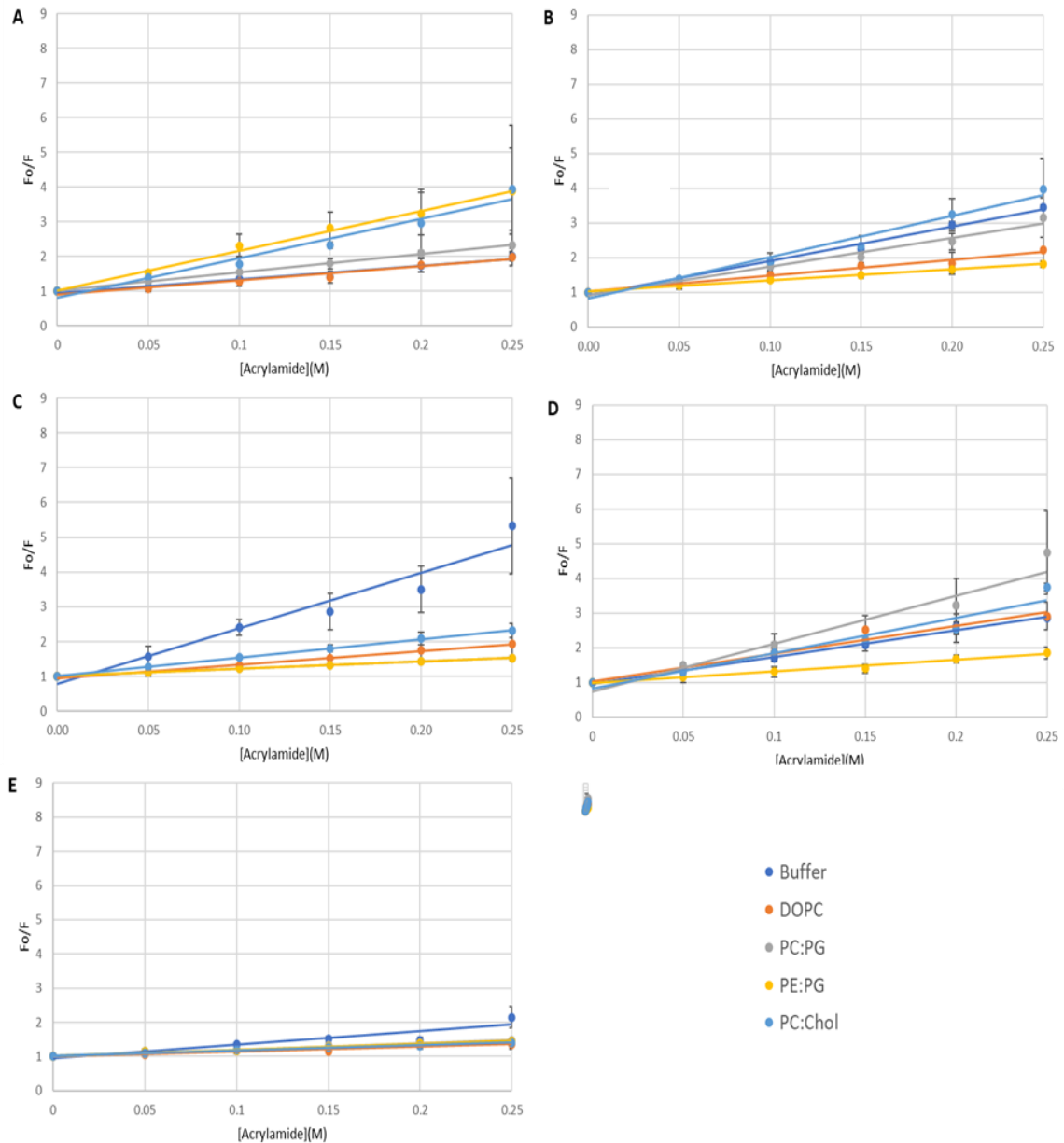
Table 3*Fluorescence Quenching*

	Acrylamide quenching (Ksv [M ⁻¹])				
	PBS	DOPC	PC:PG	PE:PG	PC:Chol
L1V	12.14 ± 1.59	4.18 ± 0.15	16.86 ± 6.47	5.64 ± 0.38	12.19 ± 1.54
L1I	10.5 ± 0.67	4.90 ± 1.51	8.72 ± 2.09	3.39 ± 2.25	12.65 ± 0.63
L1L	4.26 ± 0.97	4.08 ± 2.10	3.51 ± 0.17	2.22 ± 4.04	8.92 ± 0.94
L1A	8.19 ± 0.90	8.51 ± 0.46	10.9 ± 0.26	3.59 ± 0.58	10.79 ± 0.27
L1F	4.18 ± 4.79	1.57 ± 3.49	2.06 ± 0.97	1.80 ± 0.77	1.63 ± 0.20

Note. Abbreviations: DOPC, 1,2-dioleoyl-sn-glycero-3-phosphocholine; DOPG, 1,2-dioleoyl-sn-glycero-3-phospho-(1'-rac-glycerol). Data are averages of 3 replicates with SD.

Figure 5

Acrylamide Quenching



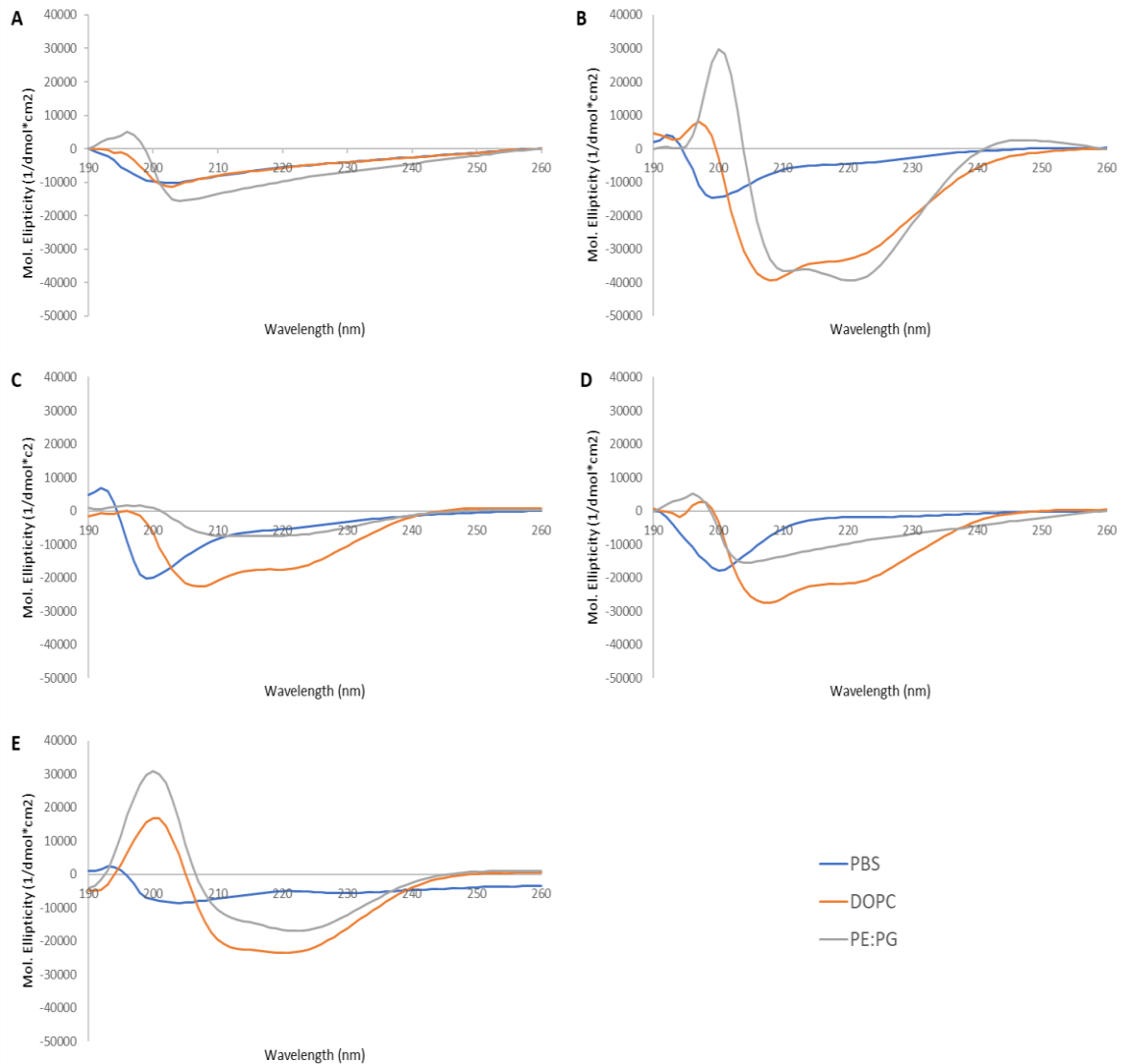
Note. Acrylamide quenching was done on (A) LIV, (B) LII, (C) LIL, (D) LIA, (E) LIF. Samples contained either no lipid vesicles (Dark Blue) or (Orange) PC, (Grey) PC:PG, (Yellow) PE:PG, and (Light Blue) PC:Chol. All samples contained a peptide concentration of 2 μ M and lipid concentration of 250 μ M for those that contained lipid vesicles. Data is corrected for inner filter effects and are background subtracted. Data represents an average of three replicates with SD shown by the error bars.

Peptide Secondary Structure

While many venom peptides that act as AMPs adopt helical secondary structures, it is also known that amino acids have differing propensities to form alpha-helical structures. Circular dichroism (CD) spectroscopy was used to characterize the secondary structure of the peptides in the absence and presence of lipid vesicles. The CD spectra were recorded of the peptides in buffer or in the presence of DOPC vesicles. DOPC was selected as 4/5 peptides appear to interact with these bilayers and the favorable spectroscopic profile of DOPC vesicles compared to those containing PG. The CD results are shown in Figure 5. In buffer alone, all peptides exhibited canonical spectral signatures consistent with disordered secondary structure except L1V. When in the presence of lipid vesicles, L1F, L1L, and L1A clearly adopt α -helical conformations while L1I appears to have some helical character but not nearly as much as the other 3 peptides. Interestingly, there was almost no difference in CD spectra for the L1V peptide in the presence or absence of vesicles. The L1V peptide exhibited a strong negative band at ~204 nm which is inconsistent with disordered structures, α -helix, or β -strand [100].

Figure 6

Circular Dichroism (CD) Spectrum



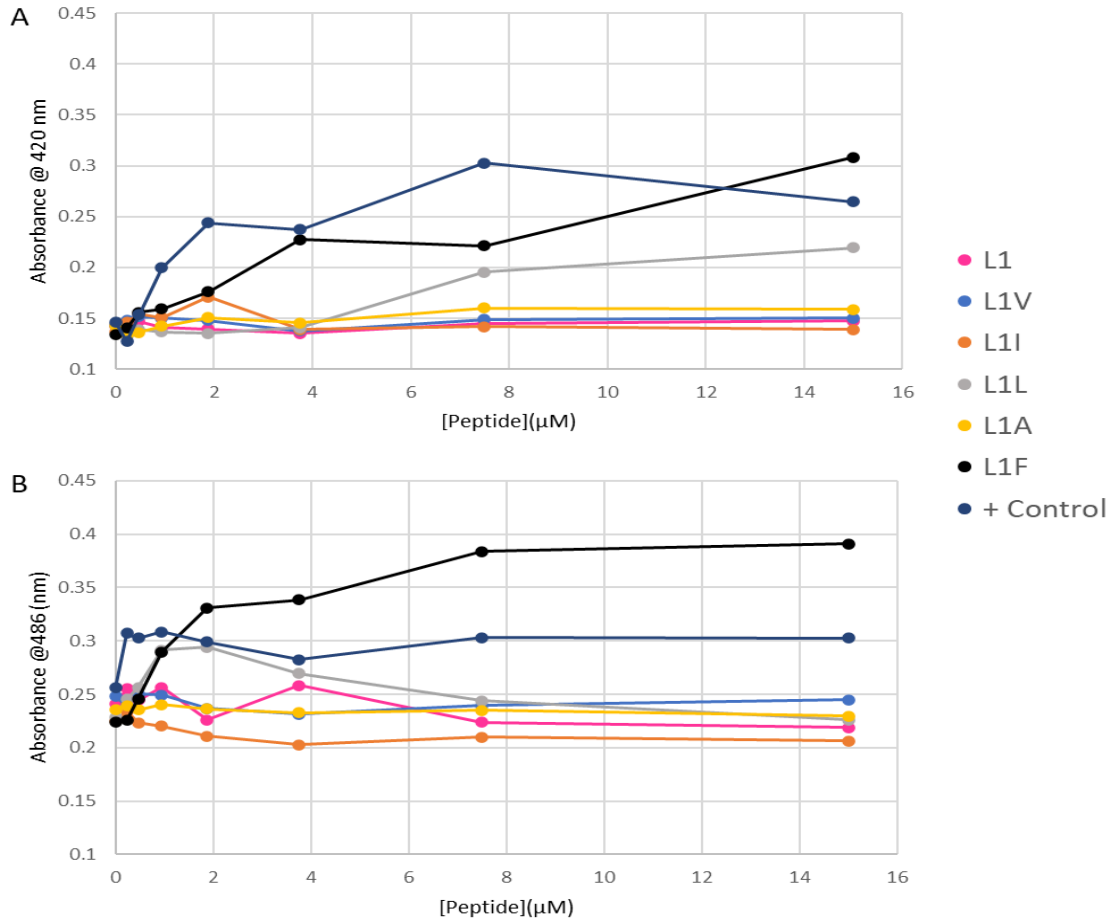
Note. Spectra of all peptide variants represented by panels (A) L1V , (B) L1I, (C) L1L, (D) L1A, (E) L1F, each with a final concentration of $3\mu\text{M}$. Spectra of all peptides were collected in 10X diluted PBS represented with blue, DOPC represented by orange, and 3:1 PE:PG represented by grey. All spectra collected with lipids were done in the presence of $200\mu\text{M}$ lipid vesicles. All data represent the average of 64 scans with correction of background spectra lacking peptide.

Membrane Permeabilization

The mechanism of action of the L1 venom peptide is likely a membrane disruptive mechanism, the effect of the hydrophobic substitutions on membrane permeabilization was investigated using *E. coli* and ovine red blood cells (RBCs). The permeabilization of the *E. coli* outer membrane was assayed using an enzyme-substrate pair in which the enzyme (β -lactamase) is located in the periplasmic space while the substrate (the chromogenic nitrocefin) is added to the exterior of cells. Normally, nitrocefin has limited permeability across the bilayer, but as peptides or other membrane active agents disrupt bilayer integrity, the nitrocefin can more easily cross the outer membrane into the periplasm where it is hydrolyzed by β -lactamase into a colored product. A snapshot of the results after 30 minutes of exposure are shown in Figure 6A, with full time courses shown in Figure 7. In this assay, L1L and L1F showed increased permeability of the outer membrane, but L1F induced permeabilization more quickly and at lower concentrations than L1L. Notably, several other peptides induced some extent of delayed permeabilization at the highest concentrations tested, however L1I, despite the similar biophysical behavior demonstrated earlier, exhibited no membrane disruption above background. Similarly, the permeabilization of the *E. coli* inner membrane was assessed using a cytoplasmic enzyme, β -galactosidase, and a chromogenic substrate, ONPG. A snapshot of the results after 30 minutes of exposure are shown in Figure 6B, with full time courses shown in Supplemental 8. In this case, only L1L and L1F exhibited any inner membrane permeabilizing activity, regardless of the time of peptide exposure.

Figure 7

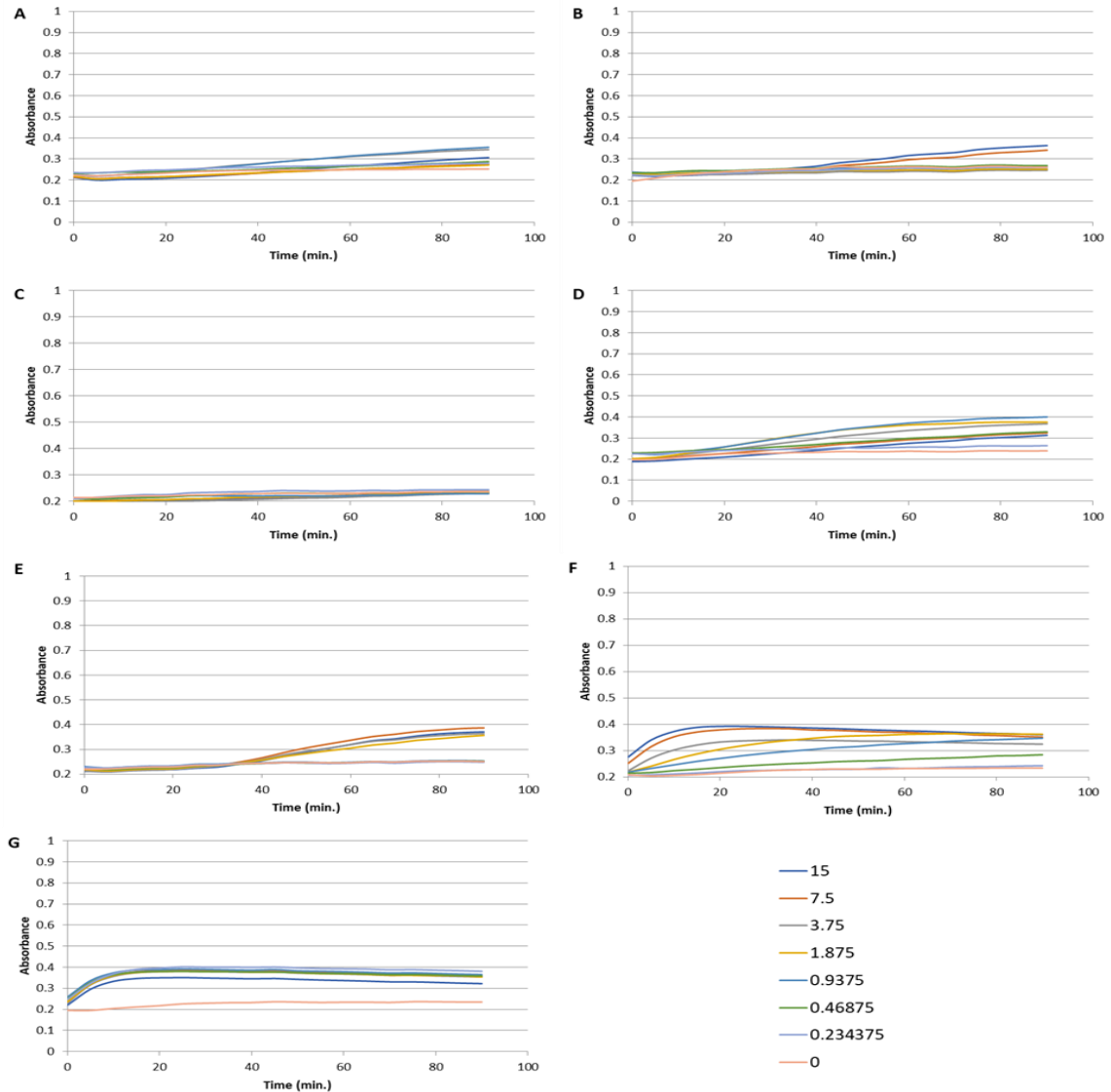
Membrane Permeabilization of E. coli



Note. *E. coli*, (A) outer membrane and (B) inner membrane permeabilization. For both panels L1 is shown in pink, L1V in blue, L1I in orange, L1L in grey, L1A in yellow, L1F in black, and positive control in dark blue. All data are averages of three replicates and SD represented by error bars. Error bars are smaller than the size of the symbols.

Figure 8

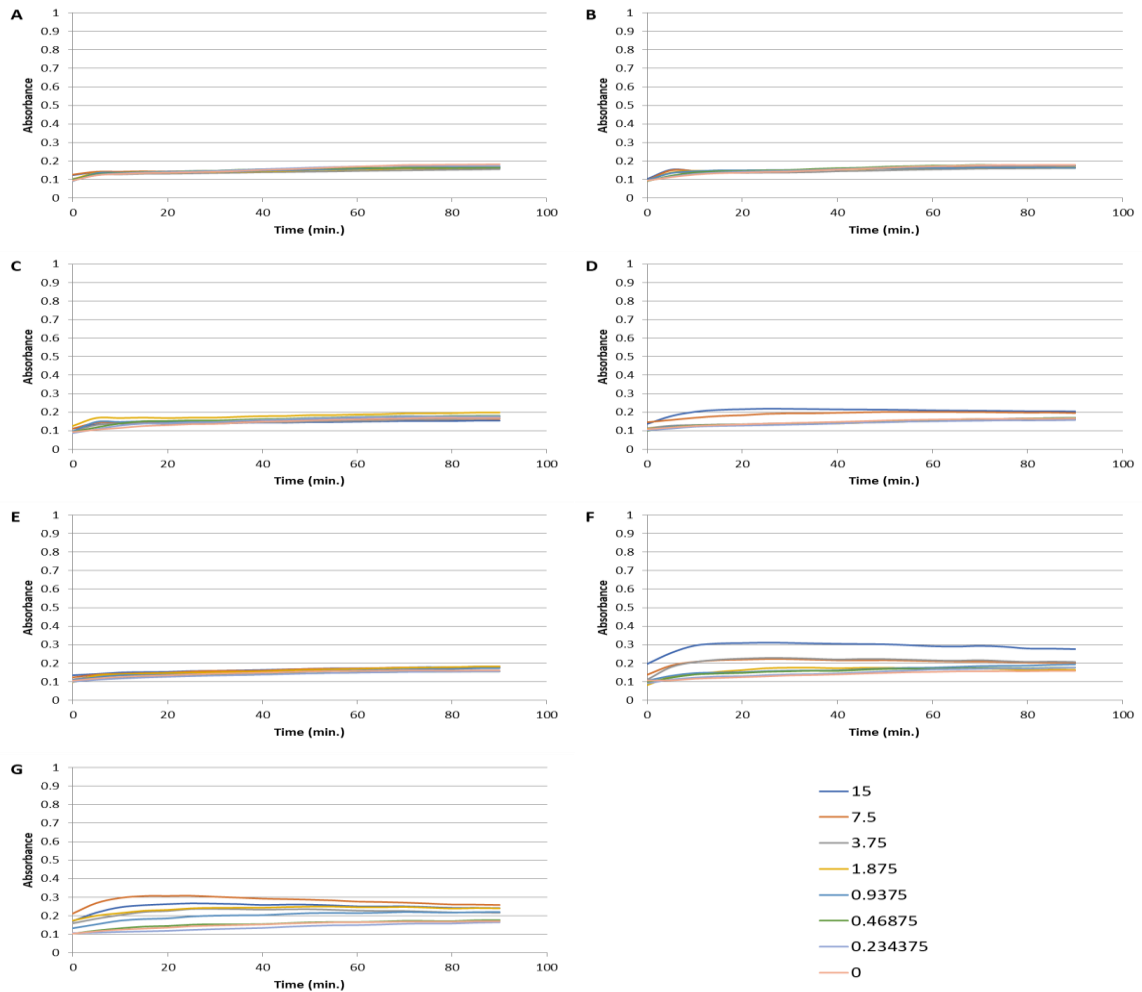
E. coli Outer Membrane Permeabilization Assay



Note. The data sets show absorbance at 486 which indicates the periplasmic enzyme β -lactamase breaking down the substrate nitrocefin. Bacteria were exposed to (A) L1, (B) L1V, (C) L1I, (D) L1L, (E) L1A, (F) L1F, (G) Polymyxin. The legend shows the colors that represent each concentration that starts from 15 μ M and diluted down to 0.234 μ M and 0 μ M being the negative control. Data represents the average and SD of 3-6 samples.

Figure 9

E. coli Inner Membrane Permeabilization Assay

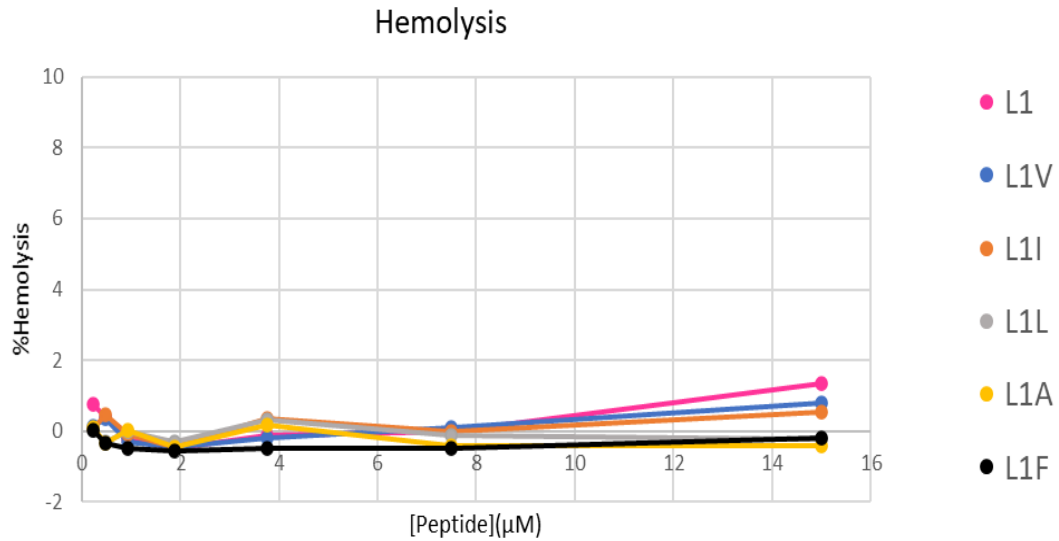


Note. These data sets show the breakdown of the ONPG substrate by the periplasmic enzyme β -galactosidase which is represented by the absorbance at 420 nm. Varying concentrations of (A) L1, (B) L1V, (C) L1I, (D) L1L, (E) L1A, (F) L1F, (G) CTAB. The legend shows the colors that represent each concentration that starts from 15 μ M and diluted down to 0.234 μ M and 0 μ M being the negative control. Data represents the average and SD of 3-6 samples.

Hemolytic activity of venom peptides and, more broadly AMPS in general, has often been a first approximation toward assessing potential for further development. Highly hemolytic peptides are unlikely to become useful clinical therapeutics due to the toxicity to the host. Venom peptides, often suffer from high hemolytic activity due to the evolutionary nature of these molecules and the original purpose in the source organism. Additionally, it has been demonstrated that the overall hydrophobicity of antimicrobial polymers directly impacts the cytotoxic and hemolytic activity of these molecules, thus screening these hydrophobic-substituted peptides for hemolysis is an important step. The peptides were co-incubated with freshly isolated ovine red blood cells and peptide-induced hemolysis was determined by comparing hemoglobin leakage from treated cells with the detergent Triton X-100 to that of untreated cells as a positive control. The results of hemolysis assays are shown in Figure 10. The results indicate that none of the L1 variants induced any measurable hemolysis up to 15 μ M peptide. These results are consistent with the previous results from on the L1 parent sequence and other sequence variants of L1 [90].

Figure 10

Hemolysis of Human Red Blood Cells (RBCs)



Note. Hemolysis of RBCs. Data sets in 10, were normalized with the experimental data done on untreated RBCs (0% hemolysis) and RBCs treated with Triton X-100 (100% hemolysis). For this panels L1 is shown in Pink, L1V in Blue, L1I in Orange, L1L in Grey, L1A in Yellow, and L1F in Black. All data are averages of three replicates and SD represented by error bars. Error bars are smaller than the size of the symbols.

Discussion

Effects of Hydrophobic Residues

The work presented herein describes an investigation into hydrophobic amino acids and how a uniform substitution strategy impacts the biophysical and microbiological activity of the venom derived peptide Ponericin L1. Overall, the behavior of the peptide can be dramatically impacted by the substitution of hydrophobic residues in different ways, depending on the identity of the substitutions.

While many AMPs have evolved to selectively target bacterial cell membranes over host cell membranes, the same selective pressure is not present for venom peptides. Notably, venom peptides generally act as an offensive weapon against predators or prey and would generally benefit from being more broad-spectrum in activity in this role [89,101,102]. However, any hope of development of a membrane-active peptide into a clinical therapeutic must have the ability to discriminate between host cell membranes and bacterial cell surfaces. The biophysical results clearly show differences in affinity to model lipid vesicles. The L1L, L1I, and L1F all show a significant change in emission barycenter upon exposure to anionic lipid vesicles. This indicates that the peptides are interacting with the vesicles and the Trp residue undergoes a change in local environment into a more non-polar environment. This is consistent with the physical properties of the peptides as these three molecules have a net positive charge and are the three most hydrophobic peptides when evaluated using the Wimley-White hydrophobicity scale [103]. However, the L1F is the only peptide to bind zwitterionic lipid vesicles over similar concentration ranges and resulting in similar extent of spectral shift (~14 nm). L1F was also the only peptide variant that showed enhanced binding to lipid composition

PC:Chol. However, it has been seen in other published work that the aromatic structure in phenyl alanine has a specific affinity for binding to cholesterol which is a likely cause for the binding displayed [161]. This is also likely driven by the increased hydrophobicity of the molecule compared to L1L and L1I. On the other hand, the L1A and L1V peptides did not show nearly as much binding to the vesicles. While these are less hydrophobic in general, the L1V exhibited the least shift despite being more hydrophobic than L1A.

The interaction with anionic model lipid bilayers appears to follow the same pattern as the MIC results. The weakest binding L1A and L1V peptides showed no antimicrobial activity at the highest concentrations tested (15 μ M). Conversely, L1L, L1I, and L1F exhibited broad spectrum activity against both Gram-positive and Gram-negative strains. Similarly, these three peptides exhibited the least quenching by acrylamide. Taken together, the binding to bilayer surfaces and the ability to interact with the nonpolar core of the bilayer appears to be a good screening tool for these peptides. Beyond this, the hydrophobic component in binding appears to have a threshold effect on both the blue-shift of the Trp fluorescence and the antimicrobial activity. Spectroscopically, the more hydrophobic peptides likely partition deeper into the bilayer, burying the Trp in a more non-polar environment shield from acrylamide. Similarly, this partitioning depth has been shown by our group and others to be a contributor to antimicrobial activity [72,104-106]. However, the correlation of binding to antimicrobial activity is not universal. Prior work from our group on a different peptide, C18G-His, demonstrated that peptide exhibited a strong blue shift upon binding at neutral pH but did not have strong antimicrobial activity at that pH regime [107]. Thus, while this correlation between binding and activity is suggestive for L1, care must be taken to

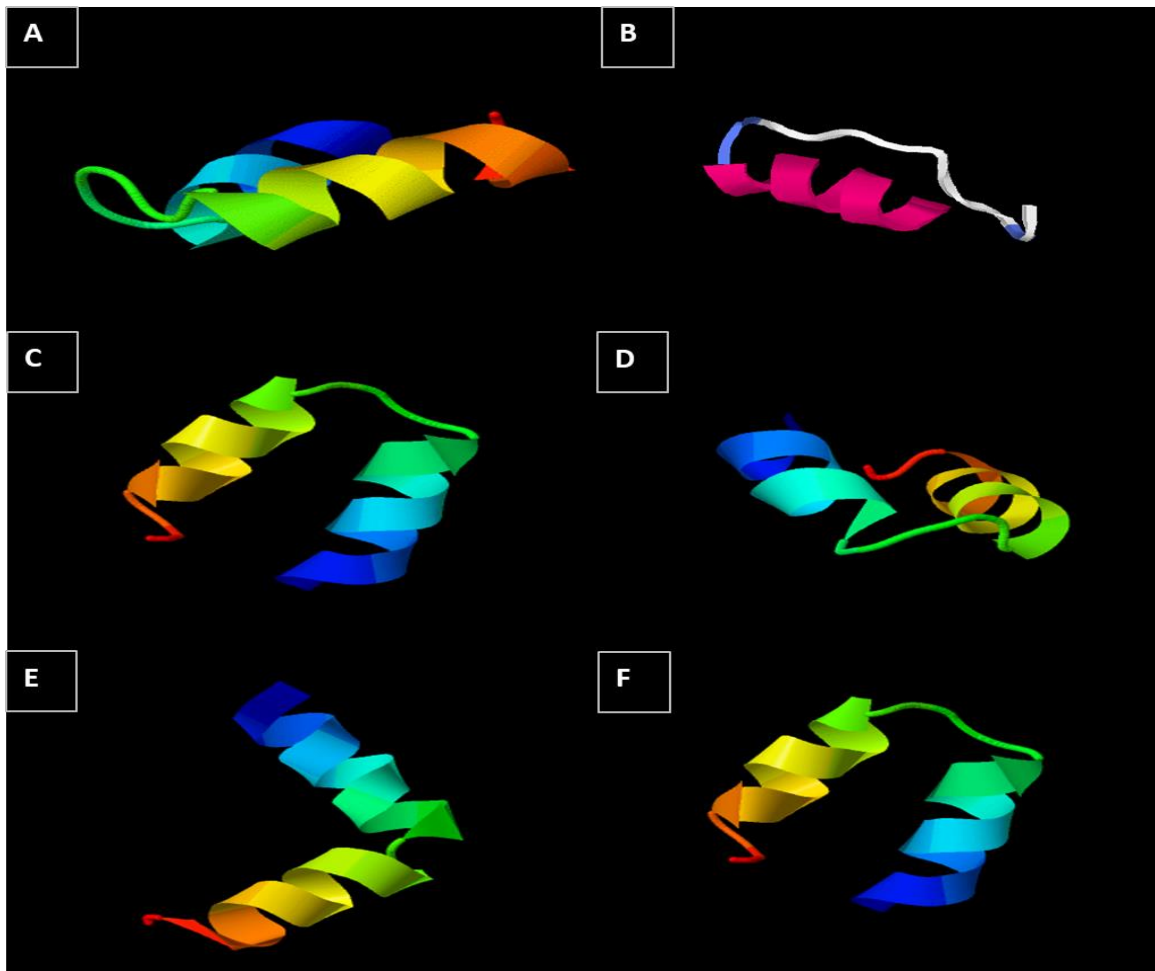
ensure that multiple avenues are examined when using experiments to guide design of novel peptide antimicrobials.

An interesting result from this work is the complete lack of activity exhibited by L1V. This was somewhat surprising due to the hydrophobic nature of the peptide coupled with the strong cationic net charge. An examination of the data indicates that this is likely driven by structure formation in the peptide while in solution. The L1V peptide exhibited the highest quenching by TCE in solution as well as exhibiting the highest degree of red-edge shift, indicative of solution interactions in the peptide. The CD spectra show no difference in the absence or presence of lipid vesicles, supporting the binding results that L1V does not interact with bilayers. Additionally, the CD spectra for L1V exhibit a minimum ~205nm, somewhat red-shifted for a disordered structure and blue-shifted for a β -strand. However, similar spectra have been reported for β -turn AMPs by several different groups [108,109]. This formation of some β -strand structure is consistent with valine having a lower helical propensity than the other residues examined [110,111]. The structure prediction algorithm, iTasser, was used to generate predicted structures of L1L and L1V which also support the formation of β -strand formation in L1V. Although this was accurate for L1V, this did not support all structures that was shown by the circular dichroism. This could be due the fact iTasser uses a “B-factor” which indicates the inherent thermal mobility of the Trp residue. This is deduced by using a threading template of proteins in combination of sequence profiles [112]. This would not account for solvent differences and will vary in secondary structure, thus the α -helical confirmations predicted were incorrect for the peptides in solution. Taken

together, the data support the hypothesis that the activity of the peptides is a balance between hydrophobicity, cationic charge, and secondary structure.

Figure 11

iTasser Structures



Note. Models presented are predictions generated through the algorithm, iTasser. The panels (A) L1, (B) L1V, (C) L1I, (D) L1L, (E) L1A, (F) L1F represent the most likely structure out of 5 total predicted structures for each variant.

Finally, the lack of hemolytic activity of these peptides is striking. While not totally unexpected based on prior results with L1-based sequences with substitutions to the cationic residues, it is exciting that these molecules retain this beneficial property even upon hydrophobic substitutions. Prior studies with AMP-mimetic polymers show a clear relationship between overall hydrophobicity and cytotoxicity and/or hemolytic activity [113,114]. In those works, the Kuroda group performed hemolysis assays on a series of heteropolymers in which the fraction and type of hydrophobic monomers were varied. These results clearly showed as the fraction of hydrophobic monomers increased, or the hydrophobicity of the monomers increased (methyl vs. butyl), the hemolytic activity also increased [113,114]. However, it appears in the L1 background that even the most hydrophobic substitutions (L1L and L1F) do not cross the threshold for inducing hemolytic activity. Speculatively, the strong interactions between L1F and zwitterionic bilayers may indicate that the hemolytic threshold is not far off, as it indicates the peptide should be able to bind to RBC or other zwitterionic mammalian membranes.

Chapter 3

Effect of Charge and Hydrophobicity in Antimicrobial Polymethacrylates

Antimicrobial Polymers

As discussed AMPs have promising potential as potential therapeutic agents. As briefly mentioned in chapter 1, macromolecular approaches have also shown potential for therapeutic agents. Polymers potential as antimicrobial agents have been discovered since 1965 and have been gaining attraction in both academic and industrial research [126]. By 2013 there were 27,845 patent issued for antimicrobial polymers. Many promising antimicrobial polymers have been reported, and the amount of FDA-approved antimicrobial polymers have drastically increased in the past decades [127]. Antimicrobial polymers can have two different types of action that include either passive or active action. Passive polymer layers that reduce protein adsorption, preventing bacterial adhesion on their surface. Active polymers actively kill bacteria that adhere to their surface. Interestingly enough both types of polymers rely on electrostatic interactions. However, passive polymers have repelling characteristics and do not actively interact or kill the bacteria. Active polymers can act much like AMPs and interact with cell membranes in disruption [126].

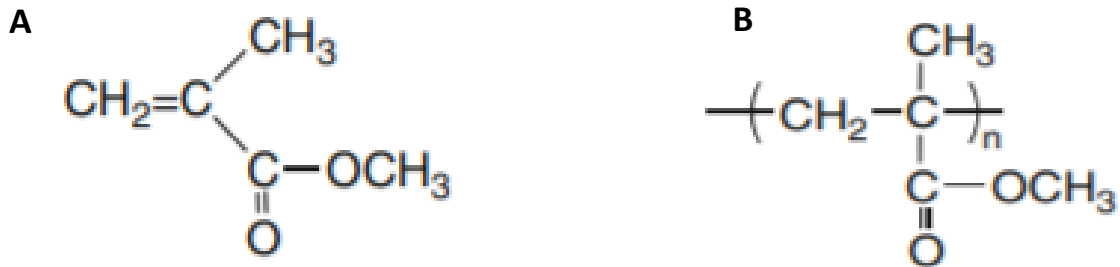
Polymethacrylates

Synthetic polymers have cationic, amphiphilic structures designed for membrane disruption. However, the major drawback to synthetic polymers is that they are often toxic to human cells or there is a lack of understanding of their toxic profiles. One of the ways to combat this issue is to design synthetic polymers mimicking functional and structural properties of less toxic host defense peptides like AMPs. Over the last decade

new antimicrobial polymers have been developed including copolymers of β -lactams [128], polynorbornenes [129], polymethacrylates [130,131], and polystyrenes [132,133]. Polymethacrylates are a class of materials that have a wide range of properties and many commercial applications including: high-performance engineering plastics, energy storage materials, functional coatings, and biomaterials. One favorable trait of polymethacrylates is the adjustability. The diverse range of ester groups that can be incorporated is one reason why polymethacrylates have such varied properties [134].

Figure 12

MMA & PMMA



Note. Figure 12A and 12B were modified from a scientific article from the Encyclopedia of Polymeric Nanomaterials [151]. (A) is methyl methacrylate (MMA) and (B) is the poly (methyl methacrylate) (PMMA) monomer.

Synthetic polymers have been widely used as biocides or used in combination with other antimicrobials [152-154]. These synthetic biocides are cationic, amphiphilic structure that are designed to cause membrane disruption. The drawback to most of these polymers is the inherent cytotoxicity of polymers to human cells. To combat these issues the design of these polymers were oriented around the much less toxic host-defense peptides. These peptidomimetic polymers over the last decade have been further finely tuned to increase favorable traits such as functionality, amphiphilic balances, polymer sizes, antimicrobial activity, and decrease hemolytic activity [152,155-158]. Polymethacrylates can be finely tuned for antimicrobial activity and selectivity through the modification of the composition of cationic and hydrophobic groups much like AMPs. This is evident by a recent study on the role of hydrophobicity and hemolytic activity of polymethacrylate derivatives. In the study it was elucidated for these polymethacrylate derivatives that as hydrophobicity increased, so did antimicrobial activity and hemolytic. Although there was a lack of selectivity that could be caused by the inherent property of those synthetic polymers, this study gives insight that composition can dictate overall activity [150].

Indole Polymers

In biological and biochemical structures indoles are ubiquitous with attracted interest in multiple areas such as pharmaceuticals, fragrances, agrochemicals, and dyes. This can be attributed to their unique electrical, chemical, and optical properties [135-136]. The multiple reaction sites on the indole group allow for easy tunability [137,138]. Side chain tryptophan-substituted polymers have gained traction for their inherent fluorescence, making it easy for tracking in biological systems and molecular imaging

[139]. Fluorescence of proteins through the excitation of L-tryptophan residues is well known and a commonly practice diagnostic tool to explore their conformation [140]. It also has been demonstrated that L-tryptophan-rich peptides play a significant role in membrane penetration [141,142].

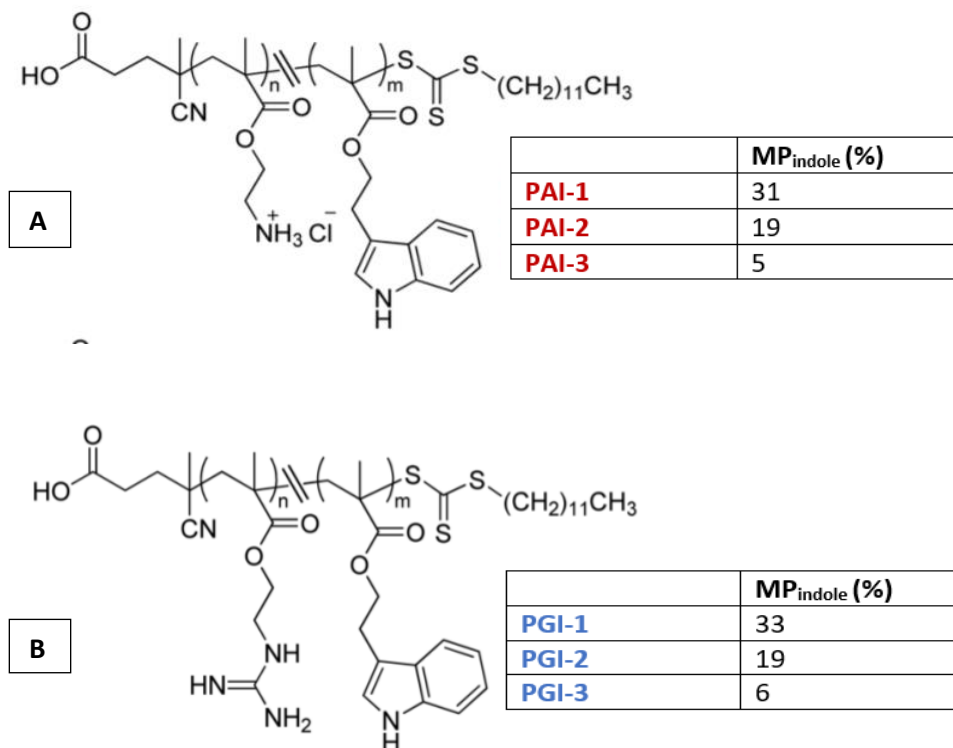
Due to structure and characteristics of indole polymers, they may mimic other traditional Trp-rich peptides. For example indole polymers may serve as good mimetics of AMPs like indolicidin and tritrypticin. Indolicidin, a 13 residue peptide in which 5 of them are Trp residues, is one of the shortest naturally occurring and linear AMPs. This AMP is a fairly attractive lead molecule for its potency, selectivity, and wide range of activity [147]. Tritrypticin is a member of the cathelicidin family and is another Trp-rich (3 Trp residues), short sequenced AMP. However, tritrypticin has an extra positive charge compared to indolicidin with four positively charged residues localized at the C- and N-terminus [148]. Interestingly enough these AMPs do have a traditional mode of action. Trp-rich AMPs (TrAMPs) like these cross the bacterial membrane and interact with intercellular targets. Although these peptides have a broad range of activity, they do not affect the integrity of the membrane.[149] For example both these peptides cross the bacterial membrane and interact with DNA to inhibit protein synthesis, causing cell death [147,148].

Of the many types of antimicrobial polymers that have been developed, cationic polymers have gained the most attention. They mainly consist of cationic and hydrophobic functional groups with mechanisms mimicking AMPs [143]. The cationic functional groups, much like AMPs, facilitate the adsorption on to the surface of the cellular membrane. This coupled with hydrophobic properties of the L-tryptophan side

chains could lead to increased antimicrobial activity. For example, there was a study done on synthesized cationic star-shaped polypeptides with 3 to 8 arms evaluating their antimicrobial activities. The study showed that increasing the amount of arms of the polypeptide resulted in an increase of antimicrobial activity, anything passed 8 arms had no significant increase. More importantly for each number of arms, when the L-lysine was modified to be an indole group, it resulted in the best antimicrobial activity. It also exhibited improved cytotoxicity without compromising the hemolytic activities [144]. This shows a potential in controlling the composition of indole and cationic groups to increase selectivity and antimicrobial activity.

Figure 13

Polymethacrylate Structures



Note. Both figures 9A and 9B are modified figures from a publication from ACS Macro Letters [145]. Both series of polymethacrylates were synthesized and synthesized by our collaborators at Commonwealth Scientific and Industrial Research Organization (CSIRO) in Melbourne Australia. Random copolymers containing Amine-Indole side chains (PAI-1, PAI-2, PAI-3 (red)) as Lysine-Tryptophan mimics and Guanidine-Indole side chains (PGI-1, PGI-2, PGI-3 (blue)) as Arginine-Tryptophan Mimics.

Materials and Methods

Preparation of Polymethacrylates

Random copolymer series PAI and PGI were synthesized and obtained by our collaborators in Australia Common Wealth Scientific and Industrial Research Organization (CSIRO). The average molecular weight for each series was calculated using H NMR end group analysis. PAI-1, PAI-2, PAI-3 had average molecular weights of 5600, 6300, 5300 g/ mol respectively. PGI-1, PGI-2, and PGI-3 had average molecular weights of 6000, 6500, and 5700 g/ mol respectively [145]. PAI (Amine-indole side chain) was synthesized to mimic as Lysine-Tryptophan mimics. Each polymer has a different mass percentage of the indole side chain, PAI-1 (31%), PAI-2 (19%), and PAI-3 (5%). PGI (Guanidine-indole side chains) was synthesized to mimic Arginine-Tryptophan Mimics. Each polymer has a different mass percentage of indole side chain PGI-1 (33%), PGI-2 (19%), PGI-3 (6%). 4 mgs of polymer was weighed out and dissolved in .5 mL of dH₂O to make an 8 mg / mL stock for experiments.

Lipid Preparation

Lipids were obtained prepared in the same manner and concentrations as previous chapter.

Binding Experiments

Binding experiments were prepared and preformed in the same manner as previous chapter. However, a PC:Chol composition was not tested and the final polymer concentration was .1 mg / mL in the same PBS buffer from chapter 2.

Acrylamide Quenching

Acrylamide quenching experiments were prepared and performed in the same manner as chapter 2 without a PC:Chol composition and with a final polymer concentration of .1mg / mL in the same PBS buffer as chapter 2.

10-DN Quenching

10-Doxyl nonadecane (10-DN) was purchased from Avanti Polar Lipids (Albaster, Alabama). 10-DN stock was made by taking a single ampule and diluting it with 1 mL of 200 proof ethanol for a final concentration of 2.7 mM. Lipid vesicles in the same manner as acrylamide quenching with the exception of drying down 10-DN with lipid compositions. To do this, 10% of the final lipid concentration used in the acrylamide protocol would be replaced with 10-DN. The following changes to lipid compositions are as follows: 100% DOPC will be change to 90:10 (DOPC:10-DN) , for PC:PG the new ratio will be 65:25:10 (PC:PG:10-DN), and for PE:PG the new ratio will be 6:25:10 (PE:PG:10-DN). Fluorescence readings were taken at excitation: 280 nm and emission: 340 nm.

Inner and Outer Membrane Permeabilization

Both experiments were prepared and performed in the same manner as the previous chapter, with the exception that the final concentration of Polymer started at .1 mg / mL and then serially diluted down to .0016 mg / mL , with a negative control in the last well.

Hemolysis

Hemolysis was prepared and performed in the same manner as the previous chapter, with the exception that the final concentration of Polymer started at .1 mg / mL and then serially diluted down to .0016 mg / mL , with a negative control in the last well.

Results

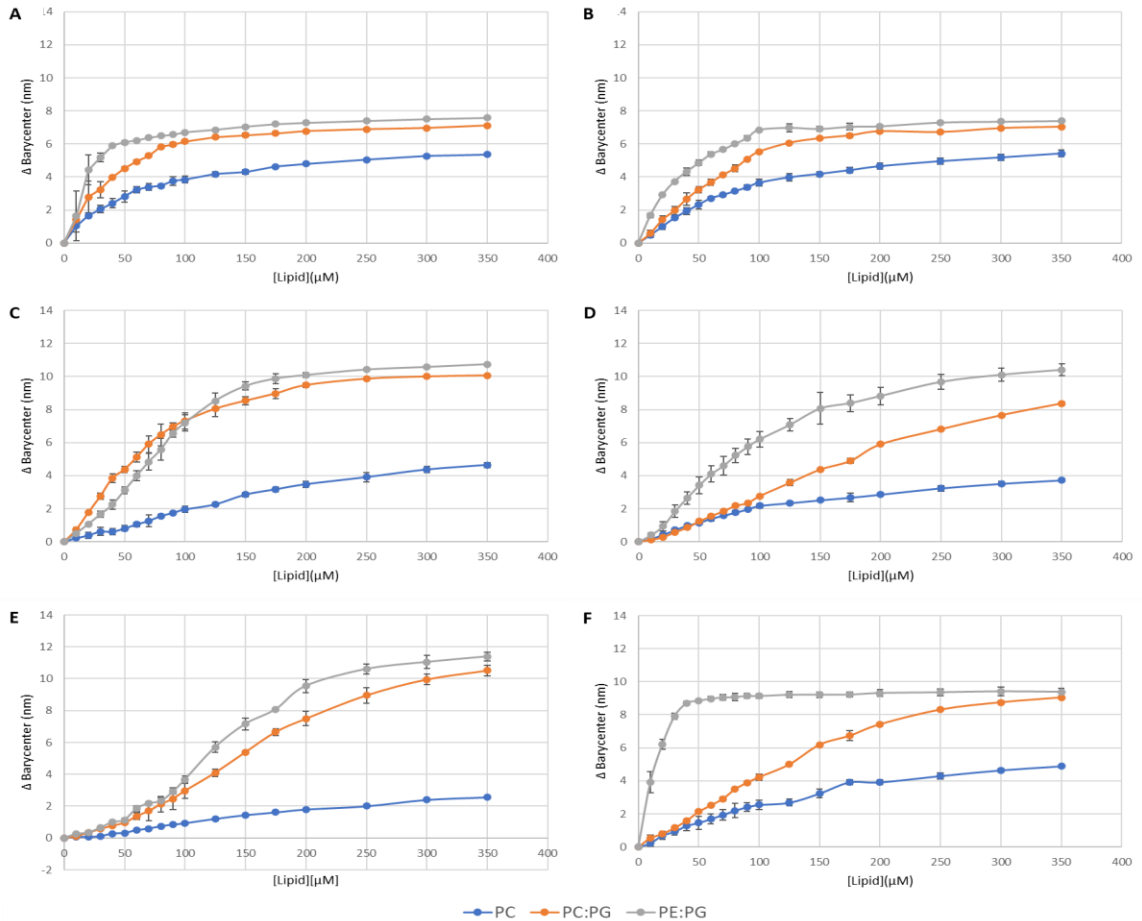
Lipid interactions

The mechanism to cationic biocides are likely to mimic that of traditional membrane disrupting AMPs. To do this the first step would be to bind to the surface of the bacterial cell. Similarly, to chapter 2, the inherent environmental sensitivity of the indole side chain was utilized to elucidate the membrane binding capabilities of each polymethacrylate series. Much like the Trp residue in the previously discussed AMPs, the indole side chain will exhibit a red shifted emission barycenter in aqueous solution, and when bound to lipid bilayers the emission will blue shift to lower wavelengths. The change in the emission barycenter compared to that in absence of vesicles was plotted as a function of total lipid concentration (Figure 14). Lipid composition of vesicles was either 100% DOPC, 3:1 DOPC:DOPG, 3:1 POPE:POPG. The results of this experiment show that there is varied behavior between indole percentage, lipid composition, and between the two different series (PAI & PGI). For PAI there is a larger blue shift at lower concentrations when the indole percentage is the highest, especially for anionic lipid compositions. The PAI series exhibits that when the indole percentage is the highest there is more significant binding at lower concentrations, however at 350 μ M of lipid vesicle the lowest indole percentage shows the greatest shift. PGI shows similar results in the sense that when the indole percentage is 19% at 350 μ M there is more binding than when the indole percentage is higher. However, at lower concentrations when the indole percentage is 19% the binding is significantly less. Both show

significantly larger barycenter shifts when binding PG-containing, indicating that electrostatic forces are a strong driver in the bilayer association of these peptides.

Figure 14

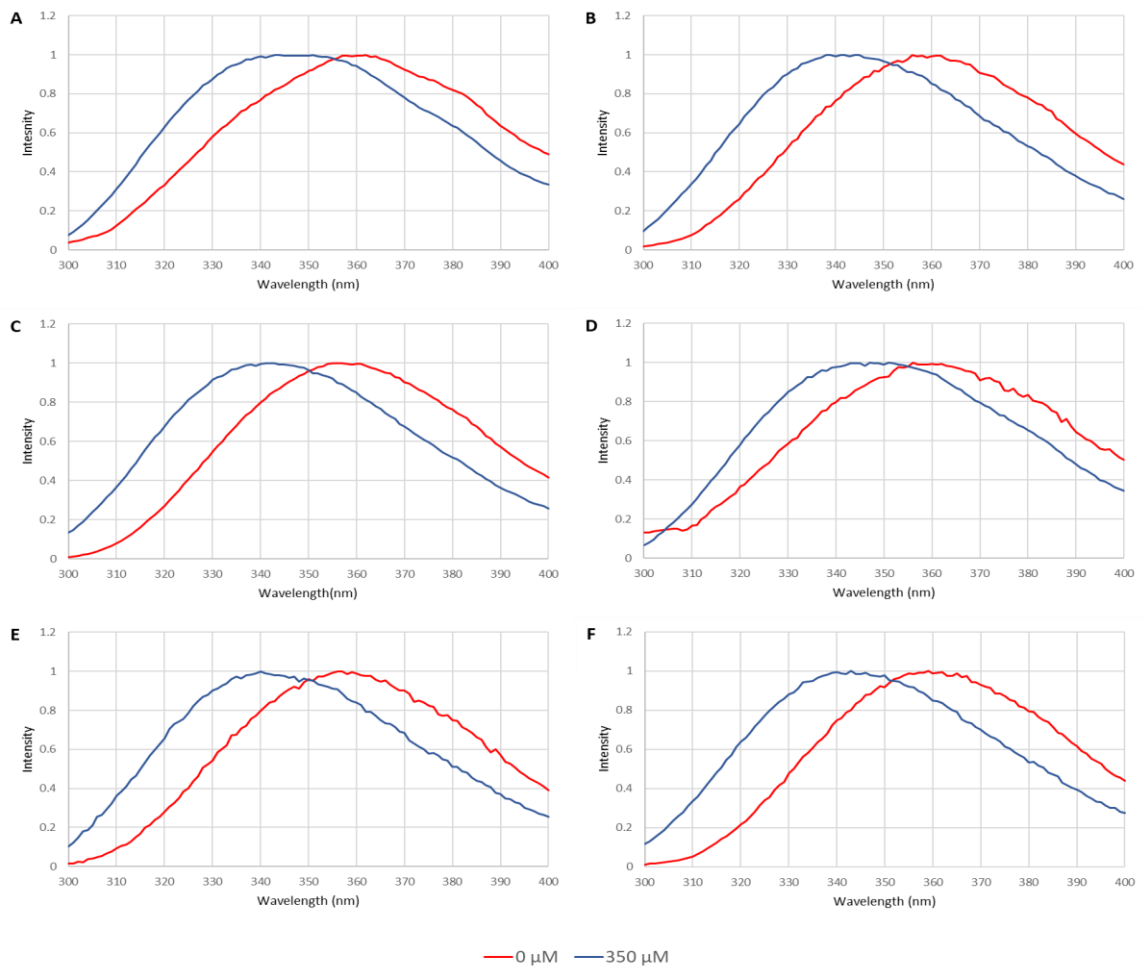
Binding to Lipid Vesicles



Note. Polymer binding was assayed using fluorescence by titrating SUVs into a polymer containing sample with a final concentration of 2 μ M. After each addition the spectral barycenter was calculated and then a Δ barycenter was calculated by taking the difference between the initial barycenter and that of each addition. Polymethacrylates that were assayed were (A) PAI-1, (B) PGI-1, (C) PAI-2, (D) PGI-2, (E) PAI-3, and (F) PGI-3. In all panels blue represents PC, orange 3:1 PC:PG, and grey 3:1 PE:PG. All data are averages of 3 replicates and SD is represented by error bars.

Figure 15

Normalized Barycenter Shifts



Note. Normalized emission spectra for PAI-1 (A), PGI-1 (B), PAI-2 (C), PGI-2 (D), PAI-3 (E), and PGI-3 (F) polymers before (red) and after (blue) interacting with lipid vesicles. Data are representative spectra after subtraction of a background spectrum. All shifts representative of samples containing 0 μM and 350 μM lipide (PC:PG).

To gather more information into the bilayer interactions, the same quenching technique was used from the previous chapter were utilized. Acrylamide strongly quenches fluorescence of Trp residues in an aqueous environment but does not exert this effect if buried into the lipid bilayer. In this case, the fluorescence of the indole was monitored for quenching by acrylamide. Stern-volmer quenching plots were created to analyze the data and K_{sv} (slopes of a linear fit to the data) are shown in Table 3. The trends represented by the data in table 3 are consistent with the barycenter shift data from figure 14. As stated previously the barycenter shift was greatest when the lipid composition contained an anionic component. The quenching assay confirms this by the reduction of quenching between the polymer being solution (free) state and when bound to the anionic vesicles. When comparing the interactions between zwitter ionic vesicles and anionic vesicles, there is a significantly smaller KSV when bound to anionic vesicles than zwitterionic. However, an interesting result is that at higher indole percentage for either series shows a significantly lower K_{sv} value. This would mean that the indole side chain PAI-1 and PGI could be significantly less exposed to the aqueous environment.

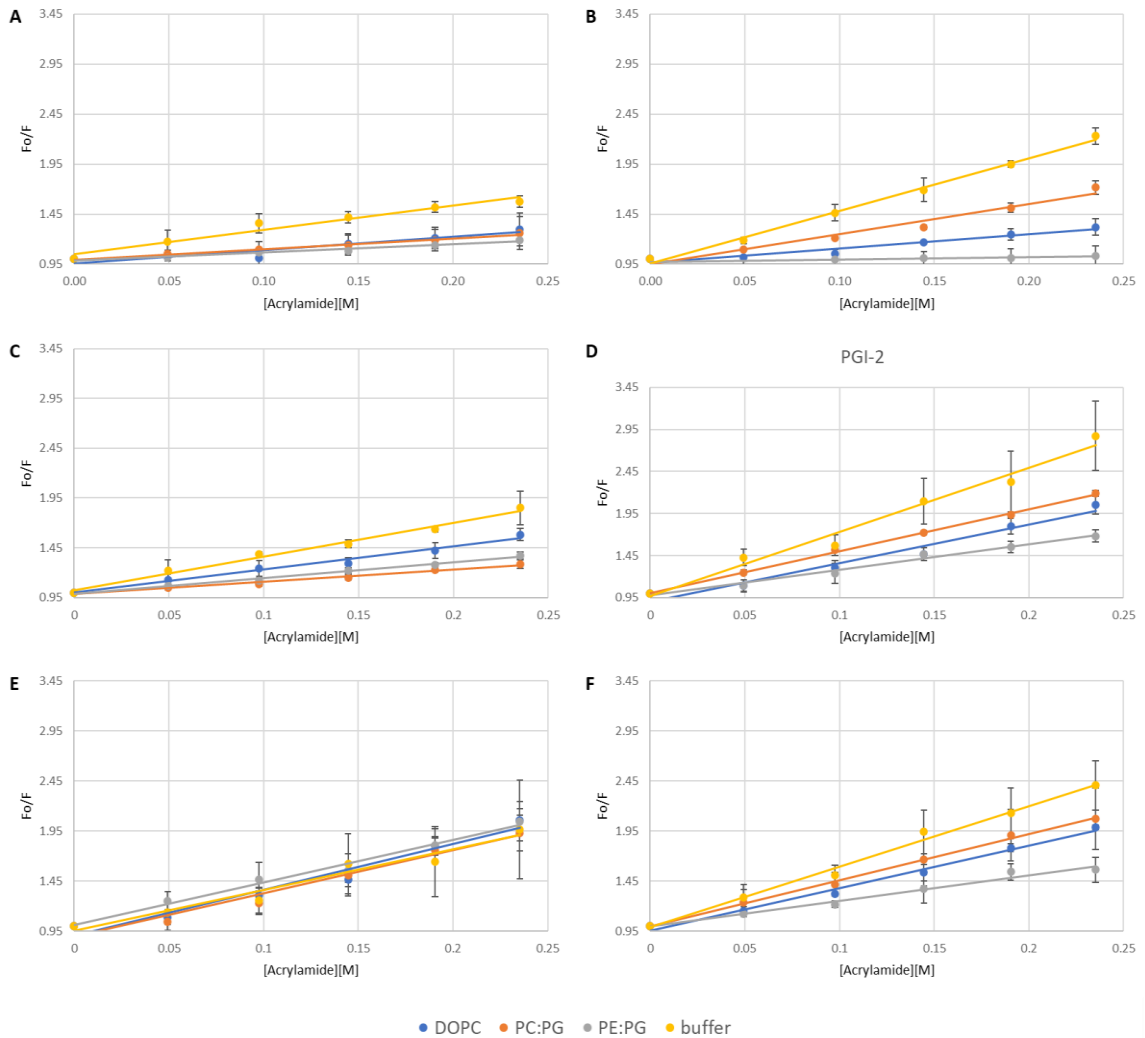
Table 4*Fluorescence Quenching*

	Acrylamide Quenching ((Ksv(M-1))											
	PBS			DOPC			PC:PG			PE:PG		
PAI-1	2.42	±	0.45	1.07	±	0.78	1.07	±	0.78	0.81	±	0.11
PAI-2	3.40	±	0.43	2.33	±	0.47	1.24	±	0.15	1.57	±	0.20
PAI-3	4.07	±	2.55	4.59	±	0.28	4.30	±	0.82	4.24	±	0.89
PGI-1	5.26	±	0.48	5.27	±	0.48	3.00	±	0.35	0.36	±	0.24
PGI-2	7.64	±	2.66	6.97	±	0.74	4.99	±	0.25	3.05	±	0.26
PGI-3	6.07	±	1.95	4.27	±	0.02	4.64	±	1.57	2.57	±	0.69

Note. Abbreviations: DOPC, 1,2-dioleoyl-sn-glycero-3-phosphocholine; DOPG, 1,2-dioleoyl-sn-glycero-3-phospho-(1'-rac-glycerol). Data are averages of 3 replicates with SD.

Figure 16

Acrylamide Quenching



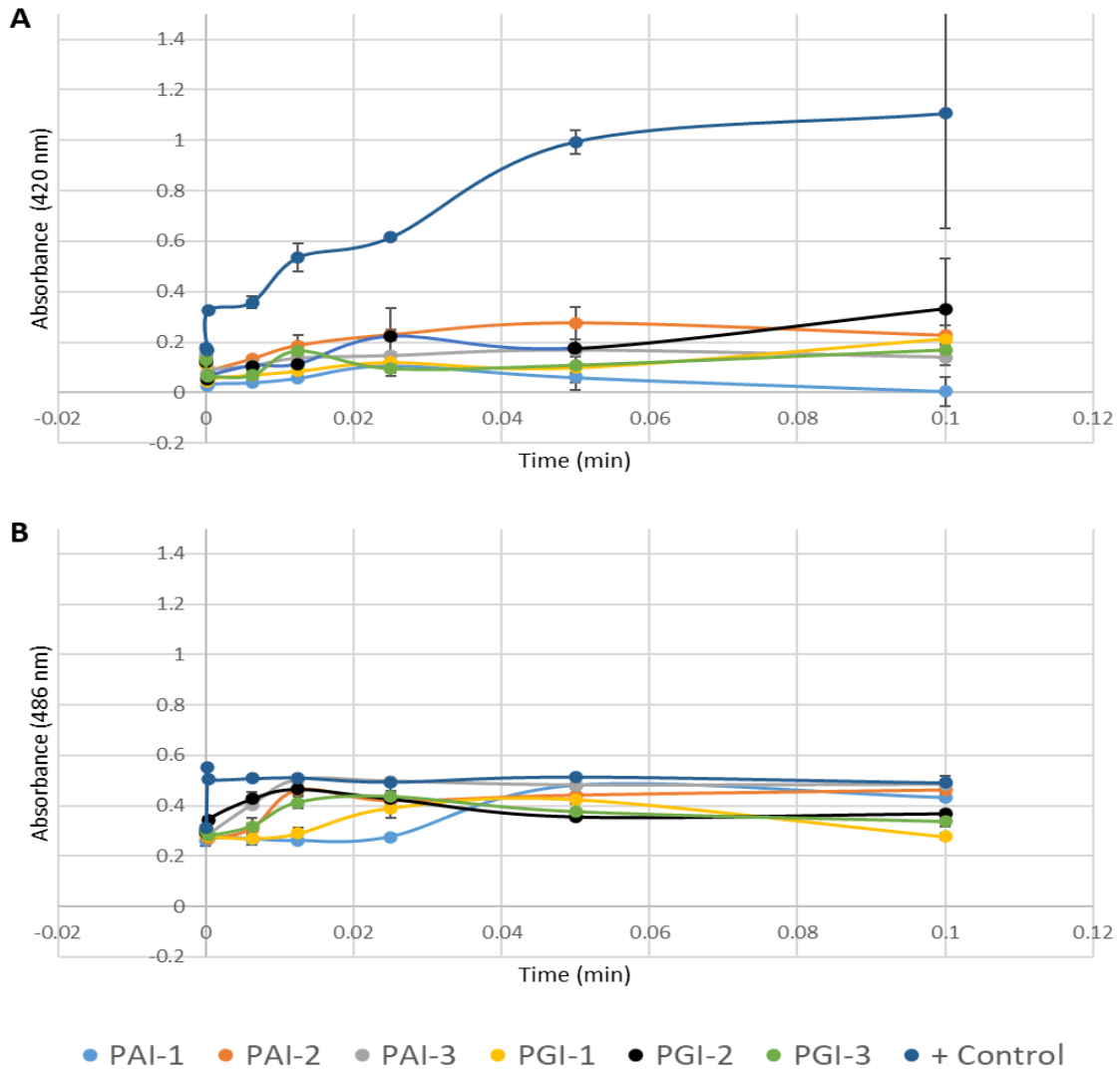
Note. Acrylamide quenching was performed on (A) PAI-1, (B) PGI-1, (C) PAI-2, (D) PGI-2, (E) PAI-3, and (F) PGI-3. Samples contained either no lipid vesicles (yellow), (blue) DOPC, (orange) PC:PG, and (grey) PE:PG. All samples contained a peptide concentration of 2 μM and lipid concentration of 250 μM for those that contained lipid vesicles. Data is corrected for inner filter effects, dilution, and are background subtracted. Data represents an average of three replicates with SD shown by the error bars.

Membrane Permeabilization

The mechanism to cationic biocides are likely to mimic that of traditional membrane disrupting AMPs. Due to the similarities of the mode of actions the effect of charge and hydrophobicity on membrane permeabilization can be investigated the same as the previous chapter. A snapshot of the outer membrane permeabilization 30 minutes after the bacterial culture was exposed to polymers is shown in Figure 13B, with full time courses shown in figure 14. The lysine-tryptohan mimicing polymers (PAI) showed similar trends to that of the arginine-tryptophan mimicking polymers (PGI) however, PAI induced permeabilization more quickly. PAI-3 showed to have permeabilized the quickest between all polymer variations. One possible explanation could be that the positively charged amide in the side chain allows for better electrostatic interactions. Interestingly enough, both series exhibited permeabilization occurred better at lower than max concentrations of the assay. Both polymer series exhibited this trend but it was most evident in the PGI series where smaller concentrations exhibited enhanced permeabilization. This could be attributed to aggregation occuring that would prevent interactions with the membrane. The PGI variants display this concept the best. The postively charged side chain that allows for better electrostatic interactions with the surface of the membrane may prevent aggregation, or reduce the effects aggregation may have on permeabilization. Although these polymers permeabilize the outer membrane, the results from the inner permeabilization assay displayed the opposite. A snap shot of the results after 30 minutes of exposure are displayed in figure 13A and a full time course in figure 15. These results elucidate that neither polymer series are capable of permeabilizing the inner membrane.

Figure 17

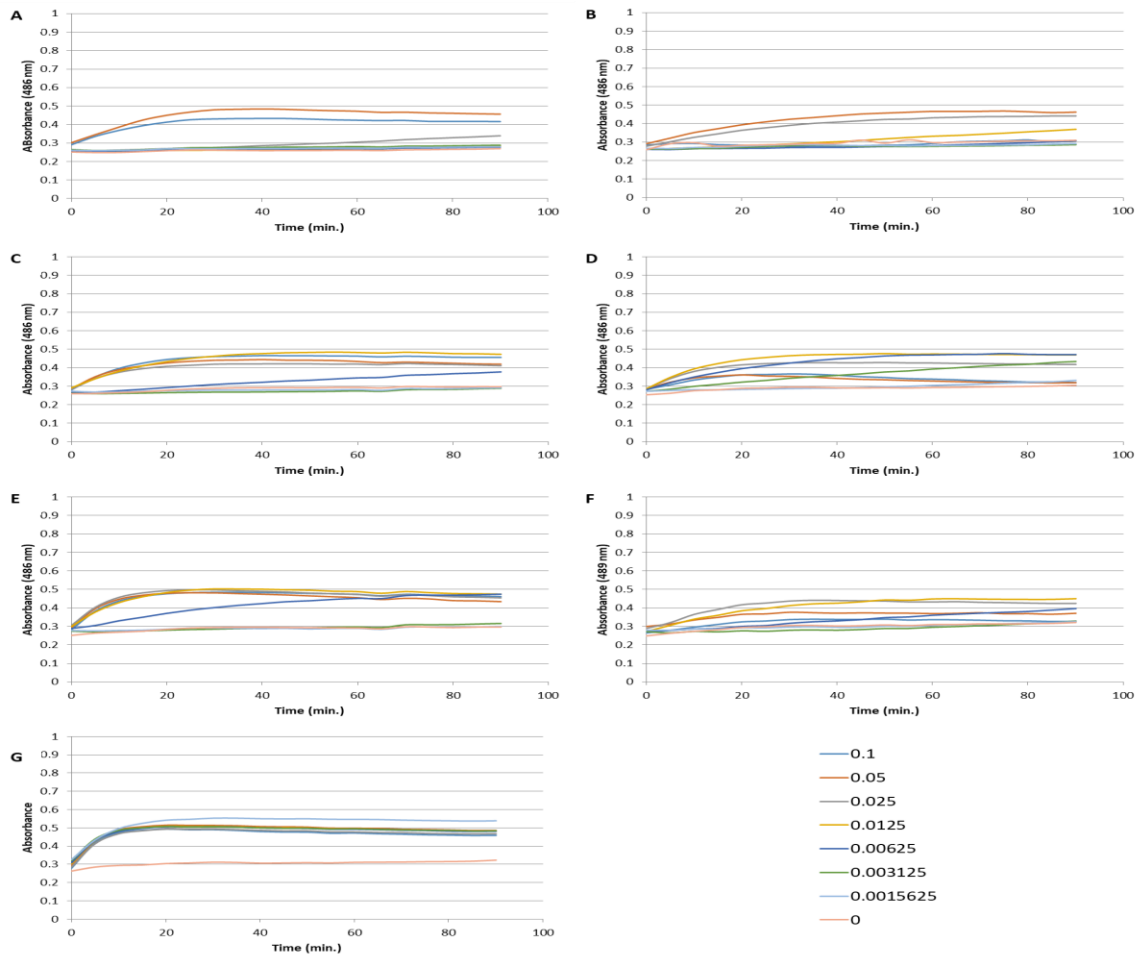
Membrane Permeabilization of E. coli



Notes. *E. coli* , (A) Inner membrane and (B) outer membrane permeabilization. For both panels PAI-1 is shown in blue, PAI-2 in orange, PAI-3 in grey, PGI-1 in yellow, PGI-2 in black, PGI-3 in green, and positive control represented by dark blue. All data are averages of three replicates and SD represented by error bars. Error bars are smaller than the size of the symbols.

Figure 18

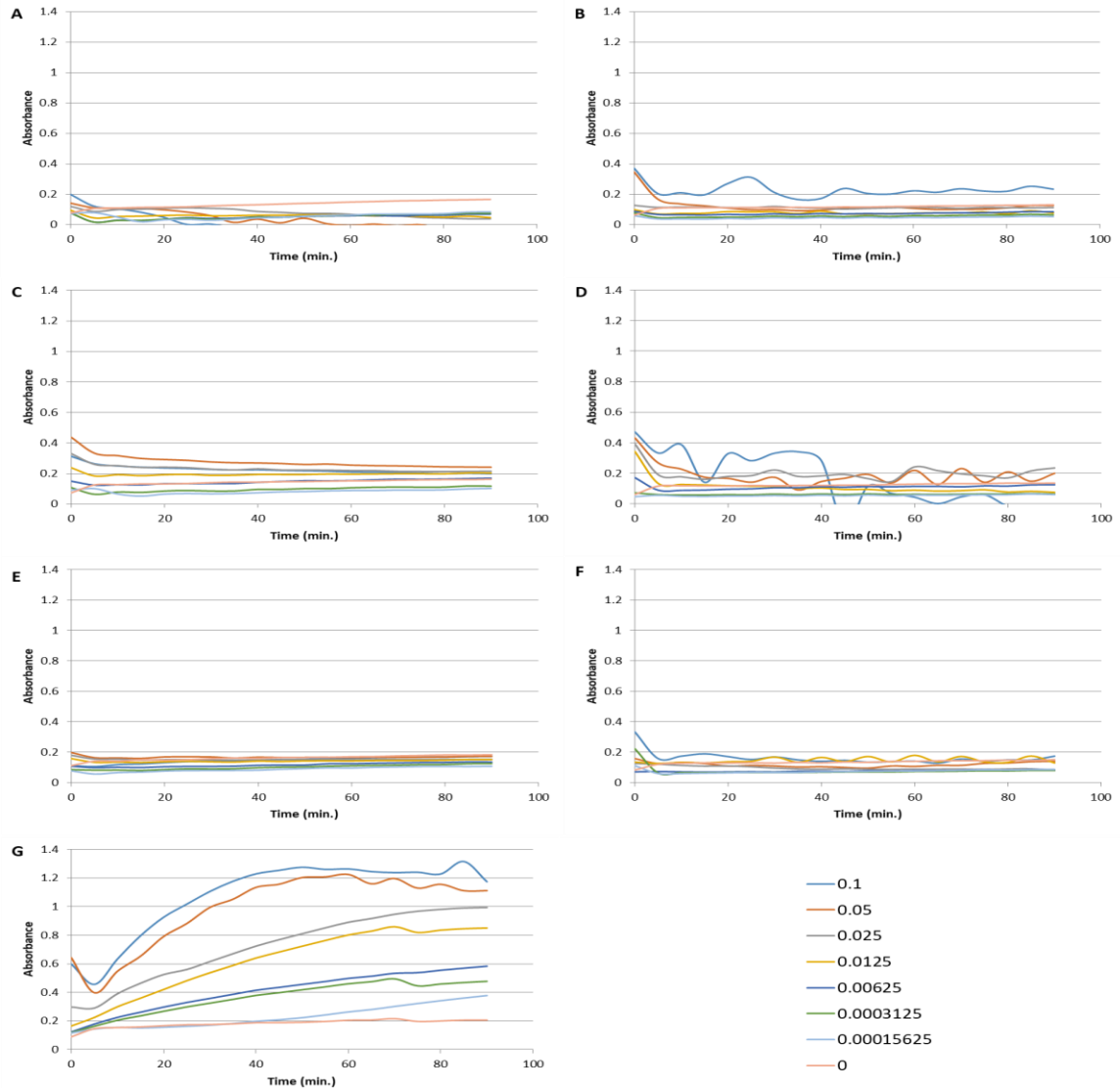
E.coli Outer Membrane Permeabilization Assay



Note. The data sets show absorbance at 486 which indicates the periplasmic enzyme β -lactamase breaking down the substrate nitrocefin. Bacteria were exposed to (A) PAI-1, (B) PGI-1, (C) PAI-2, (D) PGI-2, (E) PAI-3, (F) PGI-3, (G) Polymyxin. The legend shows the colors that represent each concentration that starts from 1 mg/mL serially diluted down to .00156 mg/mL and 0 mg/mL being the negative control. Data represents the average and SD of 3-6 samples.

Figure 19

E. coli Inner Membrane Permeabilization Assay

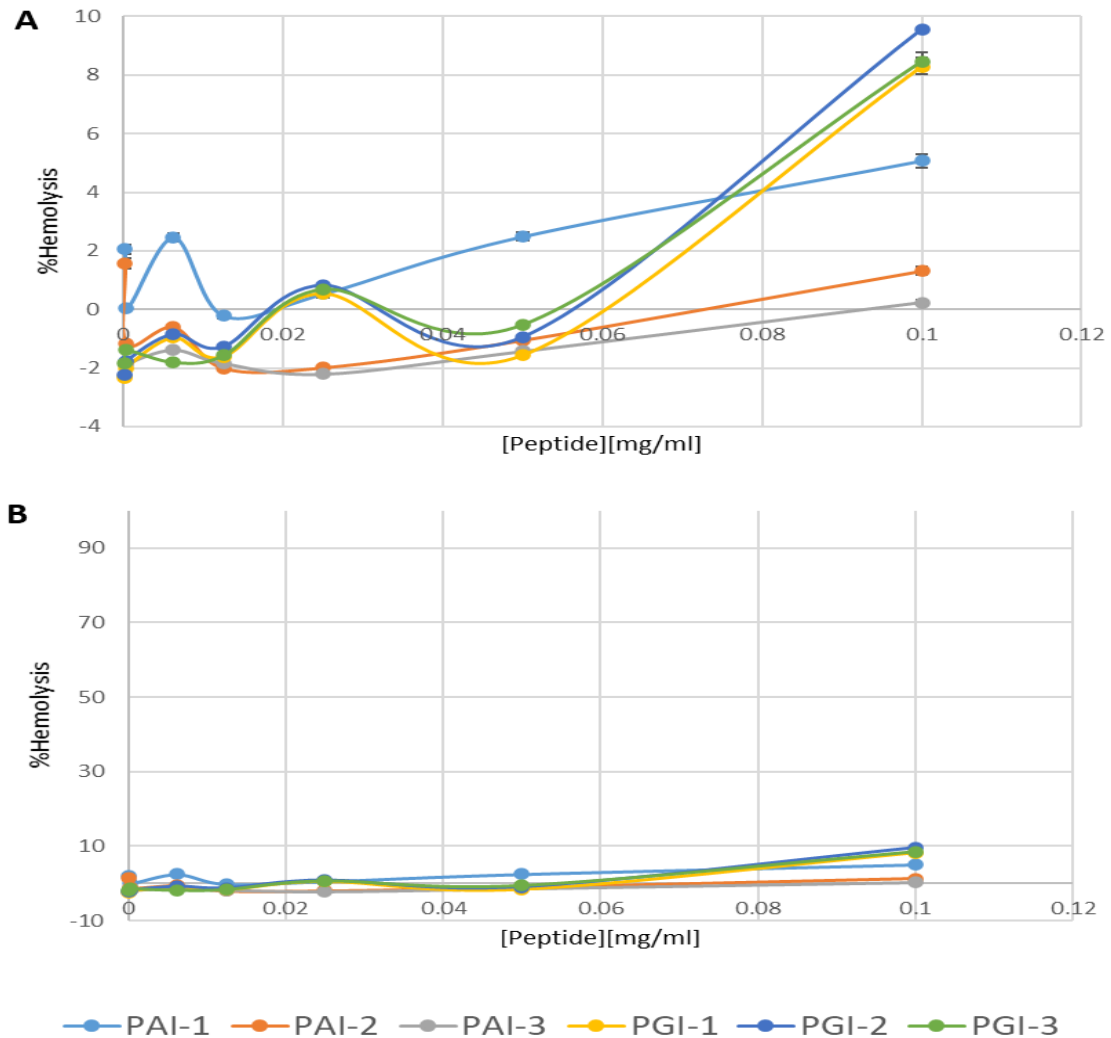


Note. These data sets show the breakdown of the ONPG substrate by the periplasmic enzyme β -galactosidase which is represented by the absorbance at 420 nm. Varying concentrations of (A) PAI-1, (B) PGI-1, (C) PAI-2, (D) PGI-2, (E) PAI-3, (F) PGI-3, (G) CTAB. The legend shows the colors that represent each concentration that starts from 1 mg/mL serially diluted down to .00156 mg/mL and 0 mg/mL being the negative control. Data represents the average and SD of 3-6 samples.

Hemolytic activity can be utilized in the same manner as it is for venom peptides and other AMPs. This activity is a valid approximation in assessing the potential for further research and development. If the hemolytic activity is too high for low concentrations than it wouldn't be useful to develop that compound further . One of the bigger disadvantages to using polymers as antimicrobial agents is the cytotoxicity. The hemolysis assay was preformed using the same ovine blood (RBC) and positive control as described in chapter 2. The results of the hemolysis assay for all polymer variants are displayed in figure 13C. These results indicate a small amount of hemolytic activity coming from the largest concentration (0.1mg/mL). The largest percent of hemolytic activity came from PGI-2 (9.5%) and the lower end coming from PAI-1 (>1%).

Figure 20

Hemolysis



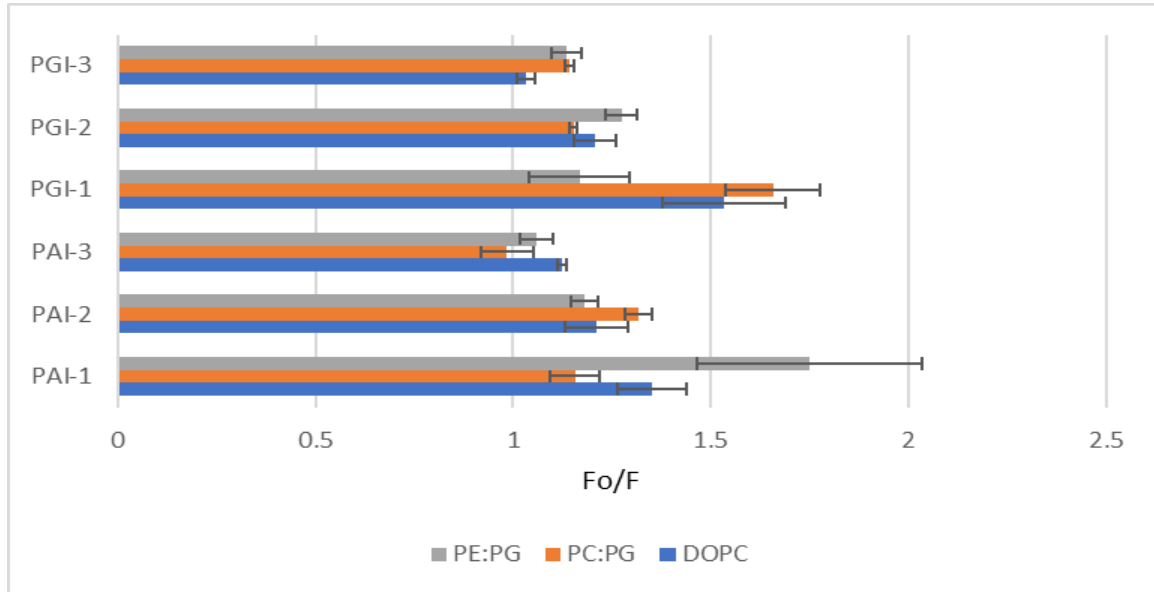
Notes. Hemolysis of RBCs. Data sets were normalized with the experimental data done on untreated RBCs (0% hemolysis) and RBCs treated with Triton X-100 (100% hemolysis). In these panels PAI-1 is shown in blue, PAI-2 in orange, PAI-3 in grey, PGI-1 in yellow, PGI-2 in black, and PGI-3 in green. Panel (A) is a smaller scale (-4% to 10%) of panel (B) (-10% to 100%). All data are averages of three replicates and SD represented by error bars. Error bars are smaller than the size of the symbols.

10-DN Quenching

10-Doxyl nonadecane (10-DN) has similar quenching features as acrylamide. However, acrylamide quenches the fluorescence of the Trp residue in aqueous solution [159-160]. 10-DN quenches fluorescence if the Trp residue is in a non-polar environment much like the lipid bilayer. This would suggest that the results from this quenching are almost the reciprocal to that of acrylamide, quenching will not happen if the Trp remains in aqueous environment. In this case, the quenching of fluorescence caused by the indole was monitored by using this assay to investigate the penetration of the indoles into the bilayer. The change in fluorescence intensity for each polymer variation is displayed in figure 21. The lipid composition of vesicles were either 100% DOPC, 3:1 PC:PG and 3:1 PE:PG. These results showed no trend in quenching in comparison to the results from the acrylamide quenching assay. For example, the results from the lipid binding experiment and acrylamide quenching assay suggest that the polymer has enhanced binding to anionic lipid compositions. However, as clear as those results were, an assessment like that cannot be made through these results.

Figure 21

10-DN Quenching



Note. The following figure shows fluorescence intensity for each polymer exposed to different lipid compositions. Blue represents DOPC, orange represents PC:PG, and grey represents PE:PG. All data was corrected for background with and without 10-DN, SD is represented by error bars.

Discussion

The work presented explains the investigation into the effects of charge and hydrophobicity on polymethacrylate polymers. These results indicate that a balance between hydrophobicity and cationic composition effect the antimicrobial activity greatly. When the cationic composition is higher, it leads to greater binding across a myriad of concentrations, however when looking the PGI series that lacks the cationic side chain only lower concentrations favored activity.

Cationic biocide polymers act in a similar fashion as AMPs where as their cationic nature allows for electrostatic interactions with the negatively charged bacterial membrane [146]. Synthesized polymers can and have been used to mimick the features of AMPs while reducing the draw backs such as manufacturing expense, easibility of production and chemical alterations, and amendability in the intergration to drug delivery systems [84]. Cationic biocide polymers must be able to preform selectively between host cells and bacterial cell surfaces to have any further development as a potential therapeutic. These results show a significant difference in binding affinity to model lipid vesicles. Both polymer series PAI and PGI show a significantly larger shift to binding to anionic lipid vesicles. This is indicative of the indole side chain undergoing a change in local environment a more non-polar one. All polymer variants caused a barycenter shift in zwitterionic lipid vesicles but the difference between that and 100% DOPC was drastically different. This would imply that the anionic component of those vesicles were the primary cause for binding. PAI-1 , PAI-2, PAI-3 seemed to show a greater affinity of binding compared to their PGI counterpart. The postively charged side chain could be responsible for this, allowing for more electrostatic interactions.

This can be further elucidated through the results of the acrylamide quenching assay. This is shown by a consistently lower Ksv displayed by the PAI series. Interestingly enough, the acrylamide quenching assay showed that for the anionic lipid model that the more cationic variants had significantly more quenching. For example, there is larger shift in barycenter for PAI-3 (6% indole) than PAI-1 (33% indole) but PAI-1 showed significantly less quenching. This could mean that although the electrostatic interactions allowed for the initial binding to the membrane, the greater hydrophobicity allowed for a deeper penetration into lipid bilayer. This becomes more evident by comparing the results of PAI-3 and PGI-3, where PGI-3 had even less quenching and more hydrophobicity. Currently, the aggregation state of the polymers as a function of concentration is being carried out using dynamic light scattering (DLS). This could effectively give the size of the polymethacrylate derivatives in solution. This study could give information on the relationship of aggregation and concentration. This could possibly show that 0.1 mg/mL is a high enough concentration to cause aggregation, preventing any significant quenching by 10-DN.

Finally there is a rather small amount of hemolytic activity which isn't totally unexpected. Hydrophobicity has been known to directly impact the cytotoxic and hemolytic activity of polymers [110,150]. To get a better understanding of the toxic profile of these polymers the hemolysis assay was an essential step. These results showed that as the ratio of cationic composition increased, the hemolytic activity was significantly less. This was interesting to see considering that the lipid binding models showed binding to the zwitterionic indicating that polymers should be able to bind to RBC or other zwitterionic mammalian membranes.

Chapter 4

Conclusions

L1 Ponericin Data

The data present in this thesis displays the hydrophobic substituted variants of the L1 peptide are membrane binding and can adopt an α -helical structure upon binding. The identity of the hydrophobic substituents play a significant role in the antimicrobial activity of this peptide. A bulkier hydrophobic substituent like phenylalanine had an overall better job at binding and permeabilizing of the membrane than smaller substituents like alanine and valine. Confirmation of the substituents could also play a role in antimicrobial activity. For example, L1L (leucine) showed significantly less binding and permeabilization than L1I (isoleucine), the substituents are isomers of each with isoleucine having a more rigid structure. These peptide variants showed secondary structures in zwitter ionic and anionic vesicles that could correlate to antimicrobial activity with the exception of the L1A variant. Peptides adopting α -helical secondary structures is a common feature when investigating the membrane disrupting abilities of AMPs. However, as shown L1A forms a α -helical structure with little to no binding in lipid models as well as antimicrobial activity. This is evidence suggesting that the degree of hydrophobicity has a direct impact. The venom peptide L1 shows great potential as a selective antimicrobial platform because of its low hemolytic activity and tunable antimicrobial activity. Future studies can be done on the overall net charge, in combination of hydrophobic/hydrophilic balance. Another useful study could be done on using non-natural amino acids in attempts to solve problems with bioavailability while

maintaining the antimicrobial activity profile and provide important fundamental understandings for designing more effective and selective antimicrobial molecules.

Polymethacrylate Data

The data presented in this thesis shows that these polymethacrylate variants have similar characteristics as traditional membrane disrupting AMPs. This becomes more prevalent in the lipid binding studies. The polymers bind better to anionic lipid vesicles than zwitter ionic suggesting electrostatic interactions is a primary mode of action. The data also suggests that there is a balance between the cationic charge and hydrophobicity of the polymethacrylate. When the side chain was cationic, binding to lipid models as well as antimicrobial activity was significantly higher. This balance also had an important role in hemolytic activity. The PAI series that contained the cationic side chain showed significantly less hemolytic activity regardless of the indole percentage. The increase hydrophobicity may have also lead to aggregation resulting in higher activity at lower concentrations of polymer. Future studies can be done to investigate the effects of the identity of cationic groups on antimicrobial activity. Overall, this study shows polymethacrylates as valid AMP mimetic polymer and a potential platform for a therapeutic agent.

References

- [1] R. Gaynes, "The Discovery of Penicillin—New Insights After More Than 75 Years of Clinical Use," *Emerging Infectious Diseases*, vol. 23, no. 5, pp. 849-853, 2017, doi: 10.3201/eid2305.161556.
- [2] S. Y. Tan and Y. Tatsumura, "Alexander Fleming (1881-1955): Discoverer of penicillin," (in eng), *Singapore medical journal*, vol. 56, no. 7, pp. 366-367, 2015, doi: 10.11622/smedj.2015105.
- [3] R. I. Aminov, "A brief history of the antibiotic era: lessons learned and challenges for the future," (in eng), *Front Microbiol*, vol. 1, pp. 134-134, 2010, doi: 10.3389/fmicb.2010.00134.
- [4] J. Davies, "Origins and Evolution of Antibiotic resistance " *Microbiology and Molecular Biology Reviews*, pp. p.417-433, September. 2010 2010.
- [5] K. Duncan Seraphin, "Weird Science: Penicillin and the Cell Wall," ed: Exploring Our Fluid Earth 2021.
- [6] F. D. Lowy, "Antimicrobial resistance: the example of *Staphylococcus aureus*," (in eng), *J Clin Invest*, vol. 111, no. 9, pp. 1265-1273, 2003, doi: 10.1172/JCI18535.
- [7] "Antibiotics 1928-2000," ed: Australian Broadcasting Corporation
- [8] M. A. Kohanski, D. J. Dwyer, and J. J. Collins, "How antibiotics kill bacteria: from targets to networks," (in eng), *Nat Rev Microbiol*, vol. 8, no. 6, pp. 423-435, 2010, doi: 10.1038/nrmicro2333.
- [9] J. B. Sauberan and J. S. Bradley, "292 - Antimicrobial Agents," in *Principles and Practice of Pediatric Infectious Diseases (Fifth Edition)*, S. S. Long, C. G. Prober, and M. Fischer Eds.: Elsevier, 2018, pp. 1499-1531.e3.
- [10] B. Kocsis, J. Domokos, and D. Szabo, "Chemical structure and pharmacokinetics of novel quinolone agents represented by avarofloxacin, delafloxacin, finafloxacin, zabofloxacin and nemonoxacin," *Annals of Clinical Microbiology and Antimicrobials*, vol. 15, no. 1, p. 34, 2016/05/23 2016, doi: 10.1186/s12941-016-0150-4.
- [11] M. Kidwai, P. Misra, and R. Kumar, "The fluorinated quinolones," (in eng), *Curr Pharm Des*, vol. 4, no. 2, pp. 101-18, Apr 1998.
- [12] M. X. Ho, B. P. Hudson, K. Das, E. Arnold, and R. H. Ebright, "Structures of RNA polymerase-antibiotic complexes," (in eng), *Curr Opin Struct Biol*, vol. 19, no. 6, pp. 715-723, 2009, doi: 10.1016/j.sbi.2009.10.010.

- [13] A. Feklistov *et al.*, "Rifamycins do not function by allosteric modulation of binding of Mg²⁺ to the RNA polymerase active center," (in eng), *Proc Natl Acad Sci U S A*, vol. 105, no. 39, pp. 14820-14825, 2008, doi: 10.1073/pnas.0802822105.
- [14] A. Feklistov *et al.*, "Rifamycins do not function by allosteric modulation of binding of Mg²⁺ to the RNA polymerase active center," (in eng), *Proc Natl Acad Sci U S A*, vol. 105, no. 39, pp. 14820-14825, 2008, doi: 10.1073/pnas.0802822105.
- [15] P. Sarkar, V. Yarlagadda, C. Ghosh, and J. Haldar, "A review on cell wall synthesis inhibitors with an emphasis on glycopeptide antibiotics," (in eng), *Medchemcomm*, vol. 8, no. 3, pp. 516-533, 2017, doi: 10.1039/c6md00585c.
- [16] "Protein Sythesis Inhibitors." (accessed July 05, 2021).
- [17] E. Martin, G. Lina, and O. Dumitrescu, "STAPHYLOCOCCUS | Staphylococcus aureus," in *Encyclopedia of Food Microbiology (Second Edition)*, C. A. Batt and M. L. Tortorello Eds. Oxford: Academic Press, 2014, pp. 501-507.
- [18] P. Blanco *et al.*, "Bacterial Multidrug Efflux Pumps: Much More Than Antibiotic Resistance Determinants," (in eng), *Microorganisms*, vol. 4, no. 1, p. 14, 2016, doi: 10.3390/microorganisms4010014.
- [19] H. Nikaido, "Multidrug resistance in bacteria," (in eng), *Annu Rev Biochem*, vol. 78, pp. 119-146, 2009, doi: 10.1146/annurev.biochem.78.082907.145923.
- [20] P. Cornejo-Juárez, D. Vilar-Compte, C. Pérez-Jiménez, S. A. Ñamendys-Silva, S. Sandoval-Hernández, and P. Volkow-Fernández, "The impact of hospital-acquired infections with multidrug-resistant bacteria in an oncology intensive care unit," *International Journal of Infectious Diseases*, vol. 31, pp. 31-34, 2015, doi: 10.1016/j.ijid.2014.12.022.
- [21] K. Kumar and I. Abubakar, "Clinical implications of the global multidrug-resistant tuberculosis epidemic," *Clinical Medicine*, vol. 16, no. 6, pp. 565-570, 2016, doi: 10.7861/clinmedicine.16-6-565.
- [22] T. Tängdén, "Combination antibiotic therapy for multidrug-resistant Gram-negative bacteria," (in eng), *Ups J Med Sci*, vol. 119, no. 2, pp. 149-153, 2014, doi: 10.3109/03009734.2014.899279.
- [23] W. Chin *et al.*, "A macromolecular approach to eradicate multidrug resistant bacterial infections while mitigating drug resistance onset," *Nature Communications*, vol. 9, no. 1, 2018, doi: 10.1038/s41467-018-03325-6.
- [24] C. Brives and J. Pourraz, "Phage therapy as a potential solution in the fight against AMR: obstacles and possible futures," *Palgrave Communications*, vol. 6, no. 1, 2020, doi: 10.1057/s41599-020-0478-4.

- [25] K. E. Kortright, B. K. Chan, J. L. Koff, and P. E. Turner, "Phage Therapy: A Renewed Approach to Combat Antibiotic-Resistant Bacteria," *Cell Host & Microbe*, vol. 25, no. 2, pp. 219-232, 2019, doi: 10.1016/j.chom.2019.01.014.
- [26] R. J. Turner, "Metal-based antimicrobial strategies," (in eng), *Microb Biotechnol*, vol. 10, no. 5, pp. 1062-1065, 2017, doi: 10.1111/1751-7915.12785.
- [27] G. M. Teitzel and M. R. Parsek, "Heavy metal resistance of biofilm and planktonic *Pseudomonas aeruginosa*," (in eng), *Appl Environ Microbiol*, vol. 69, no. 4, pp. 2313-2320, 2003, doi: 10.1128/AEM.69.4.2313-2320.2003.
- [28] A. A. Bahar and D. Ren, "Antimicrobial peptides," (in eng), *Pharmaceuticals (Basel)*, vol. 6, no. 12, pp. 1543-1575, 2013, doi: 10.3390/ph6121543.
- [29] B. El Shazely, G. Yu, P. R. Johnston, and J. Rolff, "Resistance Evolution Against Antimicrobial Peptides in *Staphylococcus aureus* Alters Pharmacodynamics Beyond the MIC," (in English), *Front Microbiol*, Original Research vol. 11, no. 103, 2020-February-14 2020, doi: 10.3389/fmicb.2020.00103.
- [30] "Antimicrobial Peptides: Their History, Evolution, and Functional Promiscuity," in *Antimicrobial Peptides*, pp. 1-37.
- [31] K. P. Sai *et al.*, "Tigerinins: Novel Antimicrobial Peptides from the Indian Frog *Rana tigerina*," *Journal of Biological Chemistry*, vol. 276, no. 4, pp. 2701-2707, 2001, doi: 10.1074/jbc.m006615200.
- [32] J. Lei *et al.*, "The antimicrobial peptides and their potential clinical applications," (in eng), *Am J Transl Res*, vol. 11, no. 7, pp. 3919-3931, 2019. [Online]. Available: <https://pubmed.ncbi.nlm.nih.gov/31396309>.
- [33] N. Antcheva, F. Guida, and A. Tossi, "Chapter 18 - Defensins," in *Handbook of Biologically Active Peptides (Second Edition)*, A. J. Kastin Ed. Boston: Academic Press, 2013, pp. 101-118.
- [34] G. Ye *et al.*, "LAMP2: a major update of the database linking antimicrobial peptides," *Database: The Journal of Biological Databases and Curation*, vol. 2020, 2020.
- [35] M. H. Cardoso *et al.*, "Computer-Aided Design of Antimicrobial Peptides: Are We Generating Effective Drug Candidates?," (in English), *Front Microbiol*, Review vol. 10, no. 3097, 2020-January-22 2020, doi: 10.3389/fmicb.2019.03097.
- [36] S. Elnagdy and M. Alkhazindar, "The Potential of Antimicrobial Peptides as an Antiviral Therapy against COVID-19," *ACS Pharmacology & Translational Science*, vol. 3, no. 4, pp. 780-782, 2020, doi: 10.1021/acspsci.0c00059.

- [37] N. Delattin, K. Brucker, K. Cremer, B. P. Cammue, and K. Thevissen, "Antimicrobial Peptides as a Strategy to Combat Fungal Biofilms," (in eng), *Curr Top Med Chem*, vol. 17, no. 5, pp. 604-612, 2017, doi: 10.2174/1568026616666160713142228.
- [38] M. Torrent, D. Pulido, L. Rivas, and D. Andreu, "Antimicrobial peptide action on parasites," (in eng), *Curr Drug Targets*, vol. 13, no. 9, pp. 1138-47, Aug 2012, doi: 10.2174/138945012802002393.
- [39] G.-M. Kong *et al.*, "Melittin induces human gastric cancer cell apoptosis via activation of mitochondrial pathway," (in eng), *World J Gastroenterol*, vol. 22, no. 11, pp. 3186-3195, 2016, doi: 10.3748/wjg.v22.i11.3186.
- [40] H.-T. Lee, C.-C. Lee, J.-R. Yang, J. Z. C. Lai, and K. Y. Chang, "A large-scale structural classification of antimicrobial peptides," (in eng), *Biomed Res Int*, vol. 2015, pp. 475062-475062, 2015, doi: 10.1155/2015/475062.
- [41] M. Dathe and T. Wieprecht, "Structural features of helical antimicrobial peptides: their potential to modulate activity on model membranes and biological cells," *Biochimica et Biophysica Acta (BBA) - Biomembranes*, vol. 1462, no. 1-2, pp. 71-87, 1999, doi: 10.1016/s0005-2736(99)00201-1.
- [42] Y. Huan, Q. Kong, H. Mou, and H. Yi, "Antimicrobial Peptides: Classification, Design, Application and Research Progress in Multiple Fields," (in English), *Front Microbiol*, Review vol. 11, no. 2559, 2020-October-16 2020, doi: 10.3389/fmicb.2020.582779.
- [43] P. Petkov, E. Lilkova, N. Ilieva, and L. Litov, "Self-Association of Antimicrobial Peptides: A Molecular Dynamics Simulation Study on Bombinin," (in eng), *Int J Mol Sci*, vol. 20, no. 21, p. 5450, 2019, doi: 10.3390/ijms20215450.
- [44] Z. G. Wang, "Curvature instability of diblock copolymer bilayers," *Macromolecules*, vol. 25, no. 14, pp. 3702-3705, 1992/07/01 1992, doi: 10.1021/ma00040a015.
- [45] N. W. Schmidt and G. C. L. Wong, "Antimicrobial peptides and induced membrane curvature: geometry, coordination chemistry, and molecular engineering," (in eng), *Curr Opin Solid State Mater Sci*, vol. 17, no. 4, pp. 151-163, 2013, doi: 10.1016/j.cossms.2013.09.004.
- [46] H.-K. Kang, C. Kim, C. H. Seo, and Y. Park, "The therapeutic applications of antimicrobial peptides (AMPs): a patent review," *Journal of Microbiology*, vol. 55, no. 1, pp. 1-12, 2017, doi: 10.1007/s12275-017-6452-1.

- [47] M. Stöckl, P. Fischer, E. Wanker, and A. Herrmann, "Alpha-synuclein selectively binds to anionic phospholipids embedded in liquid-disordered domains," (in eng), *J Mol Biol*, vol. 375, no. 5, pp. 1394-404, Feb 1 2008, doi: 10.1016/j.jmb.2007.11.051.
- [48] H. Sato and J. B. Feix, "Peptide–membrane interactions and mechanisms of membrane destruction by amphipathic α -helical antimicrobial peptides," *Biochimica et Biophysica Acta (BBA) - Biomembranes*, vol. 1758, no. 9, pp. 1245-1256, 2006, doi: 10.1016/j.bbamem.2006.02.021.
- [49] Y. Wang, D. E. Schlamadinger, J. E. Kim, and J. A. McCammon, "Comparative molecular dynamics simulations of the antimicrobial peptide CM15 in model lipid bilayers," *Biochimica et Biophysica Acta (BBA) - Biomembranes*, vol. 1818, no. 5, pp. 1402-1409, 2012, doi: 10.1016/j.bbamem.2012.02.017.
- [50] T. M. Domingues, K. R. Perez, A. Miranda, and K. A. Riske, "Comparative study of the mechanism of action of the antimicrobial peptide gomesin and its linear analogue: The role of the β -hairpin structure," *Biochimica et Biophysica Acta (BBA) - Biomembranes*, vol. 1848, no. 10, Part A, pp. 2414-2421, 2015/10/01/ 2015, doi: <https://doi.org/10.1016/j.bbamem.2015.07.012>.
- [51] B. S. Perrin, Jr. and R. W. Pastor, "Simulations of Membrane-Disrupting Peptides I: Alamethicin Pore Stability and Spontaneous Insertion," (in eng), *Biophys J*, vol. 111, no. 6, pp. 1248-1257, Sep 20 2016, doi: 10.1016/j.bpj.2016.08.014.
- [52] H. Ulm, M. Wilmes, Y. Shai, and H.-G. Sahl, "Antimicrobial Host Defensins – Specific Antibiotic Activities and Innate Defense Modulation," (in English), *Frontiers in Immunology*, Opinion vol. 3, no. 249, 2012-August-14 2012, doi: 10.3389/fimmu.2012.00249.
- [53] M. Yasir, D. Dutta, and M. D. P. Willcox, "Comparative mode of action of the antimicrobial peptide melimine and its derivative Mel4 against *Pseudomonas aeruginosa*," *Scientific Reports*, vol. 9, no. 1, 2019, doi: 10.1038/s41598-019-42440-2.
- [54] M. Mardirossian *et al.*, "The Host Antimicrobial Peptide Bac71-35 Binds to Bacterial Ribosomal Proteins and Inhibits Protein Synthesis," *Chemistry & Biology*, vol. 21, no. 12, pp. 1639-1647, 2014, doi: 10.1016/j.chembiol.2014.10.009.
- [55] P. Kumar, J. N. Kizhakkedathu, and S. K. Straus, "Antimicrobial Peptides: Diversity, Mechanism of Action and Strategies to Improve the Activity and Biocompatibility In Vivo," (in eng), *Biomolecules*, vol. 8, no. 1, p. 4, 2018, doi: 10.3390/biom8010004.

- [56] J. Lei *et al.*, "The antimicrobial peptides and their potential clinical applications," (in eng), *Am J Transl Res*, vol. 11, no. 7, pp. 3919-3931, 2019.
- [57] M. Zasloff, "Magainins, a class of antimicrobial peptides from *Xenopus* skin: isolation, characterization of two active forms, and partial cDNA sequence of a precursor," *Proceedings of the National Academy of Sciences*, vol. 84, no. 15, pp. 5449-5453, 1987, doi: 10.1073/pnas.84.15.5449.
- [58] K. Matsuzaki, K.-I. Sugishita, M. Harada, N. Fujii, and K. Miyajima, "Interactions of an antimicrobial peptide, magainin 2, with outer and inner membranes of Gram-negative bacteria," *Biochimica et Biophysica Acta (BBA) - Biomembranes*, vol. 1327, no. 1, pp. 119-130, 1997, doi: 10.1016/s0005-2736(97)00051-5.
- [59] K. Matsuzaki, K. Sugishita, N. Fujii, and K. Miyajima, "Molecular Basis for Membrane Selectivity of an Antimicrobial Peptide, Magainin 2," *Biochemistry*, vol. 34, no. 10, pp. 3423-3429, 1995/03/01 1995, doi: 10.1021/bi00010a034.
- [60] K. Matsuzaki, "Control of cell selectivity of antimicrobial peptides," *Biochimica et Biophysica Acta (BBA) - Biomembranes*, vol. 1788, no. 8, pp. 1687-1692, 2009, doi: 10.1016/j.bbamem.2008.09.013.
- [61] R. M. Eppard, C. Walker, R. F. Eppard, and N. A. Magarvey, "Molecular mechanisms of membrane targeting antibiotics," (in eng), *Biochim Biophys Acta*, vol. 1858, no. 5, pp. 980-7, May 2016, doi: 10.1016/j.bbamem.2015.10.018.
- [62] G. Ehrenstein and H. Lecar, "Electrically gated ionic channels in lipid bilayers," (in eng), *Q Rev Biophys*, vol. 10, no. 1, pp. 1-34, Feb 1977, doi: 10.1017/s0033583500000123.
- [63] K. A. Brogden, "Antimicrobial peptides: pore formers or metabolic inhibitors in bacteria?," (in eng), *Nat Rev Microbiol*, vol. 3, no. 3, pp. 238-50, Mar 2005, doi: 10.1038/nrmicro1098.
- [64] F. Costa, I. F. Carvalho, R. C. Montelaro, P. Gomes, and M. C. Martins, "Covalent immobilization of antimicrobial peptides (AMPs) onto biomaterial surfaces," (in eng), *Acta Biomater*, vol. 7, no. 4, pp. 1431-40, Apr 2011, doi: 10.1016/j.actbio.2010.11.005.
- [65] N. Papo, Z. Oren, U. Pag, H. G. Sahl, and Y. Shai, "The consequence of sequence alteration of an amphipathic alpha-helical antimicrobial peptide and its diastereomers," (in eng), *J Biol Chem*, vol. 277, no. 37, pp. 33913-21, Sep 13 2002, doi: 10.1074/jbc.M204928200.

- [66] H. V. Westerhoff, D. Juretić, R. W. Hendler, and M. Zasloff, "Magainins and the disruption of membrane-linked free-energy transduction," (in eng), *Proc Natl Acad Sci U S A*, vol. 86, no. 17, pp. 6597-6601, 1989, doi: 10.1073/pnas.86.17.6597.
- [67] Z. Liu *et al.*, "Length effects in antimicrobial peptides of the (RW)_n series," (in eng), *Antimicrob Agents Chemother*, vol. 51, no. 2, pp. 597-603, 2007, doi: 10.1128/AAC.00828-06.
- [68] Z. Jiang, A. I. Vasil, J. D. Hale, R. E. W. Hancock, M. L. Vasil, and R. S. Hodges, "Effects of net charge and the number of positively charged residues on the biological activity of amphipathic alpha-helical cationic antimicrobial peptides," (in eng), *Biopolymers*, vol. 90, no. 3, pp. 369-383, 2008, doi: 10.1002/bip.20911.
- [69] Z. Ye and C. Aparicio, "Modulation of supramolecular self-assembly of an antimicrobial designer peptide by single amino acid substitution: implications on peptide activity," *Nanoscale Advances*, vol. 1, no. 12, pp. 4679-4682, 2019, doi: 10.1039/c9na00498j.
- [70] K. D. Saint Jean, K. D. Henderson, C. L. Chrom, L. E. Abiuso, L. M. Renn, and G. A. Caputo, "Effects of Hydrophobic Amino Acid Substitutions on Antimicrobial Peptide Behavior," (in eng), *Probiotics Antimicrob Proteins*, vol. 10, no. 3, pp. 408-419, Sep 2018, doi: 10.1007/s12602-017-9345-z.
- [71] D. Andreu, R. B. Merrifield, H. Steiner, and H. G. Boman, "N-terminal analogues of cecropin A: synthesis, antibacterial activity, and conformational properties," (in eng), *Biochemistry*, vol. 24, no. 7, pp. 1683-8, Mar 26 1985, doi: 10.1021/bi00328a017.
- [72] H. Sato and J. B. Feix, "Peptide–membrane interactions and mechanisms of membrane destruction by amphipathic α -helical antimicrobial peptides," *Biochimica et Biophysica Acta (BBA) - Biomembranes*, vol. 1758, no. 9, pp. 1245-1256, 2006, doi: 10.1016/j.bbamem.2006.02.021.
- [73] Y. Zai *et al.*, "Aggregation and Its Influence on the Bioactivities of a Novel Antimicrobial Peptide, Temporin-PF, and Its Analogues," *Int J Mol Sci*, vol. 22, no. 9, p. 4509, 2021, doi: 10.3390/ijms22094509.
- [74] B. H. Gan, J. Gaynord, S. M. Rowe, T. Deingruber, and D. R. Spring, "The multifaceted nature of antimicrobial peptides: current synthetic chemistry approaches and future directions," *Chemical Society Reviews*, 2021, doi: 10.1039/d0cs00729c.
- [75] Z. Cui *et al.*, "Molecular engineering of antimicrobial peptide (AMP)–polymer conjugates," *Biomaterials Science*, 2021, doi: 10.1039/d1bm00423a.

- [76] S. D. Petrova, V. N. Atanasov, and K. Balashev, "Chapter 5 - Vipoxin and Its Components: Structure–Function Relationship," in *Advances in Protein Chemistry and Structural Biology*, vol. 87, C. Christov and T. Karabancheva-Christova Eds.: Academic Press, 2012, pp. 117-153.
- [77] A. Lahiani, E. Yavin, and P. Lazarovici, "The Molecular Basis of Toxins' Interactions with Intracellular Signaling via Discrete Portals," (in eng), *Toxins (Basel)*, vol. 9, no. 3, p. 107, 2017, doi: 10.3390/toxins9030107.
- [78] R. J. Lewis and M. L. Garcia, "Therapeutic potential of venom peptides," *Nature Reviews Drug Discovery*, vol. 2, no. 10, pp. 790-802, 2003, doi: 10.1038/nrd1197.
- [79] R. Sinha and P. Shukla, "Antimicrobial Peptides: Recent Insights on Biotechnological Interventions and Future Perspectives," (in eng), *Protein Pept Lett*, vol. 26, no. 2, pp. 79-87, 2019, doi: 10.2174/0929866525666181026160852.
- [80] P. Cardoso *et al.*, "Molecular engineering of antimicrobial peptides: microbial targets, peptide motifs and translation opportunities," *Biophysical Reviews*, vol. 13, no. 1, pp. 35-69, 2021, doi: 10.1007/s12551-021-00784-y.
- [81] H. Takahashi, G. A. Caputo, and K. Kuroda, "Amphiphilic polymer therapeutics: an alternative platform in the fight against antibiotic resistant bacteria," *Biomaterials Science*, vol. 9, no. 8, pp. 2758-2767, 2021, doi: 10.1039/d0bm01865a.
- [82] K. E. S. Locock *et al.*, "Guanylated Polymethacrylates: A Class of Potent Antimicrobial Polymers with Low Hemolytic Activity," *Biomacromolecules*, vol. 14, no. 11, pp. 4021-4031, 2013, doi: 10.1021/bm401128r.
- [83] K. E. S. Locock, T. D. Michl, H. J. Griesser, M. Haeussler, and L. Meagher, "Structure–activity relationships of guanylated antimicrobial polymethacrylates," *Pure and Applied Chemistry*, vol. 86, no. 8, pp. 1281-1291, 2014, doi: doi:10.1515/pac-2014-0213.
- [84] C. A. Schmidt and S. O. Shattuck, "The Higher Classification of the Ant Subfamily Ponerinae (Hymenoptera: Formicidae), with a Review of Ponerine Ecology and Behavior," (in eng), *Zootaxa*, vol. 3817, pp. 1-242, Jun 18 2014, doi: 10.11646/zootaxa.3817.1.1.
- [85] R. P. Santos *et al.*, "Genetic Characterization of Some Neoponera (Hymenoptera: Formicidae) Populations Within the foetida Species Complex," (in eng), *J Insect Sci*, vol. 18, no. 4, p. 14, 2018, doi: 10.1093/jisesa/iey079.
- [86] J. Orivel *et al.*, "Ponericins, New Antibacterial and Insecticidal Peptides from the Venom of the Ant *Pachycondyla goeldii*," *Journal of Biological Chemistry*, vol. 276, no. 21, pp. 17823-17829, 2001, doi: 10.1074/jbc.m100216200.

- [87] J. Orivel *et al.*, "Ponericins, new antibacterial and insecticidal peptides from the venom of the ant *Pachycondyla goeldii*," (in eng), *J Biol Chem*, vol. 276, no. 21, pp. 17823-9, May 25 2001, doi: 10.1074/jbc.M100216200.
- [88] A. S. Senetra, M. R. Necelis, and G. A. Caputo, "Investigation of the structure-activity relationship in ponericin L1 from *Neoponera goeldii*," (in eng), *Pept Sci (Hoboken)*, vol. 112, no. 3, May 2020, doi: 10.1002/pep2.24162.
- [89] I. Wiegand, K. Hilpert, and R. E. W. Hancock, "Agar and broth dilution methods to determine the minimal inhibitory concentration (MIC) of antimicrobial substances," *Nature Protocols*, vol. 3, no. 2, pp. 163-175, 2008/02/01 2008, doi: 10.1038/nprot.2007.521.
- [90] G. Rani, K. Kuroda, and S. Vemparala, "Aggregation of methacrylate-based ternary biomimetic antimicrobial polymers in solution," (in eng), *J Phys Condens Matter*, vol. 33, no. 6, p. 064003, Feb 10 2020, doi: 10.1088/1361-648X/abc4c9.
- [91] S. Haldar, H. Raghuraman, and A. Chattopadhyay, "Monitoring Orientation and Dynamics of Membrane-Bound Melittin Utilizing Dansyl Fluorescence," *The Journal of Physical Chemistry B*, vol. 112, no. 44, pp. 14075-14082, 2008/11/06 2008, doi: 10.1021/jp805299g.
- [92] Z. Vaezi *et al.*, "Aggregation determines the selectivity of membrane-active anticancer and antimicrobial peptides: The case of killerFLIP," (in eng), *Biochim Biophys Acta Biomembr*, vol. 1862, no. 2, p. 183107, Feb 1 2020, doi: 10.1016/j.bbamem.2019.183107.
- [93] K. L. Zapadka, F. J. Becher, A. L. Gomes Dos Santos, and S. E. Jackson, "Factors affecting the physical stability (aggregation) of peptide therapeutics," (in eng), *Interface Focus*, vol. 7, no. 6, p. 20170030, Dec 6 2017, doi: 10.1098/rsfs.2017.0030.
- [94] A. S. Ladokhin, M. E. Selsted, and S. H. White, "Bilayer interactions of indolicidin, a small antimicrobial peptide rich in tryptophan, proline, and basic amino acids," (in eng), *Biophys J*, vol. 72, no. 2 Pt 1, pp. 794-805, Feb 1997, doi: 10.1016/s0006-3495(97)78713-7.
- [95] S. N. Savinov and A. P. Heuck, "Interaction of Cholesterol with Perfringolysin O: What Have We Learned from Functional Analysis?," (in eng), *Toxins (Basel)*, vol. 9, no. 12, p. 381, 2017, doi: 10.3390/toxins9120381.
- [96] G. A. Caputo and E. London, "Analyzing Transmembrane Protein and Hydrophobic Helix Topography by Dual Fluorescence Quenching," (in eng), *Methods Mol Biol*, vol. 2003, pp. 351-368, 2019, doi: 10.1007/978-1-4939-9512-7_15.

- [97] N. J. Greenfield, "Using circular dichroism spectra to estimate protein secondary structure," *Nature Protocols*, vol. 1, no. 6, pp. 2876-2890, 2006, doi: 10.1038/nprot.2006.202.
- [98] S. R. Aili *et al.*, "Diversity of peptide toxins from stinging ant venoms," (in eng), *Toxicon*, vol. 92, pp. 166-78, Dec 15 2014, doi: 10.1016/j.toxicon.2014.10.021.
- [99] S. R. Johnson, J. A. Copello, M. S. Evans, and A. V. Suarez, "A biochemical characterization of the major peptides from the Venom of the giant Neotropical hunting ant *Dinoponera australis*," (in eng), *Toxicon*, vol. 55, no. 4, pp. 702-10, Apr 1 2010, doi: 10.1016/j.toxicon.2009.10.021.
- [100] W. C. Wimley and S. H. White, "Experimentally determined hydrophobicity scale for proteins at membrane interfaces," (in eng), *Nat Struct Biol*, vol. 3, no. 10, pp. 842-8, Oct 1996, doi: 10.1038/nsb1096-842.
- [101] M. A. Hitchner *et al.*, "Activity and characterization of a pH-sensitive antimicrobial peptide," (in eng), *Biochim Biophys Acta Biomembr*, vol. 1861, no. 10, p. 182984, Oct 1 2019, doi: 10.1016/j.bbamem.2019.05.006.
- [102] E. F. Palermo and K. Kuroda, "Chemical Structure of Cationic Groups in Amphiphilic Polymethacrylates Modulates the Antimicrobial and Hemolytic Activities," *Biomacromolecules*, vol. 10, no. 6, pp. 1416-1428, 2009/06/08 2009, doi: 10.1021/bm900044x.
- [103] E. F. Palermo and K. Kuroda, "Structural determinants of antimicrobial activity in polymers which mimic host defense peptides," (in eng), *Appl Microbiol Biotechnol*, vol. 87, no. 5, pp. 1605-15, Aug 2010, doi: 10.1007/s00253-010-2687-z.
- [104] A. R. D'Souza, M. R. Necelis, A. Kulesha, G. A. Caputo, and O. V. Makhlynets, "Beneficial Impacts of Incorporating the Non-Natural Amino Acid Azulenyl-Alanine into the Trp-Rich Antimicrobial Peptide buCATHL4B," (in eng), *Biomolecules*, vol. 11, no. 3, p. 421, 2021, doi: 10.3390/biom11030421.
- [105] K. T. O'Neil and W. F. DeGrado, "A thermodynamic scale for the helix-forming tendencies of the commonly occurring amino acids," (in eng), *Science*, vol. 250, no. 4981, pp. 646-51, Nov 2 1990, doi: 10.1126/science.2237415.
- [106] N. Dong *et al.*, "Strand length-dependent antimicrobial activity and membrane-active mechanism of arginine- and valine-rich β -hairpin-like antimicrobial peptides," (in eng), *Antimicrob Agents Chemother*, vol. 56, no. 6, pp. 2994-3003, Jun 2012, doi: 10.1128/aac.06327-11.

- [107] L. M. Gottler, R. de la Salud Bea, C. E. Shelburne, A. Ramamoorthy, and E. N. G. Marsh, "Using Fluorous Amino Acids To Probe the Effects of Changing Hydrophobicity on the Physical and Biological Properties of the β -Hairpin Antimicrobial Peptide Protegrin-1," *Biochemistry*, vol. 47, no. 35, pp. 9243-9250, 2008/09/02 2008, doi: 10.1021/bi801045n.
- [108] C. N. Pace and J. M. Scholtz, "A helix propensity scale based on experimental studies of peptides and proteins," (in eng), *Biophysical journal*, vol. 75, no. 1, pp. 422-427, 1998, doi: 10.1016/s0006-3495(98)77529-0.
- [109] J. Yang and Y. Zhang, "I-TASSER server: new development for protein structure and function predictions," (in eng), *Nucleic Acids Res*, vol. 43, no. W1, pp. W174-W181, 2015, doi: 10.1093/nar/gkv342.
- [110] H. Mortazavian, L. L. Foster, R. Bhat, S. Patel, and K. Kuroda, "Decoupling the Functional Roles of Cationic and Hydrophobic Groups in the Antimicrobial and Hemolytic Activities of Methacrylate Random Copolymers," *Biomacromolecules*, vol. 19, no. 11, pp. 4370-4378, 2018/11/12 2018, doi: 10.1021/acs.biomac.8b01256.
- [111] I. Sovadinova, E. F. Palermo, R. Huang, L. M. Thoma, and K. Kuroda, "Mechanism of polymer-induced hemolysis: nanosized pore formation and osmotic lysis," (in eng), *Biomacromolecules*, vol. 12, no. 1, pp. 260-8, Jan 10 2011, doi: 10.1021/bm1011739.
- [112] M. Utsintong, T. T. Talley, P. W. Taylor, A. J. Olson, and O. Vajragupta, "Virtual screening against alpha-cobratoxin," (in eng), *J Biomol Screen*, vol. 14, no. 9, pp. 1109-1118, 2009, doi: 10.1177/1087057109344617.
- [113] K. Ebrahim, F. H. Shirazi, A. Z. Mirakabadi, and H. Vatanpour, "Cobra venom cytotoxins; apoptotic or necrotic agents?," (in eng), *Toxicon*, vol. 108, pp. 134-40, Dec 15 2015, doi: 10.1016/j.toxicon.2015.09.017.
- [114] S. H. Ferreira and M. Rocha e Silva, "Potentiation of bradykinin and eledoisin by BPF (bradykinin potentiating factor) from Bothrops jararaca venom," (in eng), *Experientia*, vol. 21, no. 6, pp. 347-9, Jun 15 1965, doi: 10.1007/bf02144709.
- [115] M. Moga, O. Dimienescu, C. Arvătescu, P. Ifteni, and L. Pleș, "Anticancer Activity of Toxins from Bee and Snake Venom—An Overview on Ovarian Cancer," *Molecules*, vol. 23, no. 3, p. 692, 2018, doi: 10.3390/molecules23030692.
- [116] Q. Liao, Y. Feng, B. Yang, and S. M. Lee, "Cnidarian peptide neurotoxins: a new source of various ion channel modulators or blockers against central nervous systems disease," (in eng), *Drug Discov Today*, vol. 24, no. 1, pp. 189-197, Jan 2019, doi: 10.1016/j.drudis.2018.08.011.

- [117] F. G. Avci, B. S. Akbulut, and E. Ozkirimli, "Membrane Active Peptides and Their Biophysical Characterization," (in eng), *Biomolecules*, vol. 8, no. 3, Aug 22 2018, doi: 10.3390/biom8030077.
- [118] G. van den Bogaart, J. V. Guzmán, J. T. Mika, and B. Poolman, "On the mechanism of pore formation by melittin," (in eng), *The Journal of biological chemistry*, vol. 283, no. 49, pp. 33854-33857, 2008, doi: 10.1074/jbc.M805171200.
- [119] C. Duffy *et al.*, "Honeybee venom and melittin suppress growth factor receptor activation in HER2-enriched and triple-negative breast cancer," *npj Precision Oncology*, vol. 4, no. 1, 2020, doi: 10.1038/s41698-020-00129-0.
- [120] J. Park, O. Kwon, H.-J. An, and K. K. Park, "Antifungal Effects of Bee Venom Components on *Trichophyton rubrum*: A Novel Approach of Bee Venom Study for Possible Emerging Antifungal Agent," (in eng), *Ann Dermatol*, vol. 30, no. 2, pp. 202-210, 2018, doi: 10.5021/ad.2018.30.2.202.
- [121] Y.-W. Kim, P. K. Chaturvedi, S. N. Chun, Y. G. Lee, and W. S. Ahn, "Honeybee venom possesses anticancer and antiviral effects by differential inhibition of HPV E6 and E7 expression on cervical cancer cell line," *Oncology Reports*, vol. 33, no. 4, pp. 1675-1682, 2015, doi: 10.3892/or.2015.3760.
- [122] J. H. Choi *et al.*, "Melittin, a honeybee venom-derived antimicrobial peptide, may target methicillin-resistant *Staphylococcus aureus*," (in eng), *Mol Med Rep*, vol. 12, no. 5, pp. 6483-6490, 2015, doi: 10.3892/mmr.2015.4275.
- [123] R. Qiao, K. Wang, and J. Zhong, "14 - Tumor-penetrating peptides," in *Peptide Applications in Biomedicine, Biotechnology and Bioengineering*, S. Koutsopoulos Ed.: Woodhead Publishing, 2018, pp. 371-386.
- [124] A. Borrelli, A. L. Tornesello, M. L. Tornesello, and F. M. Buonaguro, "Cell Penetrating Peptides as Molecular Carriers for Anti-Cancer Agents," (in eng), *Molecules (Basel, Switzerland)*, vol. 23, no. 2, p. 295, 2018, doi: 10.3390/molecules23020295.
- [125] F. Prestinaci, P. Pezzotti, and A. Pantosti, "Antimicrobial resistance: a global multifaceted phenomenon," (in eng), *Pathog Glob Health*, vol. 109, no. 7, pp. 309-318, 2015, doi: 10.1179/2047773215Y.0000000030.
- [126] K.-S. Huang, C.-H. Yang, S.-L. Huang, C.-Y. Chen, Y.-Y. Lu, and Y.-S. Lin, "Recent Advances in Antimicrobial Polymers: A Mini-Review," (in eng), *Int J Mol Sci*, vol. 17, no. 9, p. 1578, 2016, doi: 10.3390/ijms17091578.

- [127] F. Siedenbiedel and J. C. Tiller, "Antimicrobial Polymers in Solution and on Surfaces: Overview and Functional Principles," *Polymers*, vol. 4, no. 1, 2012, doi: 10.3390/polym4010046.
- [128] B. P. Mowery *et al.*, "Mimicry of Antimicrobial Host-Defense Peptides by Random Copolymers," *Journal of the American Chemical Society*, vol. 129, no. 50, pp. 15474-15476, 2007/12/01 2007, doi: 10.1021/ja077288d.
- [129] M. F. Ilker, H. Schule, and E. B. Coughlin, "Modular Norbornene Derivatives for the Preparation of Well-Defined Amphiphilic Polymers: Study of the Lipid Membrane Disruption Activities," *Macromolecules*, vol. 37, no. 3, pp. 694-700, 2004/02/01 2004, doi: 10.1021/ma035407d.
- [130] E.-R. Kenawy, F. I. Abdel-Hay, A. E.-R. R. El-Shanshoury, and M. H. El-Newehy, "Biologically active polymers: synthesis and antimicrobial activity of modified glycidyl methacrylate polymers having a quaternary ammonium and phosphonium groups," *Journal of Controlled Release*, vol. 50, no. 1, pp. 145-152, 1998/01/02/ 1998, doi: [https://doi.org/10.1016/S0168-3659\(97\)00126-0](https://doi.org/10.1016/S0168-3659(97)00126-0).
- [131] K. Kuroda and W. F. DeGrado, "Amphiphilic Polymethacrylate Derivatives as Antimicrobial Agents," *Journal of the American Chemical Society*, vol. 127, no. 12, pp. 4128-4129, 2005/03/01 2005, doi: 10.1021/ja044205+.
- [132] M. A. Gelman, B. Weisblum, D. M. Lynn, and S. H. Gellman, "Biocidal Activity of Polystyrenes That Are Cationic by Virtue of Protonation," *Organic Letters*, vol. 6, no. 4, pp. 557-560, 2004/02/01 2004, doi: 10.1021/ol036341+.
- [133] I. Sovadinova, E. F. Palermo, M. Urban, P. Mpiga, G. A. Caputo, and K. Kuroda, "Activity and Mechanism of Antimicrobial Peptide-Mimetic Amphiphilic Polymethacrylate Derivatives," *Polymers*, vol. 3, no. 3, 2011, doi: 10.3390/polym3031512.
- [134] P. F. Holmes, M. Bohrer, and J. Kohn, "Exploration of polymethacrylate structure-property correlations: Advances towards combinatorial and high-throughput methods for biomaterials discovery," (in eng), *Prog Polym Sci*, vol. 33, no. 8, pp. 787-796, Aug 2008, doi: 10.1016/j.progpolymsci.2008.05.002.
- [135] R. A. Hughes and C. J. Moody, "From amino acids to heteroaromatics--thiopeptide antibiotics, nature's heterocyclic peptides," (in eng), *Angew Chem Int Ed Engl*, vol. 46, no. 42, pp. 7930-54, 2007, doi: 10.1002/anie.200700728.
- [136] D. Du, L. Li, and Z. Wang, "N-heterocyclic carbene-catalyzed domino ring-opening/redox amidation/cyclization reactions of formylcyclopropane 1,1-diester: direct construction of a 6-5-6 tricyclic hydroxyridopyridine skeleton," (in eng), *J Org Chem*, vol. 74, no. 11, pp. 4379-82, Jun 5 2009, doi: 10.1021/jo900650h.

- [137] G. Chang, L. Yang, S. Liu, X. Luo, R. Lin, and L. Zhang, "Synthesis of indole-based functional polymers with well-defined structures via a catalyst-free C–N coupling reaction," *RSC Advances*, 10.1039/C4RA03602F vol. 4, no. 58, pp. 30630-30637, 2014, doi: 10.1039/C4RA03602F.
- [138] Y. Ahmadi, N. Moeini, M. Yadav, and S. Ahmad, "Chapter 12 - Antimicrobial polymer nanocomposite films and coatings," in *Handbook of Polymer Nanocomposites for Industrial Applications*, C. M. Hussain Ed.: Elsevier, 2021, pp. 379-397.
- [139] M. A. Walling, J. A. Novak, and J. R. Shepard, "Quantum dots for live cell and in vivo imaging," (in eng), *Int J Mol Sci*, vol. 10, no. 2, pp. 441-91, Feb 2009, doi: 10.3390/ijms10020441.
- [140] Y. Shimazaki, T. Yajima, M. Takani, and O. Yamauchi, "Metal complexes involving indole rings: Structures and effects of metal–indole interactions," *Coordination Chemistry Reviews*, vol. 253, no. 3, pp. 479-492, 2009/02/01/ 2009, doi: <https://doi.org/10.1016/j.ccr.2008.04.012>.
- [141] M.-L. Jobin *et al.*, "The role of tryptophans on the cellular uptake and membrane interaction of arginine-rich cell penetrating peptides," *Biochimica et Biophysica Acta (BBA) - Biomembranes*, vol. 1848, no. 2, pp. 593-602, 2015/02/01/ 2015, doi: <https://doi.org/10.1016/j.bbamem.2014.11.013>.
- [142] F. Lazzari, A. Manfredi, J. Alongi, D. Marinotto, P. Ferruti, and E. Ranucci, "d-, l- and d,l-Tryptophan-Based Polyamidoamino Acids: pH-Dependent Structuring and Fluorescent Properties," *Polymers*, vol. 11, no. 3, 2019, doi: 10.3390/polym11030543.
- [143] Y. Yang, Z. Cai, Z. Huang, X. Tang, and X. Zhang, "Antimicrobial cationic polymers: from structural design to functional control," *Polymer Journal*, vol. 50, no. 1, pp. 33-44, 2018/01/01 2018, doi: 10.1038/pj.2017.72.
- [144] Y.-F. Chen, Y.-D. Lai, C.-H. Chang, Y.-C. Tsai, C.-C. Tang, and J.-S. Jan, "Star-shaped polypeptides exhibit potent antibacterial activities," *Nanoscale*, 10.1039/C9NR02012H vol. 11, no. 24, pp. 11696-11708, 2019, doi: 10.1039/C9NR02012H.
- [145] K. E. S. Locock *et al.*, "Antimicrobial Polymethacrylates Synthesized as Mimics of Tryptophan-Rich Cationic Peptides," *ACS Macro Letters*, vol. 3, no. 4, pp. 319-323, 2014/04/15 2014, doi: 10.1021/mz5001527.
- [146] A. M. Carmona-Ribeiro and L. D. de Melo Carrasco, "Cationic antimicrobial polymers and their assemblies," (in eng), *Int J Mol Sci*, vol. 14, no. 5, pp. 9906-9946, 2013, doi: 10.3390/ijms14059906.

- [147] C. Subbalakshmi and N. Sitaram, "Mechanism of antimicrobial action of indolicidin," *FEMS Microbiology Letters*, vol. 160, no. 1, pp. 91-96, 1998, doi: 10.1111/j.1574-6968.1998.tb12896.x.
- [148] D. J. Schibli, L. T. Nguyen, S. D. Kernaghan, Ø. Rekdal, and H. J. Vogel, "Structure-function analysis of tritrypticin analogs: potential relationships between antimicrobial activities, model membrane interactions, and their micelle-bound NMR structures," (in eng), *Biophysical journal*, vol. 91, no. 12, pp. 4413-4426, 2006, doi: 10.1529/biophysj.106.085837.
- [149] A. K. Mishra, J. Choi, E. Moon, and K.-H. Baek, "Tryptophan-Rich and Proline-Rich Antimicrobial Peptides," (in eng), *Molecules (Basel, Switzerland)*, vol. 23, no. 4, p. 815, 2018, doi: 10.3390/molecules23040815.
- [150] K. Kuroda, G. A. Caputo, and W. F. Degrado, "The Role of Hydrophobicity in the Antimicrobial and Hemolytic Activities of Polymethacrylate Derivatives," *Chemistry - A European Journal*, vol. 15, no. 5, pp. 1123-1133, 2009, doi: 10.1002/chem.200801523.
- [151] R. Goseki and T. Ishizone, "Poly(methyl methacrylate) (PMMA)," 2014, pp. 1-11.
- [152] T. Ikeda, H. Hirayama, H. Yamaguchi, S. Tazuke, and M. Watanabe, "Polycationic biocides with pendant active groups: molecular weight dependence of antibacterial activity," (in eng), *Antimicrob Agents Chemother*, vol. 30, no. 1, pp. 132-136, 1986, doi: 10.1128/AAC.30.1.132.
- [153] E.-R. Kenawy, S. D. Worley, and R. Broughton, "The Chemistry and Applications of Antimicrobial Polymers: A State-of-the-Art Review," *Biomacromolecules*, vol. 8, no. 5, pp. 1359-1384, 2007/05/01 2007, doi: 10.1021/bm061150q.
- [154] H. Takahashi, E. F. Palermo, K. Yasuhara, G. A. Caputo, and K. Kuroda, "Molecular Design, Structures, and Activity of Antimicrobial Peptide-Mimetic Polymers," *Macromolecular Bioscience*, vol. 13, no. 10, pp. 1285-1299, 2013, doi: 10.1002/mabi.201300126.
- [155] T. Eren *et al.*, "Antibacterial and Hemolytic Activities of Quaternary Pyridinium Functionalized Polynorbornenes," *Macromolecular Chemistry and Physics*, vol. 209, no. 5, pp. 516-524, 2008, doi: <https://doi.org/10.1002/macp.200700418>.
- [156] Y. Ishitsuka *et al.*, "Amphiphilic poly(phenyleneethynylene)s can mimic antimicrobial peptide membrane disordering effect by membrane insertion," (in eng), *J Am Chem Soc*, vol. 128, no. 40, pp. 13123-9, Oct 11 2006, doi: 10.1021/ja061186q.

- [157] D. Liu *et al.*, "Nontoxic membrane-active antimicrobial arylamide oligomers," (in eng), *Angew Chem Int Ed Engl*, vol. 43, no. 9, pp. 1158-62, Feb 20 2004, doi: 10.1002/anie.200352791.
- [158] G. N. Tew *et al.*, "De novo design of biomimetic antimicrobial polymers," (in eng), *Proc Natl Acad Sci U S A*, vol. 99, no. 8, pp. 5110-4, Apr 16 2002, doi: 10.1073/pnas.082046199.
- [159] G. A. Caputo and E. London, "Using a novel dual fluorescence quenching assay for measurement of tryptophan depth within lipid bilayers to determine hydrophobic alpha-helix locations within membranes," (in eng), *Biochemistry*, vol. 42, no. 11, pp. 3265-74, Mar 25 2003, doi: 10.1021/bi026696l.
- [160] L. Ronda, B. Pioselli, S. Catinella, F. Salomone, M. Marchetti, and S. Bettati, "Quenching of tryptophan fluorescence in a highly scattering solution: Insights on protein localization in a lung surfactant formulation," (in eng), *PLoS One*, vol. 13, no. 8, pp. e0201926-e0201926, 2018, doi: 10.1371/journal.pone.0201926.
- [161] R. Hao *et al.*, "Cholesterol-sensing role of phenylalanine in the interaction of human islet amyloid polypeptide with lipid bilayers," *RSC Advances*, 10.1039/C8RA07310D vol. 8, no. 71, pp. 40581-40588, 2018, doi: 10.1039/C8RA07310D.